PROCESSING AND CHARACTERISATION OF ARAMID/CARBON HYBRID FIBRE REINFORCED POLYPROPYLENE COMPOSITES

MUHAMMAD RAFIQ BIN MOHD ISA

DISSERTATION SUBMITTED IN FULFILLMENT OF THE REQUIREMENTS FOR THE DEGREE OF MASTER OF SCIENCE

DEPARTMENT OF CHEMISTRY
FACULTY OF SCIENCE
UNIVERSITY OF MALAYA
KUALA LUMPUR

2014

ABSTRAK

Komposit hibrid gentian aramid/karbon /polipropilena (PP) dengan tiga peratusan gentian keseluruhan (V_f) berbeza dan lima campuran gentian (100:0, 75:25, 50:50, 25:75 dan 0:100 V:V%) telah disediakan melalui penyemperitan dan mesin suntikan acuan. Spesimen komposit dibentuk telah dicirikan untuk sifat-sifat mekanikal, mekanikal dinamik dan sifat termal. Analisis telah diperkukuhkan dengan imej dari imbasan mikroskop elektron. Analisis termogravimetri (TGA) mendedahkan bahawa penghibridan gentian menghasilkan komposit hibrid dengan sifat haba yang lebih baik berbanding dengan komposit gentian tunggal. Analisa kalorimeter imbasan perbezaan (DSC) menunjukkan bahawa penambahan gentian tidak mengubah takat lebur komposit dengan ketara. Penghabluran matriks telah didapati sangat dipengaruhi oleh jumlah V_f. Analisis mekanikal dinamik (DMA) menunjukkan peningkatan dalam modulus penyimpanan (E'). Ini menunjukkan bahawa komposit hibrid mempunyai ketegaran yang lebih tinggi berbanding dengan komposit gentian aramid. Kandungan gentian karbon menunjukkan pengaruh yang kuat pada magnitud E'. Sifat tegangan beberapa komposit hibrid melebihi sifat-sifat komposit gentian tunggal. Walau bagaimanapun, berdasarkan imej SEM permukaan patah, didapati bahawa interaksi antara matriks dan gentian adalah lemah. Sebaliknya, penghibridan mengurangkan sifat lenturan komposit berbanding dengan komposit gentian tunggal. Sifat lenturan didapati lebih sensitif kepada jumlah V_f, di mana komposit dengan jumlah V_f yang lebih tinggi akan mempunyai modulus lenturan yang lebih tinggi. Untuk semua komposit yang telah diuji, beban puncak (P) dan faktor intensiti tekanan kritikal (K_c) meningkat dengan kandungan gentian karbon. Sebaliknya, tenaga kegagalan (W) dan kadar lepas tenaga kritikal (G_c) telah menurun dengan peningkatan kandungan serat karbon di dalam komposit hibrid. Komposit hibrid menunjukkan sifat yang lebih baik apabila dibandingkan dengan komposit gentian tunggal. Secara ringkas, penghibridan gentian meningkatkan daya tahan komposit terhadap hentaman.

ABSTRACT

Hybrid composites of aramid fibre/carbon fibre/polypropylene (PP) with three total fibre volume fraction (V_f) and five fibre proportions (100:0, 75:25, 50:50, 25:75 and 0:100 V:V %) were prepared by extrusion and injection moulding. The moulded composite specimens were characterised for thermal, dynamic mechanical and mechanical properties. The results from the analysis were supported by scanning electron microscope images. Thermogravimetric analysis (TGA) revealed that the hybridisation of fibres produces hybrid composites with better thermal properties compared to the single fibre composites. Differential scanning calorimetric (DSC) study showed that the incorporation of the fibres did not significantly alter the melting behaviour of the composites. The crystallinity of the matrix was found to be greatly affected by the total V_f. Dynamic mechanical analysis (DMA) showed an increase in the storage modulus (E') indicating higher stiffness in the hybrid composites as compared to the aramid fibre composites. Carbon fibre content showed a strong influence on the magnitude of E'. The tensile properties of some hybrid composites exceed the properties of the single fibre composites. However, based on the SEM image of the fractured surface, it was found that the interfacial interaction between the matrix and fibres is weak. On the other hand, hybridisation reduced the flexural properties of the composites compared to its single fibre counterpart. Flexural properties were found to be more sensitive to total V_f, where composites with higher total V_f would have better flexural modulus. For all composites tested, the peak load (P) and critical stress intensity factor (K_c) increased with increasing carbon fibre contents. By contrast, the fracture energy (W) and critical strain energy release rate (G_c) were decreased with increasing carbon fibre content in hybrid composites. The hybrid composite showed superior impact properties when compared to its non-hybrid counterpart. In a nutshell, hybridisation of the fibres improved the impact properties of the composites.

ACKNOWLEDGEMENT

In the name of Allah, Most Gracious, Most Merciful.

I would like to express my sincere appreciation and gratitude to my supervisor, Prof. Dr. Aziz Hassan, for his patience and guidance during the research and writing of this thesis. Thanks were forwarded to all lecturers especially to Prof. Rosiyah Yahya who have indirectly assisted me in this work.

I would also like to convey my appreciation to the technical and support staff, especially to Mr. Zulkifli Abu Hasan, Miss Ho Wei Ling and Miss Nisrin Norranis, for their continuous help during the research. I am also grateful to all the members of the polymer and composite material research group which in many ways have indirectly contributed to the completion of this study.

I am thankful to the University of Malaya for funding this research through grants PV073-2012A and RG150/11AFR.

Last but not least, I owe special gratitude to my family, especially my parents, for their continuous and unconditional support throughout the duration of this program.

LIST OF FIGURES

LIST OF TABLES

LIST OF SYMBOLS

Å	Angstrom
a/D	Notch to depth ratio
AFRC	Aramid fibre reinforced composite
ASTM	American Society for Testing and Materials
CFRC	Carbon fibre reinforced composite
DMA	Dynamic mechanical analysis
DSC	Differential scanning calorimetry
DT_p	Derivative peak temperature
E	Young's modulus
E'	Storage modulus
E"	Loss modulus
FRPC	Fibre reinforced plastic composite
FRTC	Fibre reinforced thermoplastic composite
GFRC	Glass fibre reinforced composite
G_c	Critical strain energy release rate
GPa	Giga Pascal
HDPE	High density polyethylene
K_c	Critical stress intensity factor
LDPE	Low density polyethylene
MAPP	Maleic anhydride grafted polypropylene
MPa	Mega Pascal
P	Peak load
PAN	Polyacrylonitrile

PP	Polypropylene
RPM	Revolutions per minute
S/D	Span to depth ratio
SEM	Scanning electron microscopy
SEN	Single edge notch
$T_{50\%}$	Temperature at 50% degradation
Tan δ	Tan delta
T_c	Crystallisation temperature
TGA	Thermogravimetric analysis
T_m	Melting temperature
T_{onset}	Onset temperature
UV	Ultra violet
V_f	Fibre volume fraction
W	Energy to failure
W_f	Weight fraction
wt%	Weight percent
X_c	Degree of crystallinity
ΔH_c	Enthalpy of crystallisation
ΔH_m	Enthalpy of fusion/melting

TABLE OF CONTENTS

CHAPTER 1

INTRODUCTION

1.1 Polymer composites

Tracing the history of composite materials is like taking a fascinating look at the very development of civilized life itself. Technical advancement in the ancient world is generally agreed to have depended on several main factors; one of it is the presence of suitable materials, in which the progress in composite materials have greatly contributed. This statement still holds true, even now. For example, the development of carbon fibre reinforced polymer composites has allowed significant weight reduction of turbine blades employed in wind turbines due to the excellent strength to weight ratio of the composite [1]. The maximum blade-length of a turbine is limited by both the strength and stiffness of its material. Since the strength and stiffness to weight ratio of the composite is relatively higher when compared to conventional materials, bigger and lighter blades were able to be manufactured thus improving its efficiency.

A composite is an article or substrate made up of two or more distinct phases of different substance [2]. In the plastic industry, the term broadly applies to structures of reinforcing members (dispersed phase) incorporated in compatible resinous binders (continuous phase). Such composites are subdivided into classes on the basis of the reinforcing constituents; *particulate* (dispersed phase consist of small particles), *fibrous* (dispersed phase consist of unlayered fibres), *flake* (flat flakes forming the dispersed phase) and *skeletal* (composed of a continuous skeletal matrix filled by a resin). The components remain distinct molecularly and can be separated via mechanical means. Composites display properties which none of its constituents exhibit when in isolation.

Fibre reinforced polymer composite is a specific group of materials which uses fibres with high modulus and strength embedded or bonded to a matrix with distinct interfaces (boundaries) between them [3]. Both components interact and complement each other to produce superior properties. The fibres function as load bearer where most of the load is carried by the fibres. It also provide stiffness, thermal stability, strength and, in some rare cases, electrical conductivity to the composite. Aramid, carbon, and glass fibres are some of the more common fibre reinforcements employed. On the other hand, the matrix fulfils several roles which are vital to the performance of the composite. The matrix binds the fibres together and transfers the load to the fibres. It provides the composite with rigidity, shape and also isolates the fibres so that each one can function separately. The isolation would improve the crack resistance of the composite by either stopping or slowing the crack propagation process. The matrix also protects the fibres from chemical attack, elevated temperature, humidity and mechanical wear. Depending on the materials selected as the matrix, the impact strength and ductility of the composite can be improved. Adhesion and compatibility between fibres and the matrix is very important in order to produce strong composites [4]. Higher compatibility between the fibre and matrix would significantly improves the interfacial interaction between the two components resulting in better composites.

Polymer composites offer several advantages over conventional materials. It provides the capability for parts integration. The composite also have high specific stiffness (stiffness-to-density ratio) and specific strength (strength to density ratio). Polymer composites offer the same stiffness as steel at one fifth the weight and the same stiffness as aluminium at only half the weight [5]. Typically, any component made with polymer composite is lighter when compared to its traditional counterpart. Due to this, vehicles and

airplanes made with the composite parts can travel faster and have better fuel efficiency. In addition, polymer composites are highly resistant to corrosion and have high endurance (resistant to fatigue). The coefficient of thermal expansion for polymer composites are smaller compared to metallic material granting them better dimensional stability. Apart from its superior properties, using polymer composite also offer several advantages during processing. Complex parts, special appearances and contours, some impossible to be done with metals, can be fabricated using polymer composites without the need to weld or rivet separate pieces. Net-shape or near net-shape components can also be produced which would reduce several steps of machining and assembly, therefore reducing the cycle time and cost. The cost of tooling for polymer composites is much lower than for metals due to lower pressure and temperature involved in the processing step [6].

Polymer composites also suffer from a few disadvantages. On a weight basis, the cost of materials needed to produce polymer composite is usually five to twenty times the price of aluminium or steel. In addition, most of the popular processing method for composite such as hand lay-up is not suitable for high volume production. The automotive industry for example would require between 100 – 20,000 parts per day for its manufacturing activities. Manufacturing sporting goods such as golf shafts are done on the order of 10,000 per day. Designing using polymer composite is also a challenge due to the lack of data available; unlike materials such as steel which has abundance of design and data handbooks. Temperature resistance of the polymer composite is also dependent on the thermal property of the matrix. Most of the polymer composites are not suitable for service in elevated temperature for a prolonged period of time. Polymer composites also absorb moisture which can affect its dimensional stability and mechanical strength significantly.

1.2 Research Background

Carbon fibre reinforced composites (CFRC) are increasingly employed for a variety of high performance applications especially in aeronautic and aerospace industry due to their excellent specific mechanical properties. However, the anisotropic nature of CFRC make them sensitive to accidental damages, of which low-energy impact is considered the most dangerous [7]. The internal damage (defects) caused by low-energy impact is often barely visible to the naked eye and was found to cause substantial degradation in important mechanical properties, including strength and stiffness. These defects, if disregarded, could keep growing and cause premature failure.

The complex energy absorption mechanism during the impact process includes matrix cracking, delamination and fibre kinking and fracture. Various approaches have been taken to improve the damage resistance and damage tolerance of fibre composites. One of the more popular approaches is to introduce second fibre reinforcement into the system. Pejis *et. al.* have investigated the effect of the addition of high performance PE fibres on the impact resistance of hybrid PE/carbon/epoxy structures [8]. The researchers reported that the hybrid composite exhibited significantly better resistance to impact damage when compared to all-carbon laminates due to a change in energy absorption mode. It was suggested that more energy is stored in the PE component and consequently less energy is available for damage in the structural carbon component, resulting in a reduction in impact damage and improved post-impact properties.

For the purpose of this study, aramid/carbon hybrid fibre reinforced polypropylene was prepared. Aramid fibres are introduced into the system with the main aim of improving its impact properties.

1.3 Research Objectives

The objectives of this work are:

i. To prepare the aramid/carbon hybrid fibre composite via extrusion and injection moulding.

ii. To study the thermal properties of the specimens by thermogravimetric analysis (TGA) and differential scanning calorimetry (DSC).

iii. To study the dynamic mechanical properties of the composites through the Dynamic Mechanical Analyser (DMA).

iv. To study the mechanical properties of the specimens through tensile, flexural and impact tests.

v. To study the fractured surface of the specimens in order to establish the failure mechanism (either fibre pull-out or fibre fracture) of the composites.

1.4 Research Scope

This study covers the effect of fibre reinforcement on composite performance and the effect of hybridization at different total fibre loading and fibre proportions on their mechanical, thermal as well as morphological properties. The intimately mixed hybrid fibre composites were prepared with three different total fibre volume fraction, V_f (5%, 10% and 20%) and five different fibre proportions (100:0, 75:25, 50:50, 25:75 and 0:100 V:V %).

1.5 Thesis Outline`

The main essence of this dissertation is to study the effect of fibre hybridisation on the properties of fibre reinforced polypropylene composites. It is divided into the following chapters:

Chapter one presents a general introduction to composites; advantages and applications. Research background, objectives and scope of work are also presented.

Chapter two provides a review of literature on the basic concepts of hybrid composites and examples of some of the hybrid composites developed by other researchers and its properties.

Chapter three highlights the materials and methods employed. Details of the testing method were also provided.

Chapter four focuses on the presentation of results and its discussion on the influence of hybridisation on the properties of the composite. Properties of single fibre composites were also presented.

Finally, chapter five presents the general conclusions and recommendations for future work.

CHAPTER 2

LITERATURE REVIEW

2.1 Fibre Reinforced Polymer Composites

Fibre reinforced composites can be divided to three main components. The components are the matrix (continuous phase), the fibres (dispersed phase) and the interface (region between the fibre and the matrix).

2.1.1 Matrix

In fibre reinforced polymer composites, the matrix consists of polymers. The polymers are divided into two main groups; thermoplastic and thermoset. The functions of the matrix are to bind the reinforcing fibres to form a coherent structure and to provide a medium by which to transfer applied stress from one filament to another. The nature of the matrix depends on which class of polymers are used. Thermosets tend to be brittle while thermoplastics are more ductile. Thermosets are used in applications where the composites will be exposed to extremely high temperature as the thermosets have very high thermal resistance and won't melt. In this study, the thermoplastic polypropylene was chosen as the matrix.

Polypropylene (PP) is used in various applications, both in industry and in consumer goods, and it can be used both as a structural plastic and as a fibre. PP is a highly crystalline, easily processed on conventional processing machines and an important commodity polymer. It, also, has a low processing temperature and low cost but poor

toughness, average modulus and thermal-resistant properties [9]. This plastic is often used for food containers, particularly those that need to be dishwasher safe.

PP was synthesised as early as 1869 by Berthelot using concentrated sulphuric acid [10]. The resulting viscous oil at room temperature did not exhibit interesting properties for industrial application. Its industrial importance stems from the appearance of crystalline high molecular weight PP which was first polymerised in 1955 by Natta *et al.* using organo-metallic catalysts based on titanium and aluminium [11]. Most commercial polypropylene is isotactic and has an intermediate level of crystallinity between that of low-density polyethylene (LDPE) and high-density polyethylene (HDPE). Polypropylene is normally tough and flexible, especially when copolymerised with ethylene. This allows polypropylene to be used as an engineering plastic, competing with materials such as ABS. PP's strength and versatility stem from a matrix of interlocking crystallites that allow formation of rigid and tough articles. Highly isotactic polymer, with its regular structure, forms a helical coil having three monomer units per turn. These coils stack together into thin lamellar crystallites which force the chains to fold several times as they emerge and re-enter lamellae [10].

The melting point of PP, at 160°C, is relatively very high compared to many other plastics [12]. This contrasts with polyethylene (PE), another popular plastic for containers, which has a much lower melting point. Three crystalline forms of PP are known, of which the α-form is the most stable. Rapid quenching yields the β-form with lower density and melting point of 150°C. Polymers of lower stereoregularity and random copolymers usually contain γ-crystallites in addition to the α-form [13].

Because it is composed of only carbon and hydrogen atoms, and not polar atoms such as oxygen and nitrogen, PP is a nonpolar material. PP is resistance to attack by polar chemicals such as soap, alcohols and wetting agents. However, it can swell, soften or undergo crazing in the presence of liquid hydrocarbon or chlorinated solvents. Strong oxidizing agents such as fuming nitric acid or hot, concentrated sulphuric acid can cause swelling and degradation [12].

PP is also very easy to dye and it is often used as a fibre in carpeting that needs to be rugged and durable, such as that for use around swimming pools or on miniature golf courses. Unlike nylon, which is also often used as a fibre for rugged carpeting, it doesn't soak up water, making it ideal for uses where it will be constantly subject to moisture.

PP is not as sturdy as PE, but in some situations, it can be the better choice. One of these situations is creating hinges from a plastic, such as a plastic lid on a travel mug. Over time, plastics wear out from the repetitive stress of being opened and shut, and eventually will break due to fatigue. PP is very resistant to this sort of stress, and it is the plastic most often used for lids and caps that require a hinging mechanism.

The uses of PP are numerous because of how versatile this product is. According to some reports, the global market for this plastic is 45.1 million tons, which equates to a consumer market use of about 65 billion US Dollars. It is used in products such as plastic parts for toys and automobile, carpeting, upholstery, reusable containers, laboratory equipment and many more. Like many plastics, PP has virtually endless uses, and its development has not slowed since its discovery. It is one of a handful of materials the world is literally built around.

2.1.2 Fibre

The fundamental role of fibres in a composite material is to improve the mechanical properties of the neat resin system. Fibrous fillers offer improvement in strength and stiffness of the materials. All of the different fibres used in composites have different properties and so affect the properties of the composite in different ways. The fibres chosen for this work are aramid and carbon fibres.

2.1.2.1 Aramid Fibres

Aramid fibres are highly crystalline aromatic polyamide fibres that have the lowest density and one of the highest tensile strength-to-weight ratios among the reinforcing fibres. Aramid fibres are used as reinforcement in marine and aerospace applications where lightweight, high tensile strength and resistance to impact damage (a famous example is dropping a heavy hammer on the composite component) are important. They have negative coefficient of thermal expansion in the longitudinal direction, similar to carbon fibres. The major disadvantages of aramid fibres are their low compressive strength and difficulty in cutting or machining. Aramid is difficult to dye by nature, but it is now possible to produce black threads of the same quality. Twaron® is five times stronger than steel at the same weight and is often used in bullet-proof vests, ropes and cables, sails and fire fighter suits. The molecular structure of Twaron® (aramid fibre used in this work) is illustrated in Figure 2.1. The repeating unit in its molecule contains an amide group and an aromatic ring. The aromatic ring gives it a higher chain stiffness as well as better chemical and thermal stability over other commercial organic fibres such as nylon.

Production of Twaron® fibres is divided into three main stages; polymerisation, filament yarn spinning and conversion. Twaron® is a p-phenylene terephtalamide (PpPTA), the simplest form of the AABB para polyaramide. PpPTA is a product of p-phenylene diamine (PPD) and terephtaloyl dichloride (TDC). N-methyl pyrrolidone (NMP) and calcium chloride ($CaCl_2$) were used as co-solvent in the process. At this stage, it has yet to acquire the reinforcing properties of yarn or pulp.

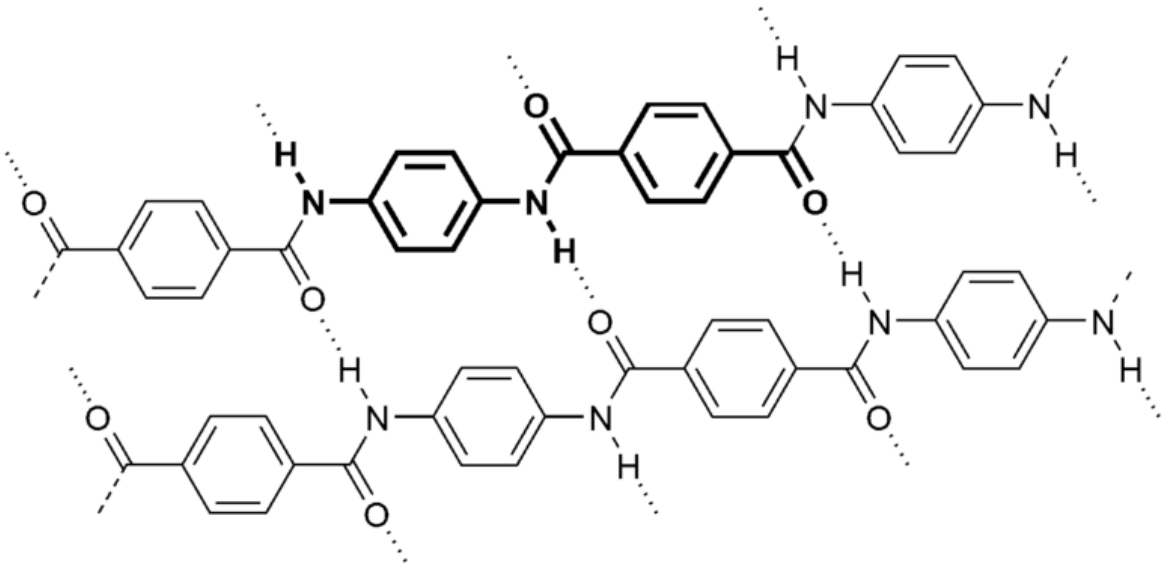

Figure 2.1: Molecular structure of Twaron®

The second stage involves dissolving the polymer in sulphuric acid to produce a liquid crystalline solution. This solution is then spun into fine, natural yellow or dope-dyed black filament yarn (the diameter of each filament is as small as 12µm). The structure of the yarn is virtually 100% para-crystalline, with molecular chains running parallel to the axis of the fiber. It is this high degree of orientation that contributes to the extraordinary properties of Twaron® filament yarns. Studies done by Young and Andrews [14], and Zwaag et. al [15] has confirmed the presence of chain stretching in aramid molecules when mechanical stress were applied.

However, aramid fibres are quite susceptible to environmental degradation. Prolonged exposure to moisture and ultraviolet (UV) rays may cause the mechanical properties of the fibres to significantly decrease. The effect of UV rays on the mechanical properties of aramid fibres (Twaron® 2000) was studied by Zhang *et al.* [16]. Exposure to UV rays causes a photo induced chain scission and end group oxidation in air to occur. The crystalline structure remained unchanged but some local rearrangement of the crystalline area might occur. With irradiation, the tenacity, tensile strain and work to break of the filaments decrease rapidly and almost linearly, and the work to break drops more quickly than the tenacity and tensile strain of the filaments. The modulus of the filaments decreases slightly with irradiation. Similar results were also reported by several other researchers with different aramid fibres (Kevlar® 149 and Technora® by Dobb *et al.* [17] and Kevlar 49 by Brown *et al.* [18]). It was also noted that the tensile failure mode of the fibres changed from fibril splitting to brittle fracture after UV ray exposure.

Tanaka *et al.* studied the effect of moisture on the interfacial interaction between aramid fibre and epoxy [19]. They found that moisture would weaken the interaction and decreases the strength of the composite. Several other researchers also have studied the detrimental impact of moisture on the performance of aramid fibres [20-23].

2.1.2.2 Carbon Fibres

Carbon fibre is any fibre consisting mainly of elemental carbon and is widely used in reinforced polymer composites [24]. Among the advantages of carbon fibres are their exceptionally high tensile strength-weight ratios as well as tensile modulus-weight ratios, very low coefficient of linear thermal expansion (provides dimensional stability), high

fatigue strength and high thermal conductivity [25]. Their weaknesses are low strain-to-failure, low impact resistance, and high electrical conductivity (advantageous in some application such as solar panels, but it may cause "shorting" if utilised in unprotected electrical machinery). Their high cost has so far excluded them from widespread commercial applications. They are used mostly in the aerospace industry, where weight saving is considered more critical than cost. The fibres are commonly prepared by controlled pyrolysis of precursors such as polyacrylonitrile (PAN) and pitch (petroleum derived pitch is also known as bitumen or asphalt). Carbon fibres made from PAN precursor have lower thermal conductivity and electrical conduct than pitch carbon fibres [26]. Figure 2.2 illustrates the manufacturing of carbon fibres.

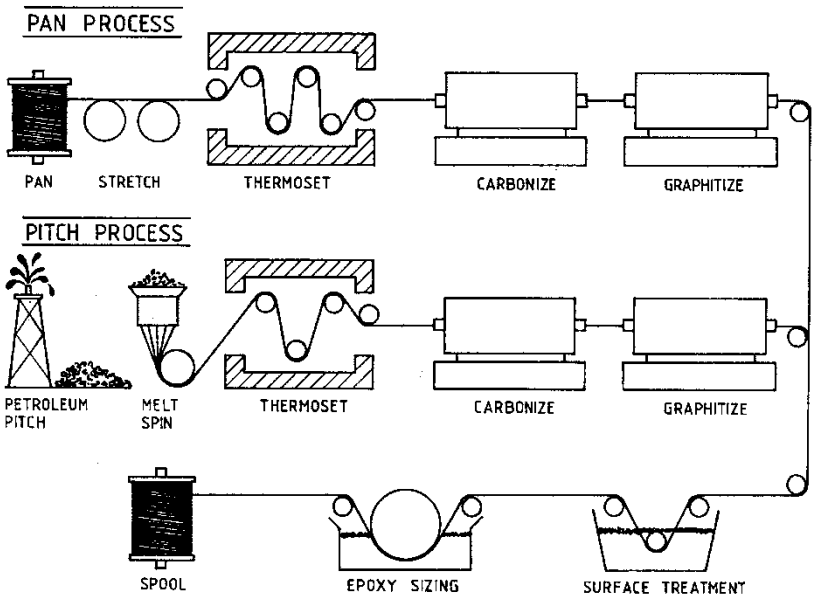

Figure 2.2: Schematic of PAN and pitch based carbon fibre manufacturing procedure.[27]

Structurally, carbon fibres consist of a blend of amorphous carbon and graphitic carbon. Their high tensile modulus results from the graphitic form, in which carbon atoms are arranged in a crystallographic structure of parallel planes or layers as seen in Figure 2.3.

The carbon atoms in each plane are arranged at the corners of interconnecting regular hexagons. The distance between the planes (3.4 Å) is larger than that between the adjacent atoms in each plane (1.42 Å). Strong covalent bond exist between carbon atoms in each plane, but the bond between the planes is due to van der Waals-type forces, which is much weaker. This results in highly anisotropic physical and mechanical properties for the carbon fibre.

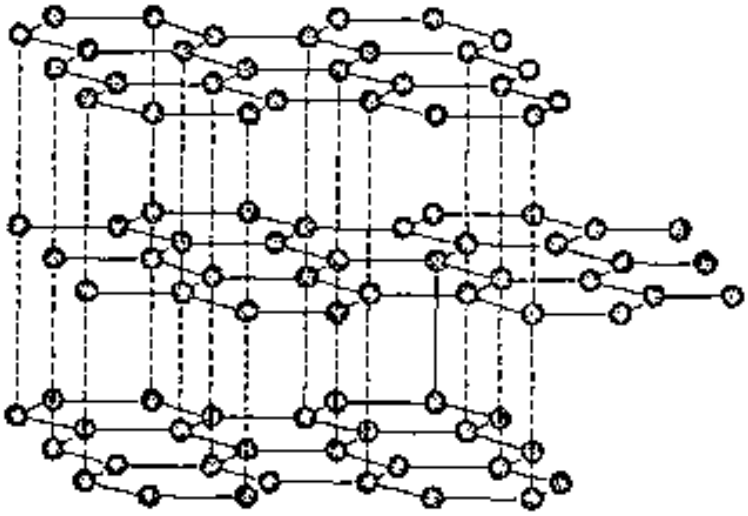

Figure 2.3: Graphite layers

2.2 Fibre Reinforced Thermoplastic Composite

Fibre reinforced thermoplastic composite (FRTC) are composites that consist of thermoplastic polymer as its matrix. There are several advantages of using thermoplastics as the matrix. Thermoplastics can be repeatedly softened by heating and can be shaped by flow into articles by moulding and extrusion in its softened state. It can be hardened simply through cooling, in opposed to the curing process required by thermosets. FRTC are also more resistant to impact damage due to its toughness.

Strength of FRTC is dependent on several factors such as the strength and modulus of the fibre, strength and chemical stability of the matrix and also the interfacial interaction between these two phases. The interfacial interaction is an important control factor which can determine the mechanical properties of the composite. Generally, composites with better interfacial interaction would have better mechanical properties. The strength of the interfacial bonding is usually governed by the affinity of the two components. Hence, the interfacial bonding can be improved either through surface treatment or introduction of a coupling agent.

FRTC can be divided into subgroups depending on the type of fibres employed. There are two main subgroups which were classified based on the fibre used. There are continuous FRTC, where the reinforcing fibres are continuous, from one end to the other end of the finished article. On the other hand, there are discontinuous FRTC, where the fibres used are in the form of discontinuous fibres. In this type of composite, tens, hundreds or even thousands of fibres were introduced into the composite as needed.

FRTC can be further classified into single fibre composites and hybrid composites. Single fibre composites are composite reinforced with only one type of fibre whereas hybrid composites may contain two or more different type of fibres.

2.3 Hybrid Fibre Reinforced Thermoplastic Composite

The incorporation of two or more types of reinforcements into a single matrix has led to the development of hybrid composites. The reinforcement can be of the same type (fibre with fibre) or it can be different (fibre with particulates). In some cases, the hybrid would contain a mixture of polymers as its matrix. The behaviour of the hybrid composite is the

weighed sum of its components in which there is more balance between its inherent advantages and disadvantages [28]. Using a hybrid composite with two fibres, the advantage of one fibre may complement with what was lacking in the other fibre. As a consequence, balance of cost and performance may be achieved with proper material design. The properties of a hybrid composite mainly depend upon several factors such as fibre content, length of individual fibres, fibre orientation, extent of intermingling of fibres, fibre to matrix bonding and arrangement of both fibres. The strength of hybrid composite is also dependent on the failure strain of individual fibres. Maximum hybrid results are obtained when the fibres fails at similar tensile strain.

Hybrid fibre composites can be classified into four general types according to its construction [29]. Schematic diagram of the hybrid types is provided in Figure 2.4.

a) Type A – Dispersed fibre

This consists of intimate mixture of two or more types of continuous fibres aligned, but randomly dispersed throughout a common resin matrix.

b) Type B – Dispersed fibre ply

Basically this consists of random or alternating mixture of two or more types of fibre ply.

c) Type C – Fibre skin and core

This type consists of outer skins of one or more sorts of fibre laminate applied to a core made of another fibre laminate. Both skins and core may be made of unidirectional or angle ply material or type A or B hybrids. It is common to have the stiffer fibre (such as carbon fibre) in the skins.

d) Type D – Fibre skin, non-fibre core

This type of hybrid, which consists of fibre skins applied to a core of foam, filled resin, some type of honeycomb, solid metal or wood, is often referred to as a sandwich structure.

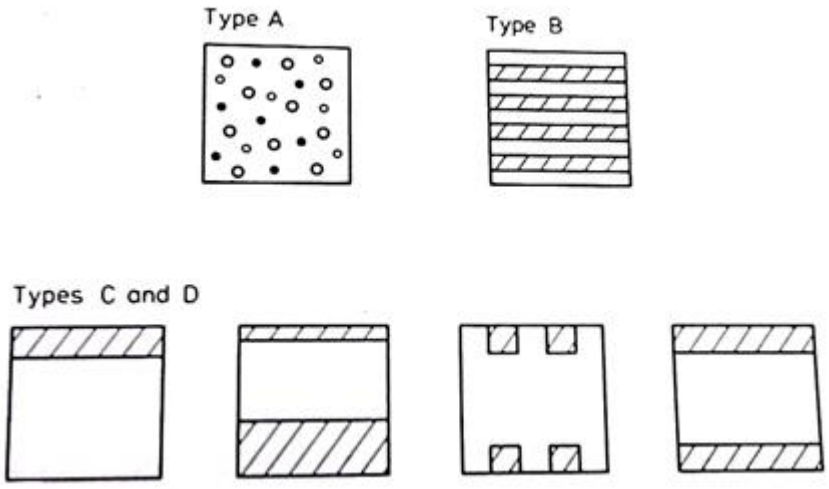

Figure 2.4: Schematic diagram of hybrid construction.

One critical issue in dealing with hybrid composites is the so-called "*hybrid effect*" or "*synergy*". It is defined by Marom *et al.* [30] as the deviation of behaviour of a hybrid structure from the "rule of mixture". The effect can either be positive or negative, depending whether it is higher or lower than the value predicted using rule of mixture. Three physical mechanisms have been identified and demonstrated to be responsible for causing the hybrid effect [31]. The first mechanism (mechanism I) is the protection enhancement afforded by the matrix to the fibres through the fragmentation process during composite extension. This enhancement effect is dependent on the along-fibre property variation (variation along fibre length) and on the fibre-matrix interfacial shears strength. Due to this enhancement, the (in situ) behaviour of the fibres in the composite will be

different from the original (ex situ) fibre behaviour determined before the fibres being embedded into the matrix. The second mechanism is related to the between-fibre property variation, i.e. variation of breaking strains between fibres of the same type. Because of this variation, the composite will break gradually according to the statistical distribution of their breaking strength or strain, eventually reducing the values of strength and breaking elongation of the composite due to the fibre-fibre interaction of the same type. These two mechanisms can also be seen in non-hybrid composites. The third mechanism is the cross coupling effects between the LE (fibre with lower breaking elongation) fibres and HE (fibre with higher breaking elongation) fibres.

2.4 Processing

Processing can be defined as the engineering activity concerned with operations carried out on polymeric materials/filler system to increase their utility. It deals with the conversion of raw materials into finished product involving compounding and shaping which leads to morphology stabilisation, and thus, value added products [32].

2.4.1 Compounding/Extrusion

In compounding, a base polymer resin in a molten form is combined in a batch or continuous mixers with fillers, reinforcements, other polymers, pigments, modifiers, and miscellaneous additives to improve properties, reduce costs, or improve processabilty. It involves dispersion of the fillers and additives in the molten polymer. Compounding may be defined as the production of a more useful and uniform product, in a more usable form [33].

There are two principal mixing mechanisms that dictate the type of equipment and mixing configuration. Dispersive mixing involves the reduction of the size of a component having cohesive character, within a continuous liquid phase. The cohesive character is due to Van der Waals forces between particles of the agglomerates or to the surface tension and elastic properties of the liquid droplets. The second mechanism is distributive mixing of components lacking a cohesive character, which results in their distribution throughout the volume. Distributive mixing depends on frequency of reorientation of flow elements under strain. Schematic diagram of the individual mixing mechanisms and their effect are are shown in Figure 2.5.

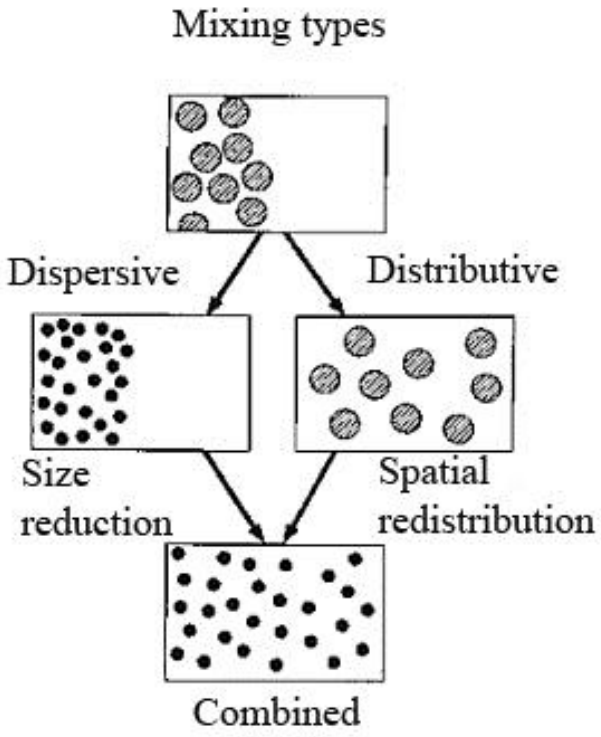

Figure 2.5: Distributive and dispersive mixing aspects

Primary mixing mechanisms for polymer blends, filled polymers or formulations are determined by the characteristics of the components. For high aspect ratio fibres (e.g.,

carbon), a distributive mixing configuration is mostly required. A combination of distributive and dispersing mechanisms is operative for compounds containing agglomerated low aspect ratio fillers such as talc.

Compounding is the first step towards the establishment for a microstructure that would control the desired properties of the finished product. For multiphase polymer systems containing a rigid dispersed phase (fibre), the melt compounding step controls the degree of dispersion and distribution of the fibres in the compounded pellets. The generated microstructure needs to remain stable in the subsequent fabrication (shaping) step.

The extruder is one of the most important pieces of machinery in polymer processing. Extrusion is defined as a plastic shaping process in which melted plastic resin is forced through an opening to produce a product that maintains relatively consistent size and shape [34]. Extrusion is highly suitable for mixing thermoplastic because the basic chemical nature of a thermoplastic usually does not change significantly as a result of the process [35]. Processing thermosets through extrusion is cumbersome. There is risk of the thermoset hardening in the barrel (due to crosslinking) which will damage the machine.

In this work, the extruder employed is an intermeshing co-rotating twin screw extruder. The rotation action of two intermeshing screws has additional capabilities that cannot be achieved by single screw extruders. The advantages are better melting and mixing, fast pressure build-up along the screw channel, narrow residence time distribution and positive conveying of polymer solid and melt along the screw channel. The intermeshing co-rotating twin screw extruder has been established as the most popular continuous mixing device [36].

2.4.2 Moulding

Moulding of plastics can be defined as the confinement of a mass of molten plastic in a cavity of defined dimensions, called a mould, while it hardens to the desired shape or finished article. There are several moulding processes such as compression moulding, thermoforming and injection moulding.

Compression moulding is widely used to manufacture products from thermosetting plastics. In compression moulding, the material is introduced directly into a heated metal hold, softened by heat and forced to conform to the shape of the mould cavity as the mould closes. A calculated amount of the material, either powder, preforms or granular form is positioned in the heated female mould cavity. The mould is then closed and the part is formed by heat and pressure. After a set amount of time, the mould is opened and ejector pin pushes the part out of the mould. Compression moulding is more widely used in the plastic industry for thermosetting polymer is due to the fact that the mould does not need to cool down prior to removing the finished article. Thermosetting polymer would cure inside the mould and harden while thermoplastic would need to cool down for it to harden. In addition, the process is not suitable for producing intricate parts or parts with fragile features.

In injection moulding, the polymer is softened and conveyed with a screw (similar to extrusion), and the molten polymer is pushed through a system of runners into cavities in the mould. The mould is cooled and after a set amount of time, the mould separates and the finished article is ejected [37]. Injection moulding has supplanted compression moulding as the premier choice of manufacturing some polymer products due to its advantages in material handling and automation. However, injection moulding is more suited to produce products in high volume due to its higher initial start-up cost (more expensive machinery).

2.5 Properties

2.5.1 Thermal properties

Thermal analysis represents a broad spectrum of analytical techniques designed to assess the response of materials to thermal stimuli, typically temperature change. Various techniques evaluate changes in enthalpy, specific heat, thermal conductivity and diffusivity, linear and volumetric expansion, mechanical and viscoelastic properties with temperature.

2.5.1.1 Differential scanning calorimetry

The differential scanning calorimeter (DSC) is the instrument that has dominated the field of thermal analysis. It measures heat flows and temperatures associated with exothermic and endothermic transitions. The ease with which important characteristics such as transitions, heat capacity, reaction, and crystallisation kinetics are characterised has made the DSC widely used in the plastics laboratory.

The DSC can operate in one of two ways: with a power-compensated design in which energy absorbed or evolved by the sample is compensated by adding or subtracting an equivalent amount electrical energy to a heater located in the sample holder. Alternatively, it can operate based on a heat flux design by which it measures the differential heat flow between a sample and an inert reference. Modulated DSC is an extension of conventional DSC in which the material is exposed to cyclic, rather than linear, heating profile. Deconvolution of the heat flow results obtained provides unique benefits, including improved resolution of closely occurring or overlapped transitions, increased sensitivity for subtle transitions, and separation or reversing and non-reversing thermal phenomena [38].

DSC is routinely used for investigation, selection, comparison and end-use performance of materials. Material properties that are routinely measured are glass transition temperature, freezing point, melting point, boiling point, decomposition temperature, crystallisation, phase changes, melting crystallisation, product stability, cure and cure kinetics, and oxidative stability.

Hartikainen *et al*. studied the thermal properties of PP composites reinforced with long glass fibre and $CaCO_3$ particulates [39]. In this study, DSC was mainly used to study the crystalllinity of the composite. However, due to the small size of the $CaCO_3$ and the surface treatment of the particulates, no significant changes were observed in the crystallinity of the composites.

Li Yu *et al.* reported that in a clay/glass fibre/epoxy hybrid nanocomposite, increasing the clay content would increase the T_g of the composite [40]. The introduction of clay would restrict the mobility of the epoxy molecules resulting in the increase.

2.5.1.2 Thermogravimetric analysis

Thermogravimetric analysis (TGA) is the second most used thermal technique. It measures weight changes in a material as a function of temperature or time under a controlled atmosphere. As the material degrades due to the temperature, it releases volatile compounds into the atmosphere, thus reducing the weight of the sample on balance. TGA is usually done either in temperature sweep mode or isothermal mode. The mode selected is based on which properties are currently being studied. The main uses include measurement of a materials thermal stability and composition. It can also be used to determine the

amount of bound and free water in polymer products and magnetic properties of composite materials.

TGA was used by Li Yu *et al.* to study the thermal stability of clay/glass fibre/epoxy composite [40]. The researchers reported that the thermal stability of the composite improved with increasing clay content. The results suggested that the increase of decomposition at the onset of decomposition is due to the improvement of barrier properties by the intercalated composites, in which clay act as barriers to decrease the permeability of degradation compounds.

2.5.2 Dynamic mechanical analysis

A dynamic mechanical analyser (DMA) is a controlled-stress or controlled-strain instrument that provides information on mechanical properties such as modulus, energy dissipation, and material stability. DMA is a powerful technique for developing a fundamental understanding of materials behaviour. A vast amount of research has led to the development of mathematically rigorous science that allows for the characterisation of polymers as well as the extrapolation of properties [38].

There are several modes of operation of DMAs. The most common is the rotational/torsional type instrument, although a number of linear tensile-compressive types are now available. These may operate either in a constant-strain or constant-stress mode. In the former, the specimen is always deflected to a defined strain while the stress is measured. Constant-stress mode is the converse. Constant stress modes are preferred for creep mode type experiment while the constant-strain mode lends themselves better to stress-relaxation studies.

Consider applying a sinusoidal strain to an ideal elastic solid as shown in Figure 2.6;

$$\varepsilon(t) = \varepsilon_o \,.\sin(\omega t) \tag{2.1}$$

where ε is the strain and ω is the angular frequency.

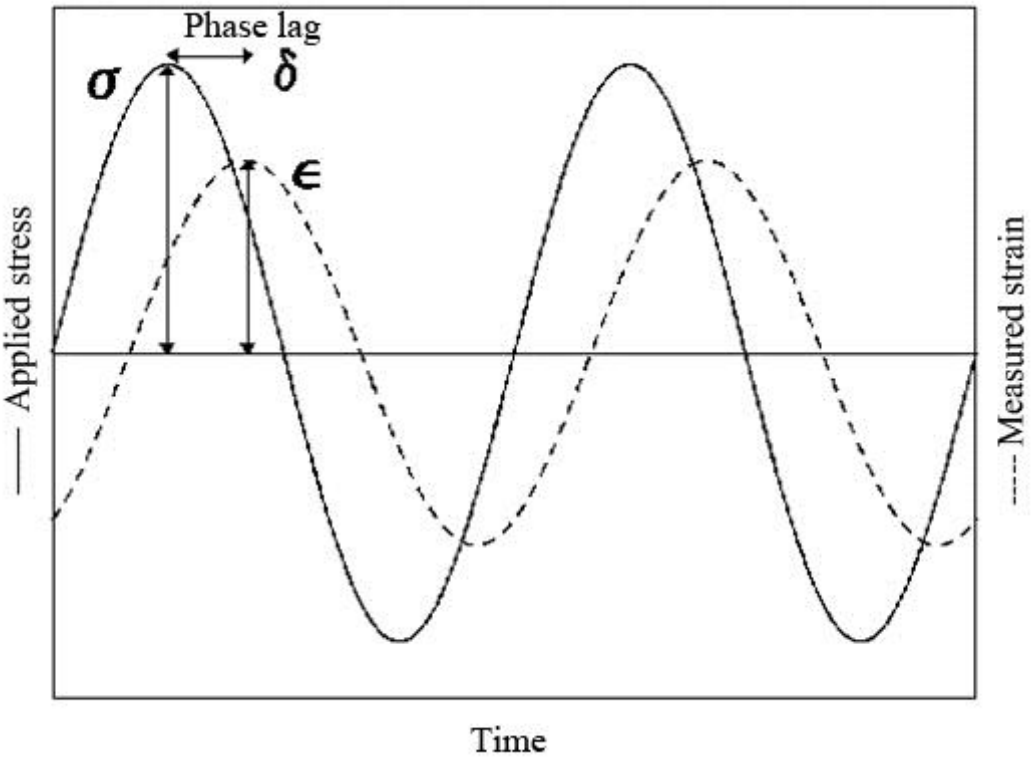

Figure 2.6: Stress and strain in dynamic mechanical analysis

At any point in time, the stress will be proportional to the strain according to Hooke's law;

$$\sigma(t) = E.\varepsilon(t) = \; E.\varepsilon_0.\sin(\omega t) = \sigma_0.\sin(\omega t) \tag{2.2}$$

where σ is the applied stress.

Thus, for an ideal solid, the stress will be sinusoidal function in-phase with the strain and the ratio of the amplitude of stress and strain will be storage modulus of the material.

$$E' = \frac{\delta_0}{\varepsilon_0}\cos(\delta) \tag{2.3}$$

where δ is the phase angle.

Now consider what happens if a sinusoidal force is applied to an ideal liquid;

$$\gamma = \gamma_o.\sin(\omega t) \tag{2.4}$$

At any point in time, the stress will be proportional to the strain rate in accordance with Newton's law of velocity;

$$\tau(t) = \eta.\gamma(t) = \frac{\eta.d\gamma(t)}{dt} = \eta.\gamma_0.\omega.\cos(\omega t) = \eta.\gamma_0.\omega.\sin\left(\omega t + \frac{\pi}{2}\right) \tag{2.5}$$

Thus, for an ideal liquid, the stress will be a sinusoidal function of 90° out of phase with the strain. This 90° phase difference between the sinusoidal stress and strain in liquids is the key to the use of DMA as a tool for characterising visco-elastic materials. A visco-elastic material has properties intermediate between those of an ideal solid and an ideal liquid, therefore it exhibits a phase lag somewhere between 0° (ideal solid) and 90° (ideal liquid). The phase lag is a measure of the relative degree of viscous character to elastic character [41].

The importance of DMA as a tool in the study of the behaviour of composite structures is paramount. It has been proved to be an effective method to study the relaxations in polymers and thereby the behaviour of materials under various conditions of

stress, temperature and phase composition of fibre composites and its role in determining the mechanical properties.

Idicula *et al.* produced an intimately mixed short banana/sisal hybrid fibre reinforced polyester composite and studied its dynamic mechanical behaviour [42]. The researchers found that at 3:1 fibre ratio with total volume fraction of 0.40, the composite produces the best stress transfer between the fibres. The composite has the lowest tan δ and highest storage modulus (E') value at glass transition temperature (T_g). Using Arrhenius equation, it was found that the composite at that formulation has the highest activation energy for glass transition. The results were confirmed by SEM images.

2.5.3 Mechanical Properties

2.5.3.1 Tensile properties

Tensile test is the most commonly performed test. Dumb-bell shaped specimens were used to prevent any artefacts in the measurement which were caused by deformation of the material in the grip region. Truly accurate measurements require extensometers, which can be either contact or non-contact.

Stress-strain behaviour represents the response of a material to loading. Tests are performed on a universal testing machine (UTM), sometimes referred to as a tensile tester because of the primary mode of deformation used to characterise this form of behaviour. Specimens are typically deformed at a constant cross-head speed. Due to the viscoelastic effect, the stress-strain relationship of a plastic composite is rate dependent. Performing tensile measurement at higher cross-head speeds results in stiffer response (higher modulus value). In addition, the properties may also vary significantly at different temperature. Tests

can be done within an environmental chamber to obtain data at elevated and sub-ambient temperatures. Several modes of deformation have been devised along the lines of the principal mode of deformation seen in the material: tension, compression, shear and flexure.

The modulus is the slope of the initial portion of the stress-strain curve. It measurement is complicated due to the fact that most plastics, unlike metals, do not have a linear relationship between stress and strain. This means that the modulus decreases with increasing strain, and the measured value depends on the strain region used as well as whether the slope is taken as a secant, a chord, or a tangent to this region [38]. There is justification for each of these methods and is chosen based on the intended application of the data. In order to ensure comparability, standards are used to define criteria for modulus measurement.

Tensile strength is the maximum stress that the material can withstand before failure. It suffers from variability in cases where the material is brittle, where the failure may be dictated by microscopic defect in the specimen. In contrast, ductile materials exhibit well defined maxima that results in repeatable tensile strength measurement.

Fu *et al.* studied the tensile properties of injection moulded carbon fibre reinforced polypropylene composite and the effect of mean fibre length [43]. The researchers found that with increase in fibre loading, the mean fibre length was decreased due to increased fibre breakage during processing. It was suggested that the combined effect of fibre volume fraction and mean fibre length determines the final tensile property of the composite. Carbon fibre reinforced polypropylene composites were shown to have higher tensile modulus when compare to polypropylene composites reinforced with glass fibre.

Composites with higher mean fibre length tend to have higher tensile strength. Modulus however is more dependent on the fibre volume fraction.

Jacob *et al.* prepared a sisal/oil palm hybrid fibre reinforced natural rubber composite and studied its mechanical properties [44]. The researchers report that increasing the total fibre loading in the composite would decrease the tensile strength and tear strength. However, the modulus of the composite increased with increase in total fibre loading. The researchers also studied the effect of fibre surface modification (alkali treatment) and bonding agent on the composite and found that the alkali treatment improved the adhesion between the matrix and the fibre thus improving its mechanical properties.

Velmurugan and Manikandan studied the mechanical properties of palmyra/glass fibre hybrid composites [45]. The researchers produced two types of hybrid composite where in one composite the palmyra fibre and glass fibre were mixed together. In the other hybrid composite, palmyra fibre reinforced composite were sandwiched by glass fibre reinforced mats. The mechanical properties such as impact, tensile, shear and bending properties were improved with introduction of glass fibre along the palmyra fibres. The sandwiched hybrid composite shown better properties when compared to the intimately mixed hybrid. In addition, the introduction of glass fibres reduced the moisture absorption of the composite.

2.5.3.2 Interfacial adhesion and compatibility between fibre and matrix

The importance of good interfacial interaction between components in a composite is well documented. The interface plays a major part during the stress transfer from the matrix to

the fibre during loading. A good adhesion would result in an efficient stress transfer thus producing a stronger and stiffer material. However, if the interfacial interaction is too strong, the material would be very brittle and notch sensitive [46]. A sufficiently strong (but not too strong) interfacial interaction is desirable especially for materials exposed to possible impact damage.

The interfacial interaction can be modified through several methods such as introduction of coupling agent or the surface modification of the fibres. For example, maleic anhydride grafted polypropylene (MAPP), a coupling agent, can be introduced into the matrix to improve the adhesion between the fibre and the matrix. Tjong *et al.* studied the effect of MAPP on the mechanical strength of short glass fibre/styrene-ethylene-butylene-styrene (SEBS) / polypropylene hybrid [47]. The researchers found that the introduction of the coupling agent improved the stiffness of the composite, indicating an improvement to the interfacial adhesion. However, improved interfacial adhesion caused the fracture toughness of the material to decrease. Rijsdijk *et al.* found that MAPP improves the flexural strength of continuous glass fibre reinforced polypropylene composites [48]. They found that both longitudinal and transverse flexural strength were improved up to 10 wt% MAPP content. When the MAPP content was further increased, the flexural properties were decreased.

The effect of moisture on the mechanical strength of composites has been widely reported and is especially notorious in composites made from hygroscopic materials such as nylon and natural fibre composites [47, 49-51]. The presence of moisture could reduce the mechanical strength of a composite by weakening its interfacial interaction. Almgren *et al.* [52] states that the interfacial stress transfer is less efficient when moisture is present is adsorbed into the interface. With a less efficient stress transfer, most of the load was carried

by the matrix instead of the fibre. Bradley *et al.* also reported that the moisture would reduce the tensile strength and interfacial shear strength of 7 different composite by up to 22% [53]. In order to counter this problem, the specimens are thoroughly dried and stored with silica gels prior to testing.

2.5.3.3 Flexural properties

Flexural analysis is the study of a material's resistance to bending. Studying the flexural properties of a composite is important because in its real life application, most of the components will be subjected to a mixture of loading which may include bending, either accidentally or intentionally. Flexural stress-strain curve are obtained by monitoring the force required to flex a material and the displacement that the material undergoes as a result of the applied force at a constant deformation rate.

Flexural modulus, an intensive property, is defined as the ratio of stress to strain in flexural deformation. It can also be defined as the tendency for the material to bend. Higher flexural modulus value indicates that the material is resistant to bending.

The flexural strength is the highest stress experienced within the material at its point of failure. When an object formed of a single material, like a wooden beam or a steel rod, is bent, it experiences a range of stresses across its depth. At the edge of the object on the inside of the bend (concave face) the stress will be at its maximum compressive stress value. At the outside of the bend (convex face) the stress will be at its maximum tensile value. These inner and outer edges of the beam or rod are known as the 'extreme fibres'. Most materials fail under tensile stress before they fail under compressive stress, so the

maximum tensile stress value that can be sustained before the beam or rod fails is its flexural strength.

Rozman *et al.* studied the flexural properties of oil palm empty fruit bunch (OPEFB)-glass fibre polypropylene composite [54]. The researchers found that increasing the amount of OPEFB in the hybrid causes the flexural strength to decrease. Natural fibres tend to be irregularly shaped, unlike man-made fibres which have uniform cross-section. The ability to support stress for non-uniform fillers such as the OPEFB is rather poor, resulting in a weaker composite. Similar observation was reported by Mishra *et al.* [55].

2.5.3.4 Impact Properties

Impact is a catastrophic event that has become very important for plastic composites. The impact properties of a material represent its ability to absorb and dissipate energies under impact or shock loading. In practice, the impact condition may range from accidental dropping of hand tools to high-speed collisions, and the response of structure may range from localized damage to total disintegration. If a material is strain rate sensitive, its static mechanical properties cannot be used in designing against impact failure. Furthermore, the fracture modes in impact conditions can be quite different than those observed in static tests.

While measurements of impact performance have always been made in the past, new applications in the aeronautics, automotive, electronics and consumer appliance industries have placed considerable importance on the quantification of this behaviour. A variety of standard impact test methods are available for metals (ASTM E23) and unreinforced polymers (ASTM D256). Some of these tests have also been adopted for fibre

reinforced composites. However, as in the case of metals and unreinforced polymers, the impact tests do not yield basic material property data that can be used for design purposes. They are useful in comparing the failure modes and energy absorption capabilities of two different materials under identical impact conditions.

Historically, Izod test has been used routinely to characterize impact. A notched rectangular bar is clamped in a vice and broken by a sharp impact from a hammer attached to a moving pendulum. Izod test have been widely criticized for being unsuitable for plastics, but it remains the most common test for impact and failure characterisation [38]. The Charpy test, widely used in Europe, has seen better acceptance by the scientific community. Here the test specimen, similarly notched, is held in a flexural mode while it is subjected to the impact. Typically, Izod impact energies are lower than Charpy impact energies.

Razaei *et. al* developed a short carbon fibre reinforced polypropylene composite for car bonnet [56]. The composite was prepared by melt blending and were moulded into the finished article using a hot press. They found that the composite has higher strength, stiffness, Izod impact energy and thermal stability when compared to neat polypropylene. They also found that composites with 10% fibre loading has comparable properties to traditional steel bonnet, with added advantage of lower weight. However, their study into the impact behaviour is not thorough as they only studied the Izod impact energy of the composite.

CHAPTER 3

EXPERIMENTAL

3.1 Material

Materials used in this experiment were TitanPRO® 6431 (unreinforced polypropylene manufactured by Titan Chemical Corporation, Malaysia), Twaron® 1488 (para-aramid fibre manufactured by Teijin Aramids BV, Netherlands) and Sigrafil® (carbon fibre manufactured by SGL Technic Ltd., Germany).

Amount of fibre and matrix required were calculated and weighed according to the desired volume fraction. The complete list of composite prepared in this work is provided in Table 3.1. To calculate the volume fraction of each fibre component in the composite, the following equation was employed,

$$V_{f1} = \frac{\frac{M_{f1}}{\delta_{f1}}}{\left(\frac{M_{f1}}{\delta_{f1}} + \frac{M_{f2}}{\delta_{f2}} + \frac{M_m}{\delta_m}\right)} \tag{3.1}$$

where M and δ are weight and density respectively; and subscripts f_1, f_2 and m referred to fibre 1, fibre 2 and matrix, respectively. The equation was modified from the one used by Hassan *et al.* in their research [57].

The components were mixed using physical mixing method. The blends were mixed in 500 g batches in order to avoid segregation of fibres in the feed hopper during extrusion. The segregation is due to the difference in density of the fibres and the matrix.

Table 3.1: List of composites produced during experiment

Designated Name	Polyproylene (v/v %)	Aramid fibre (v/v %)	Carbon fibre (v/v %)
5(5.00:0.00)	95	5	0
5(3.75:1.25)	95	3.75	1.25
5(2.50/2.50)	95	2.5	2.5
5(1.25/3.75)	95	1.25	3.75
5(0.00/5.00)	95	0	5
10(10.00:0.00)	90	10	0
10(7.50:2.50)	90	7.5	2.5
10(5.00:5.00)	90	5	5
10(2.50:7.50)	90	2.5	7.5
10(0.00:10.00)	90	0	10
20(20.00:0.00)	80	20	0
20(15.00:5.00)	80	15	5
20(10.00:10.00)	80	10	10
20(5.00:15.00)	80	5	15
20(0.00:20.00)	80	0	20

Specimens were designated according to their composition; for example, A(B:C) refers to specimen with total fibre volume fraction of A% where B is the V_f of aramid fibre and C is the V_f of carbon fibres.

3.2 Processing

3.2.1 Compounding

The materials were dried in a vacuum oven at 90°C for at least 8 hours prior to processing to remove moisture. The presence of moisture during processing would cause voids to form which could significantly affect the mechanical properties of the composites. This step is very important especially with hygroscopic materials such as aramid fibres. In addition, the presence of steam in the barrel could possibly cause some degradation to occur. The materials were compounded using a twin screw extruder (BRABENDER® KETSE 20/40 Lab Compounder, Germany). The extrusion was done at screw speed 80 RPM with the heaters set from 185°C to 195°C. The nozzle temperature was set at 200°C. The screw speed was chosen so that that fibre degradation could be kept at a minimum. The extrudate was quenched in an icy water bath and air dried prior to palletisation.

3.2.2 Injection moulding

Impact and tensile specimens were moulded using a 55 tonne BOY® 55M injection moulding machine (BOY®, Germany). The parameter for injection moulding is provided in Table 3.2. A single gated eight cavities bar shaped mould was used for the impact specimens while for the tensile specimens, a single gated four cavities bar shaped mould were used.

Table 3.2: **Parameter for injection moulding**

Parameter	Setting
Heating zone 1	190°C
Heating zone 2	195°C
Heating zone 3	200°C
Nozzle temperature	210°C
Screw speed	80 RPM
Cooling time	6 seconds
Mould temperature	25°C

3.3 Characterisation

3.3.1 Thermal properties

3.3.1.1 Thermogravimetric analysis

Thermogravimetric Analyser, TGA 6 (Perkin Elmer, USA) was used to study the degradation behaviour of the composites. About 5 - 10 mg of the sample was placed in ceramic sample cups. Tests were done from 50°C to 900°C with scan rate 10°C/min under nitrogen gas environment.

3.3.1.2 Differential Scanning Calorimetry

Diamond DSC (Perkin Elmer, USA) was used to study the phase transitions in the composites. About 5 mg of specimen were placed in an aluminium sample pan and crimped. A typical DSC run would consist of three steps. The first step involves heating from 50°C to 230°C. The sample then was cooled to -50°C and held for at least 5 minutes.

The final step involves heating from -50°C to 230°C. All these steps were done under controlled condition, with heating and cooling rate of 10°C/min. The first step was taken as precaution to remove the thermal history of the materials. The melting temperature (T_m), crystallisation temperature (T_c), melting enthalpy (ΔH_m), and crystalline enthalpy (ΔH_c) were determined from the last two steps.

3.3.2 Mechanical properties

3.3.2.1 Tensile test

Tensile tests were performed using a universal testing machine (Instron 5569, USA) equipped with a 50 kN load cell and a mechanical extensometer at a cross-head speed of 10 $mm.min^{-1}$. The specimen dimension and shape is in accordance with ASTM D638 [58]. The tests were done at room temperature and the extensometer jaw grip was set at 50 mm. Minimum of seven specimens per batch were tested to get the best reproducible results. For each batch of specimen, the average values of Young's modulus (E), tensile strength and tensile strain were calculated by the software from the stress over strain curve obtained. E was calculated at 0.5% strain.

3.3.2.2 Flexural test

Flexural tests were performed using a universal testing machine (Instron 5569, USA). The distance between the supports spans (L) were 50 mm, the cross-head speed of 1.33 mm/min. The speed of cross-head motion (R), was calculated by using the equation:

$$R = \frac{ZL^2}{6d} \tag{3.2}$$

where L and d are the specimens support span and depth respectively. Z is the rate of straining equal to 0.01. The test was conducted at a room temperature. The specimen shape and dimension is in accordance with ASTM D790 [59]. Ten specimens per batch were tested and the values of six best results were recorded. Flexural modulus and strength were calculated by the Bluehill® software from the flexural curve obtained.

3.3.2.3 Impact test

The impact test bars were notched at the center of one edge to produce single edge notch (SEN) impact test specimen using a Ray-Ran notch cutter. The notch angle was set at 45°. For each batch, they were notched with four different notch-to-depth ratios (a/D) of 0.1, 0.2, 0.3 and 0.4. The support span to depth ratio (S/D) was maintained at 4 throughout the experiment. For each batch, a minimum of ten specimens were tested and the results presented were taken from the average of at least 8 good reproducible data. The impact test was run in Charpy mode using an Instron Dynatup 9210 Falling Weight Impact Tester with a V-shaped impactor tup. The specimen dimension used is as stated in ASTM E23 [60]. Impact load used were 6.448 kg and height of 40 mm. Fracture energy and peak load were calculated by the software.

For this study, drop weight impact test was used. The test uses the free fall of a known weight to supply the energy to break a beam shaped specimen. The kinetic energy of the falling weight is adjusted by simply varying its drop height. Energy absorbed by the specimen is calculated as

$$U_t = \frac{W}{2g}(u_1^2 - u_2^2) \tag{3.1}$$

where W is weight of the striking head, g is the acceleration due to gravity, u_1 is the velocity of the striking head just before impact ($= \sqrt{2gH}$), u_2 is the measured velocity of the striking head just after impact and H is the drop height.

3.3.3 Dynamic mechanical analysis (DMA)

Samples were cut from the middle part of the tensile specimens to produce 60 mm x 13 mm x 3 mm test specimens. The DMA test was done using TA Instruments Q800 with a three point bending clamp with span length of 50 mm. The measurement was done over temperature range of -50 to 130°C at 3°C/min heating rate and frequency of 1 Hz. The sub-ambient temperature was achieved using a liquid nitrogen cooling unit.

3.3.4 Fracture surface analysis

A Zeiss Supra 35VP (Zeiss, Germany) digital scanning electron microscope (SEM) was used to study the fracture surface of selected tensile and impact test fracture surfaces. SEM micrographs were taken at 10 kV. In order to avoid an electrical charge during the examination, the fracture parts of the specimens were coated with a thin layer of gold (Au). The images were taken at several magnification values.

CHAPTER 4

RESULTS AND DISCUSSION

4.1 Thermogravimetric analysis (TGA)

TGA is a method studying the effect of temperature on the physical and chemical properties of a sample. When a sample decomposes or degrades after prolonged exposure to high temperature, the products would normally evaporate into the atmosphere, resulting in loss of weight. TGA can be done either by using constant temperature for a certain time (isothermal run) or by using a temperature sweep (scanning run). Understanding the thermal stability of a material is very important as it allows us to determine a safe service temperature range for the material. In addition, it can provide vital information that can be used by the engineers during material selection and product design. In this study, the samples were subjected to a temperature sweep from 50 to 900°C with heating rate of 10°C.min^{-1}. The resulting TGA curves are shown in Figures 4.1 – 4.3. `

From the curves, important information such as the thermal stability and weight fraction of the composite components can be obtained. The weight fractions of the components in the composite are important because it indicates the success of the mixing step. There were several precautionary steps taken during the processing step as suggested by Hassan *et al.* [61]. Prior to compounding the individual components in the extruder, the polypropylene pellets and the fibres were weighed carefully and premixed in 500 g batches. If this step is not taken, there is high probability that the component with higher density would settle down in the hopper. The weight fractions for the matrix and fibre were compared with the calculated values in Table 4.1.

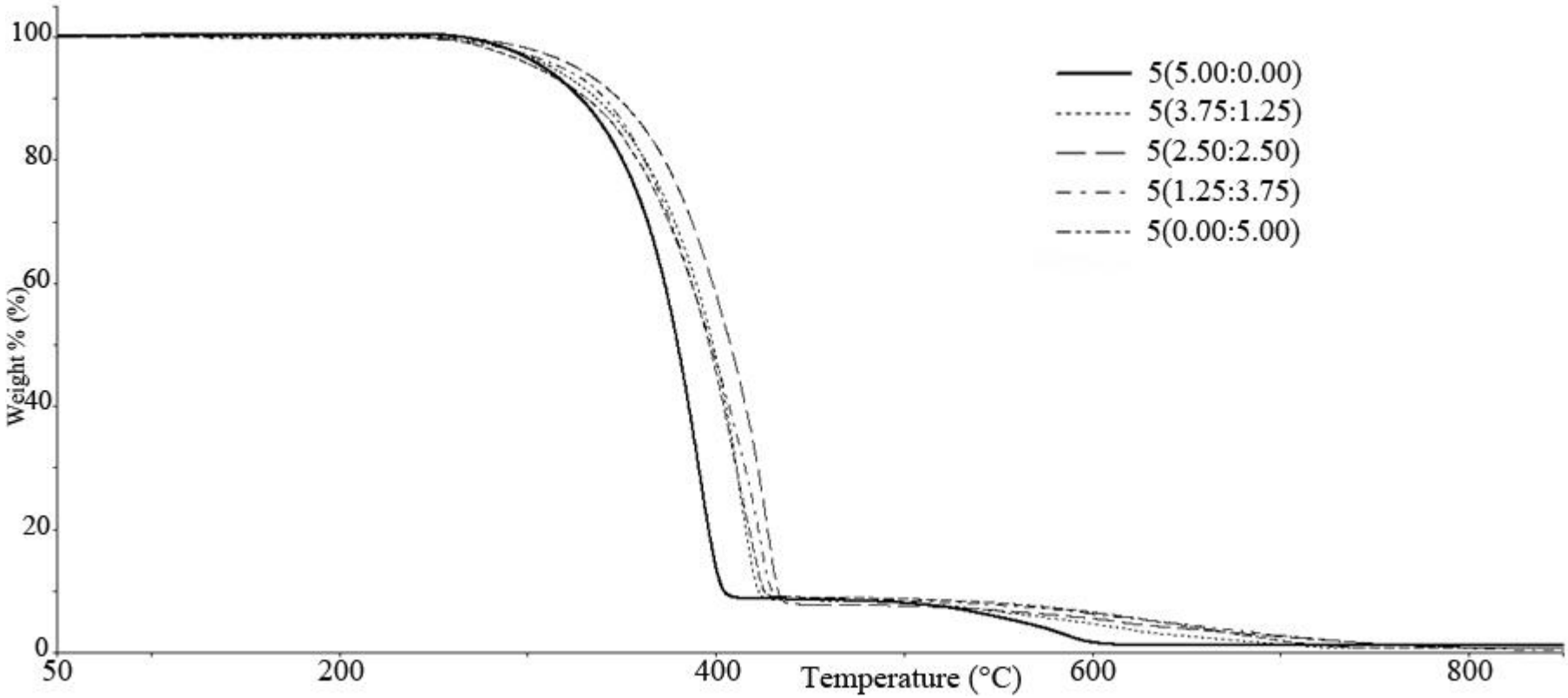

Figure 4.1: TGA thermogram of composites with 5% total V_f at different fibre proportions

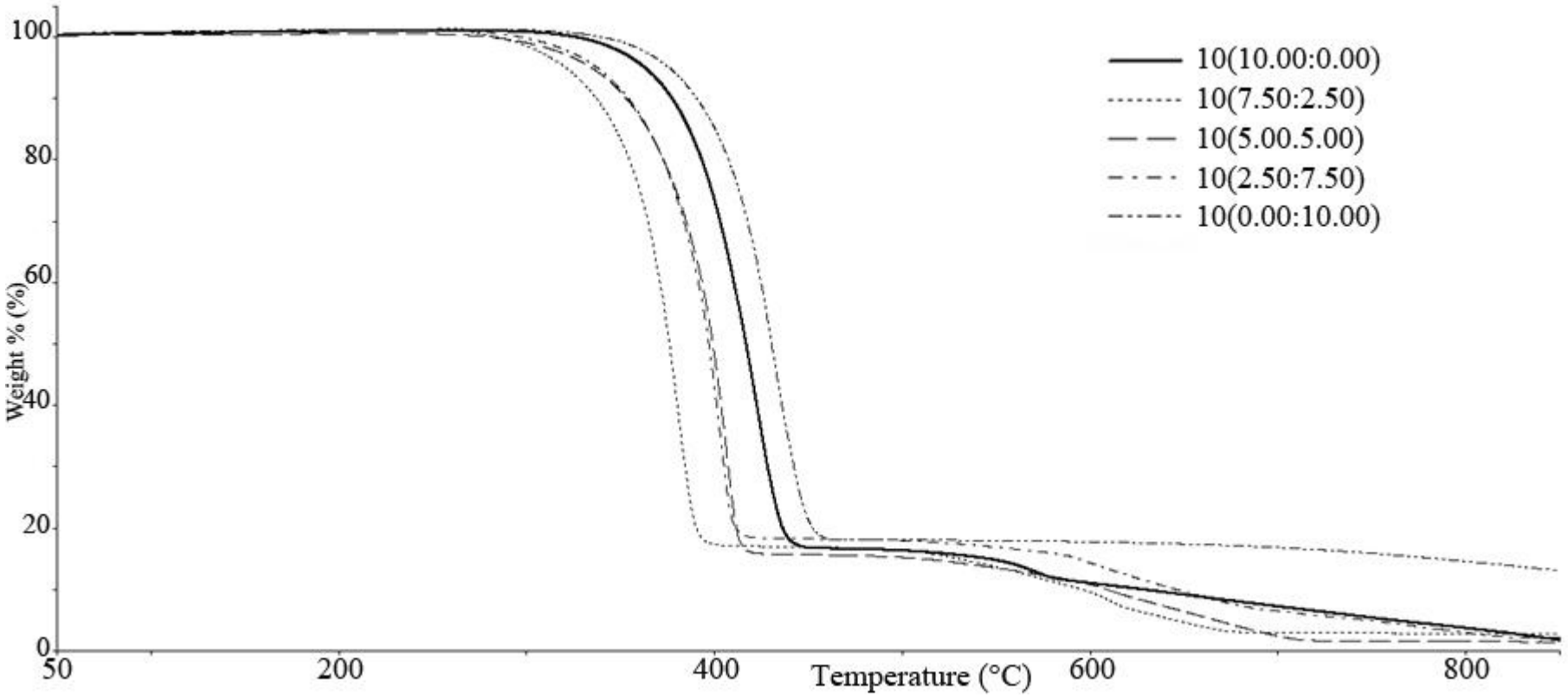

Figure 4.2: TGA thermogram of composites with 10% total V_f at different fibre proportions

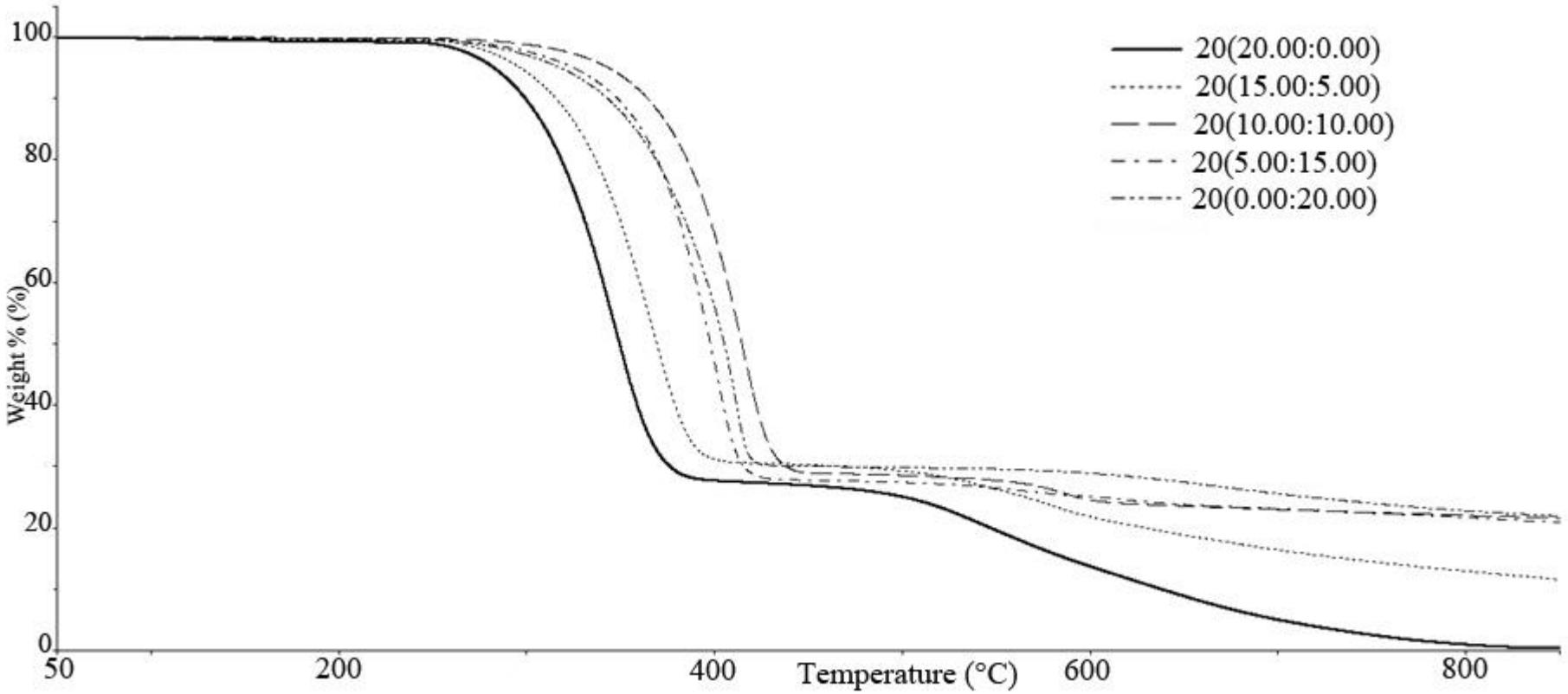

Figure 4.3: TGA thermogram of composites with 20% total V_f at different fibre proportions

Table 4.1: Calculated and experimental weight fraction for all composites.

Composite	W_m (Experimental)	W_m (Calculated)	Total W_f (Experimental)	Total W_f (Calculated)
5(5.00:0.00)	91.21	92.39	8.79	7.61
5(3.75:1.25)	91.40	92.01	8.60	7.99
5(2.50:2.50)	92.19	91.64	7.81	8.36
5(1.25:3.75)	91.30	91.27	8.70	8.73
5(0.00:5.00)	90.92	90.90	9.08	9.10
10(10.00:0.00)	83.50	85.18	16.50	14.82
10(7.50:2.50)	81.86	84.51	18.14	15.49
10(5.00:5.00)	84.28	83.85	15.72	16.15
10(2.50:7.50)	83.03	83.20	16.97	16.80
10(0.00:10.00)	82.22	82.55	17.78	17.45
20(20.00:0.00)	72.36	71.88	27.64	28.13
20(15.00:5.00)	69.46	70.80	30.54	29.20
20(10.00:10.00)	71.08	69.76	28.92	30.24
20(5.00:15.00)	72.19	68.75	27.81	31.25
20(0.00:20.00)	69.85	67.77	30.15	32.23

From Table 4.1, it can be observed that the difference between the experimental weight fraction value for the matrix and fibre components and its calculated value is small. For example, the experimental W_m for 20(0.00:20.00) is 69.85% while the calculated value is 67.77%. The difference is relatively small and it can be concluded that the mixing process produced composites with desired formulation. It is impossible to differentiate between aramid and carbon fibre in the hybrid composite using TGA. Therefore, the

comparison was done using the total fibre weight fraction instead. Incomplete degradation of the matrix (for example, charring which produce ash residue) would contribute to the slight difference between experimental and calculated W_f values.

From Figure 4.4, it can be observed that the intimately mixed composite were successfully produced from the fact that the fibres are intermingling in the matrix. No separate region containing only one type of the fibres employed were observed. Aramid and carbon fibre can be clearly differentiated from the image. Aramid fibres are the rope/ribbon like protrusions while the carbon fibres are the stiff cylindrical pipes protruding from the matrix.

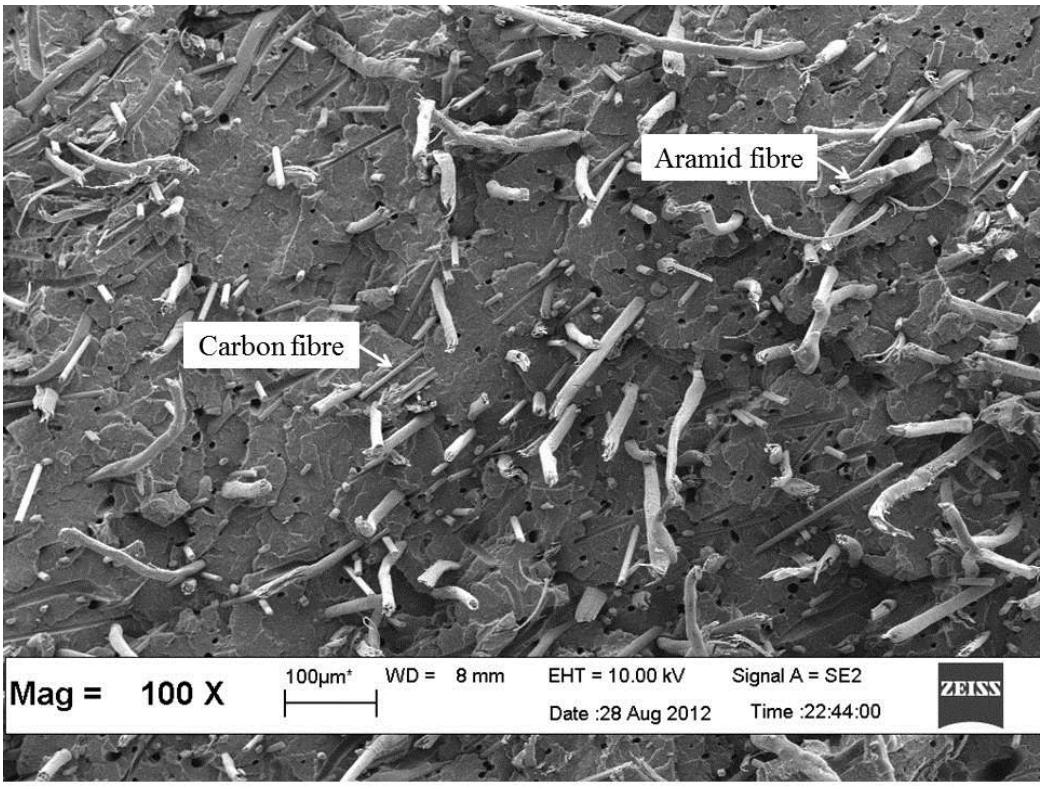

Figure 4.4: SEM micrographs taken from impact fracture surface of 10(5.00:5.00)

4.1.1 The effect of total fibre volume fraction, V_f

The thermal stability of a composite can be characterized by the onset temperature, the derivative peak temperature and the temperature at 50% weight loss, which are referred as T_{onset}, DT_p and $T_{50\%}$ respectively, as tabulated in Table 4.2. As heating occurs in an inert environment, a non-oxidative degradation occurs. $T_{50\%}$ is widely accepted as the temperature where the material will start to fail. T_{onset} indicates the temperature in which the material begins to degrade. The derivative peak temperature indicates the point of greatest rate of change on the weight loss curve.

The TGA curves for carbon fibre reinforced composite (CFRC) show a single step degradation process. The degradation of the polypropylene matrix occurred between 300°C to 450°C. Residues were present after the test. This is because under nitrogen gas environment and in the temperature range tested, carbon fibre would not degrade. In addition, some ash from the degradation of polypropylene could be present.

Increasing the amount of carbon fibre in the CFRC has affected the thermal stability of the composite. For example, as the fibre content increased from 5 to 10%, the T_{onset} increases from 360.0°C to 396.3°C. However, as the fibre content were further increased to 20%, T_{onset} value decreased to 367.0°C. The same trend was also observed in $T_{50\%}$ and DT_p values. $T_{50\%}$ values for CFRC with 5, 10 and 20% V_f are 396.4, 430.4 and 405.5°C, respectively. DT_p values for CFRC with 5, 10 and 20% V_f are 410.9, 430.5 and 412.0°C, respectively. Rezaei *et. al.* have reported that increasing the carbon fibre content increased the degradation temperature of the composites [62]. Carbon fibre has higher heat absorption capacity compared to polypropylene. As more fibres are introduced into the system, more heat was absorbed by the fibres and higher temperature was needed to achieve the threshold energy for commencement of degradation.

Table 4.2: T_{onset}, DT_p and $T_{50\%}$ for all composites.

Composition	T_{onset} (°C)	$T_{50\%}$ (°C)	DT_p (°C)
5(5.00:0.00)	346.8	379.6	390.8
5(3.75:1.25)	372.0	397.8	413.0
5(2.50:2.50)	378.0	406.7	381.7
5(1.25:3.75)	361.3	398.1	369.5
5(0.00:5.00)	360.0	396.4	410.9
10(10.00:0.00)	383.4	417.4	422.8
10(7.50:2.50)	349.6	375.6	427.2
10(5.00:5.00)	376.8	398.9	406.9
10(2.50:7.50)	372.9	397.0	415.9
10(0.00:10.00)	396.3	430.4	430.5
20(20.00:0.00)	298.9	349.5	347.9
20(15.00:5.00)	319.0	369.5	423.8
20(10.00:10.00)	373.1	414.2	403.4
20(5.00:15.00)	359.5	397.5	400.8
20(0.00:20.00)	367.0	405.5	412.0

The degradation temperature increased because as the amount of carbon fibre in the composite increased, the fibres in the composite would absorb more heat, thus higher temperature was needed to achieve the threshold energy for commencement of the degradation process, as explained by Rezaei *et al.* [62, 63]. Incorporation of fillers reduced the chain mobility in the absorption and boundary layers, which caused the decrease to the tension induced to the carbon-carbon chain by thermal excitation. Majority of the bond

breaking that occurred during thermal degradation is due to this induced tension and since the tension was reduced, the degradation was also reduced. In addition, it was also found that the fibre length plays an important role in the thermal properties of fibre reinforced composites. The researchers found that longer carbon fibres produce composites with better thermal properties. This explains the drop in thermal stability of carbon reinforced composites with 20% total V_f. At higher fibre content, the probability of fibre-fibre interaction during processing will increase. Increased fibre-fibre collision would cause fibre breakage to occur during processing and produce shorter carbon fibre fragments.

For aramid fibre reinforced composites (AFRC), the TGA curves showed a multistep degradation process. The first step, starting at 250°C, was due to degradation of the polypropylene matrix while the second step, starting around 400°C, was due to degradation of the aramid fibre. Bourbigot *et al.* studied the degradation of para-aramid fibres (Kevlar® 29 knitted fabric) using TGA and FTIR [64]. The researchers found that p-aramid fibres would start to degrade at around 550°C and formed a 38 wt. % residue at 1200°C. However, in the presence of oxygen, the fibre starts to degrade at 450°C and formed a 3 wt. % residue. This indicates that oxygen plays a big role in the degradation process. Major degradation products are C, CO, CO_2 and H_2O. HCN and ethylene species are the minor degradation products and at higher temperature, the HCN evolved reacts to produce NO through mechanism proposed by the authors. The solid residue were analysed and found to be char composed of polyaromatic compounds partially oxidised. Maity *et al.* reported that polypropylene composites reinforced with Twaron® fibres have higher degradation temperature when compared to pure PP [65]. The effect is more pronounced when the fibres were fluorinated (to improve interfacial interaction) which indicates that

better interfacial interaction between the fibre and the matrix would also improve the thermal stability of the composite.

The effect of fibre loading on the thermal stability of AFRC showed a similar trend to CFRC. For AFRC, the T_{onset} and $T_{50\%}$ increase when the aramid reinforcement increased from 5% to 10%. However, further increase in aramid content (10% to 20%) causes both parameters to decrease which indicates lower thermal stability. The T_{onset} values for AFRC with 5, 10 and 20% V_f are 346.8, 383.4 and 298.9°C, respectively. $T_{50\%}$ values for AFRC with 5, 10 and 20% V_f are 379.6, 417.4 and 349.5°C, respectively. DT_p values for AFRC with 5, 10 and 20% V_f are 390.8, 422.8 and 347.9°C, respectively.

The initial increase in the thermal stability of the composites is due to the increase in fibre content in the composite, as discussed earlier. The decrease in thermal stability as the fibre content was further increased is believed to be due to the fibre dispersion. The SEM image of composites reinforced with 20% V_f aramid has shown that there are fibre bundles in the composite, which indicates poor dispersion. The presence of undispersed aramid fibre bundles can be seen in Figure 4.5. The poor dispersion would cause the shielding effect to be less effective, hence reducing the thermal stability of the composite. The presence of fibre bundles are due to wetting problem. This is due to the inability of the viscous molten matrix to reach in between the fibres during mixing and in this case might be due to the high amount of aramid fibres. This is an interesting discovery that can serve as a guideline for future research.

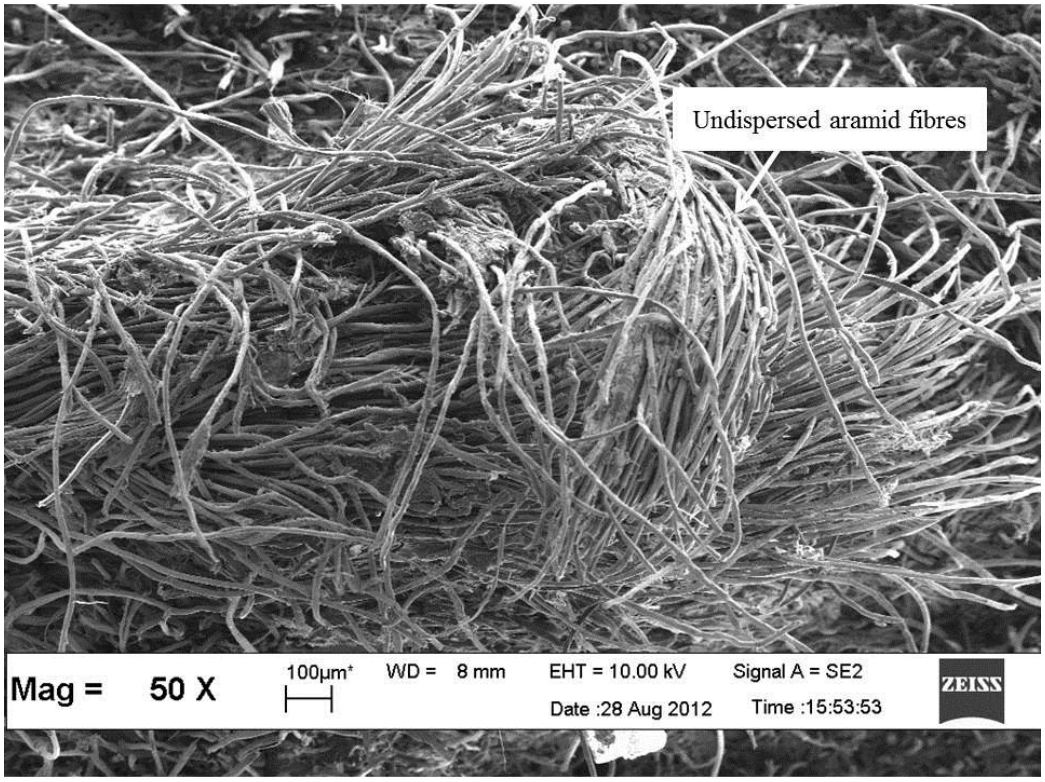

Figure 4.5: The presence of undispersed aramid fibre bundles in specimen with 20% aramid fibre content.

The effect of total V_f on the thermal stability of the hybrid composites showed mixed effect. For hybrid composite with 75:25 V:V% fibre proportions, T_{onset} and $T_{50\%}$ decreased as the total V_f was increased which indicates that the thermal stability of the hybrid decreased with higher V_f. T_{onset} for the hybrid decreased from 372.0°C to 349.6°C when total V_f was increased from 5 to 10%. It would further decrease to 319.0°C as the total V_f increased to 20%. For $T_{50\%}$, the value decreased from 397.8°C (V_f 5%) to 375.6°C (V_f 10%) and 369.5°C (V_f 20%). On the other hand, DT_p value showed increase when total V_f was increased from 5 to 10% and slightly lowered when the total V_f was further increased to 20%. DT_p values for the hybrid composites at 5, 10 and 20% total V_f are 413.0, 427.2 and 423.8°C, respectively.

Hybrid composites with 50:50 V:V% fibre proportions showed slight decrease in T_{onset} value with increasing total V_f. T_{onset} values for the composites are 378.0°C (V_f 5%), 376.8°C (V_f 10%) and 373.1°C (V_f 20%). $T_{50\%}$ showed initial decrease, from 406.7 to 398.9°C, when total V_f was increased from 5 to 10%. Increasing the total V_f further to 20% would cause the $T_{50\%}$ value to increase to 414.2°C. DT_p values for the hybrid composites at total V_f 5, 10 and 20% are 381.7, 406.9 and 403.4°C, respectively.

T_{onset} and DT_p values for hybrid composites with 25:75 V:V% fibre proportions showed similar trend. T_{onset} values initially increased from 361.3 to 372.9°C as the total V_f was increased from 5 to 10%. Further increasing the total V_f to 20% would cause the T_{onset} value to decrease to 359.5°C. DT_p values for the hybrid composites at 5, 10 and 20% total V_f are 369.5, 415.9 and 400.8°C, respectively. For hybrid with 25:75 V:V% fibre proportions, $T_{50\%}$ was not significantly affected by the increase in total V_f.

4.1.2 The effect of fibre proportion

In general, the effect of fibre proportions did not show any clear trends with regards to thermal stability. No significant increase or decrease in the thermal stability can be attributed to change in fibre proportions. Please refer to Table 4.2.

However, some of the hybrid composites were found to possess better thermal stability in certain aspects when compared to the non-hybrid composites. For example, the hybrid composite 20(10.00:10:00) starts to deteriorate significantly at 373°C and half of the composite weight was lost at 414.0°C. This is significantly higher than AFRC (20(20.00:0.00)) and CFRC (20(0.00:20.00)) with similar total volume fraction. Another hybrid, 5(2.50:2.50) starts to degrade at 378.0°C and is more thermally stable compared to its non-hybrid counterparts, 5(5.00:0.00) and 5(0.00:5.00), which starts to deteriorate at

346.8°C and 360.0°C, respectively. This indicates the presence of synergy where hybridisation of both fibres produces composites with higher thermal stability compared to its single fibre counterpart.

4.2 Differential scanning calorimetry (DSC)

Crystallisation and melting behaviour of the composites were analysed using DSC. The method has been used extensively in analysing the thermal behaviour of polymer composites [65-69]. DSC studies would allow greater understanding of the phase changes (such as melting) that the composite went through in the temperature range studied. The mechanical properties of the composite are influenced by the molecular structure of the matrix (crystalline structure, orientation of amorphous regions), especially the degree of crystallinity. Figures 4.6 – 4.8 show the DSC thermograms for the composites with total volume fraction of 5%, 10% and 20%, respectively.

Important parameters that were studied such as melting temperatures (T_m), enthalpy heat of melting (ΔH_m), degree of crystallinity (X_c), crystallisation temperature (T_c) and enthalpy heat of crystallisation (ΔH_c) for the composites are given in Table 4.3. X_c is calculated using the following equation:

$$X_c = \frac{\Delta H_m}{\Delta H_m^*} \tag{4.1}$$

where ΔH_m^* is the enthalpy heat of fusion for an 'ideally' fully crystalline PP, taken as 209 J/g [70]. The values provided in the table have been normalized according to the actual PP content in the composite. T_m and ΔH_m were obtained from the heating run while T_c and ΔH_c were obtained from the cooling run.

A single peak attributed to the matrix was observed in the heating run at around 157°C to 159°C. Neat polypropylene shows a single peak at 157.6°C. This peak indicates the melting temperature of the composite. Generally, most of the composites tested shows similar melting temperature with neat polypropylene. Melting temperature and the degradation temperature obtained from TGA is important in helping determine the suitable processing temperature during injection moulding. The temperature employed must be

above the melting temperature of the composite but not so high as to cause the material to degrade inside the barrel. Several studies have also found that fibre content does not significantly affect the melting temperature of the composites [71]. However, fillers such as carbon nanotube that would change the crystal structure (for example, α crystal to β crystal) of the matrix would cause the T_m to change accordingly [72].

4.2.1 The effect of total V_f

Melting behaviour

In general, the introduction of the reinforcing fibres did not significantly alter the melting temperature of the composites, as evident in Table 4.3. For AFRC, T_m for the composites at 5, 10 and 20% V_f are 158.9, 157.6 and 157.3°C, respectively. For CFRC, T_m for the composites at 5, 10 and 20% V_f are 159.1, 157.6 and 157.6°C, respectively.

Most of the hybrid composites also showed similar trend as observed above. Refer to Table 4.3. For example, for hybrid composites with 25:75 V:V% fibre proportions, the T_m for composites with total V_f of 5, 10 and 20% are 159.5, 157.4 and 156.0°C, respectively. However, hybrid composite 5(2.50:2.50) showed slightly lower T_m value compared to the other specimens (154.8°C). The reduction in T_m may be due to degradation that might occur when the composites were being processed. The presence of hot spots during processing might cause the polymer chains to degrade and produce polymer chains with lower molecular weight. This will cause the melting temperature to decrease [73].

Both hybrids, 5(3.75:1.25) and 5(1.25:3.75), show higher T_m value at 159.6°C and 159.5°C, respectively. There is no clear cause for the anomaly since there was no discernible trend observed.

ΔH_m is very important because its magnitude is directly proportional to the X_c of the composite. From the data, it was discovered that for AFRC, increasing the fibre content would reduce the ΔH_m of the composite. The enthalpy reduced from 93.0 J/g to 87.3 J/g when the fibre content was increased from 5% to 10%. The value went down further to 55.6 J/g when the fibre content was increased to 20%. It is possible that the presence of aramid fibres inhibits the rearrangement of the polypropylene chain during crystallisation making it more amorphous. Cao *et al.* in their study found that the addition of Kevlar fibres would promote α crystallisation of the polypropylene matrix, especially near the fibre surface [74]. However, it is worth noting that the fibres used in their work were surface treated to improve the interaction between the fibre and the matrix while the aramid fibres employed in our study were used as provided.

On the other hand, initially increasing the amount of carbon fibre increases the ΔH_m of CFRC. However, as the V_f was increased to 20%, ΔH_m decreased. ΔH_m for the composites at 5, 10 and 20% V_f are 72.9, 81.4 and 45.2 J/g, respectively. Tan *et al.* in their study found the presence of carbon fibre content accelerated the crystallisation process of polypropylene [75]. They found that most crystallite would initially appear near the crossing point of fibres. An increase in the amount of fibres would increase the number of crossing points, which would explain the initial increase in crystallinity.

Table 4.3: Thermal properties from DSC for all composites

Specimen	T_m (°C)	ΔH_m (J/g)	X_c (%)	T_c (°C)	ΔH_c (J/g)
5(5.00:0.00)	158.9	93.0	44.5	120.5	103.0
5(3.75:1.25)	159.6	103.6	49.6	120.6	101.4
5(2.50:2.50)	154.8	90.0	43.1.	114.8	95.9
5(1.25:3.75)	159.5	82.9	31.7	120.9	101.1
5(0.00:5.00)	159.1	72.9	38.4	125.6	103.0
10(10.00:0.00)	157.6	87.3	41.8	128.0	92.2
10(7.50:2.50)	157.9	71.4	34.1	127.9	102.7
10(5.00:5.00)	157.8	86.7	41.5	127.8	105.1
10(2.50:7.50)	157.4	80.3	38.4	127.7	104.6
10(0.00:10.00)	157.6	81.4	47.2	116.0	92.2
20(20.00:0.00)	157.3	55.6	26.6	121.0	95.5
20(15.00:5.00)	157.1	55.7	26.7	116.6	84.5
20(10.00:10.00)	157.3	65.8	31.5	119.7	92.5
20(5.00:15.00)	156.0	67.8	32.4	117.4	94.5
20(0.00:20.00)	157.6	45.2	32.0	116.6	95.5

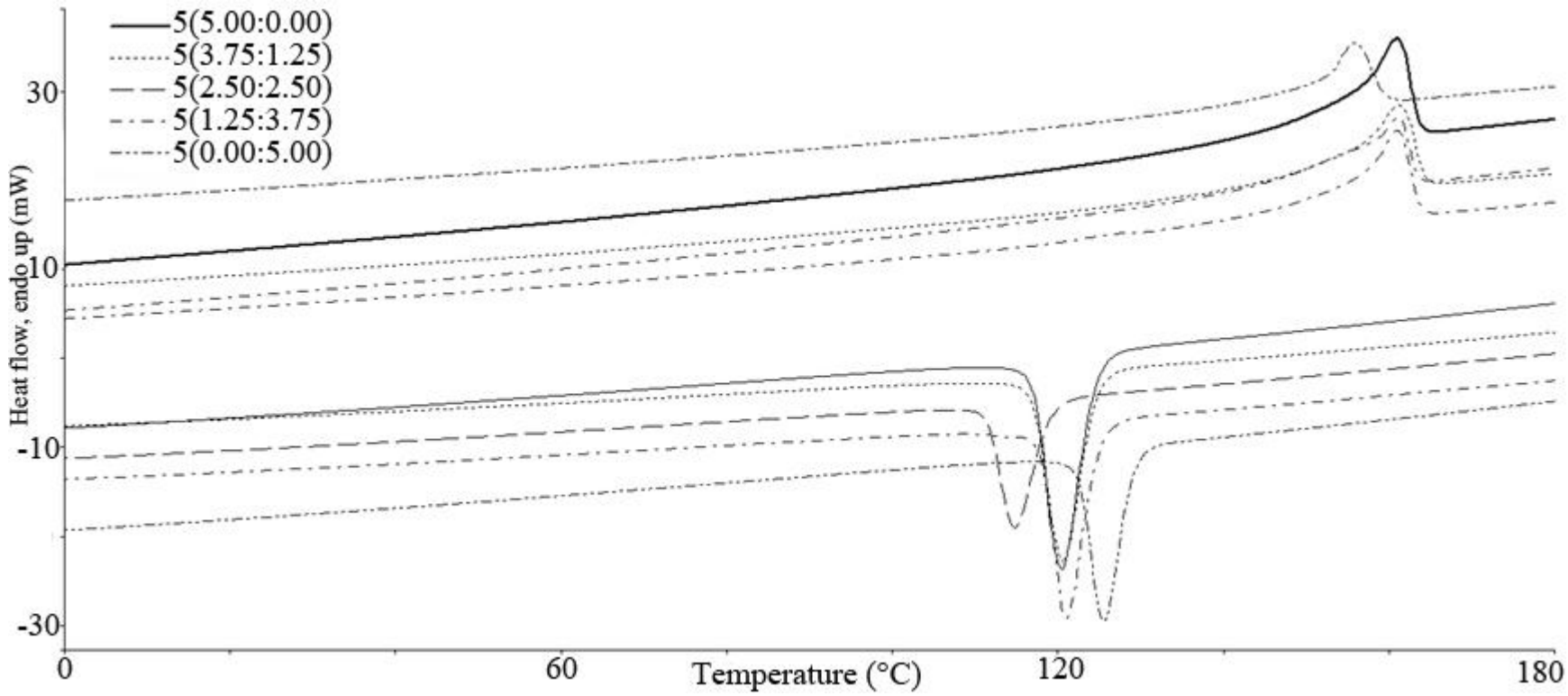

Figure 4.6: DSC curves of composites with 5% total V_f at different fibre proportion

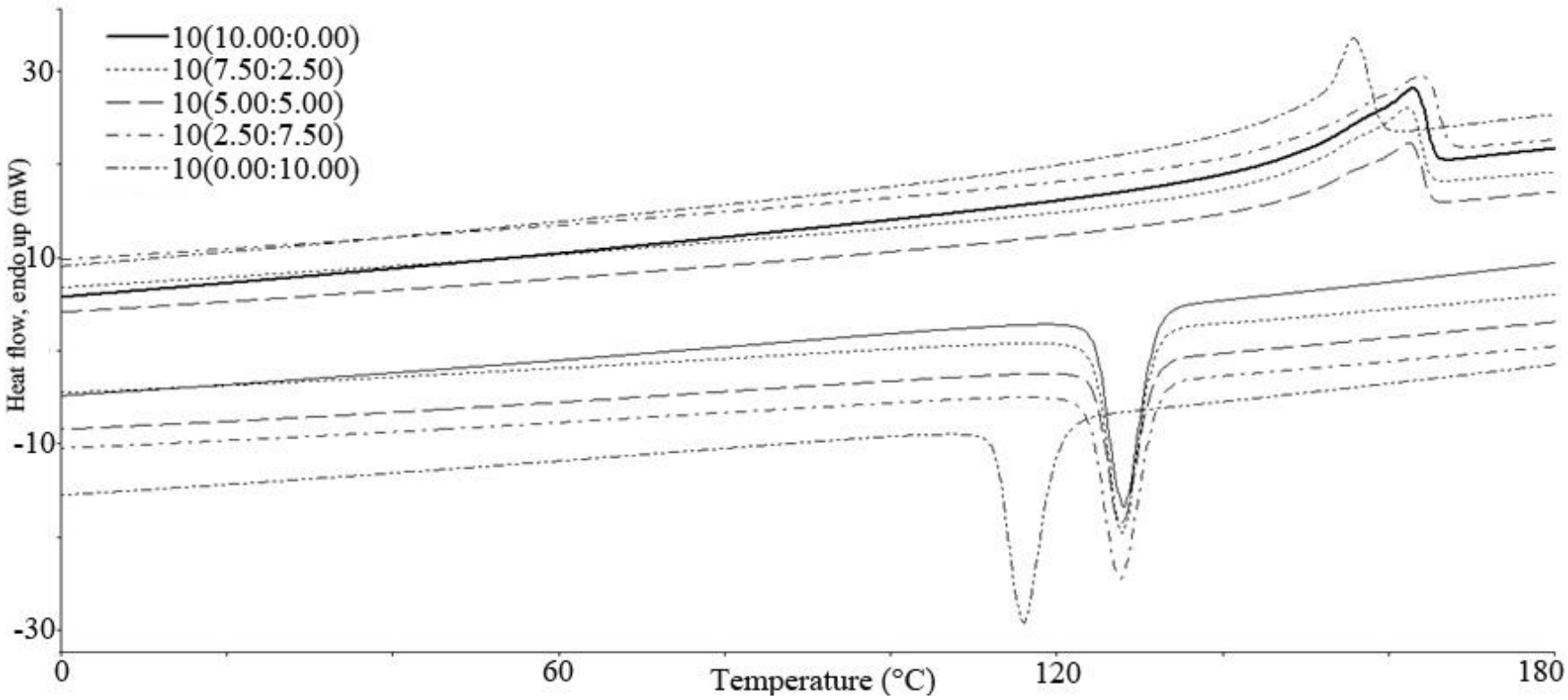

Figure 4.7: DSC curves of composites with 10% total V_f at different fibre proportion

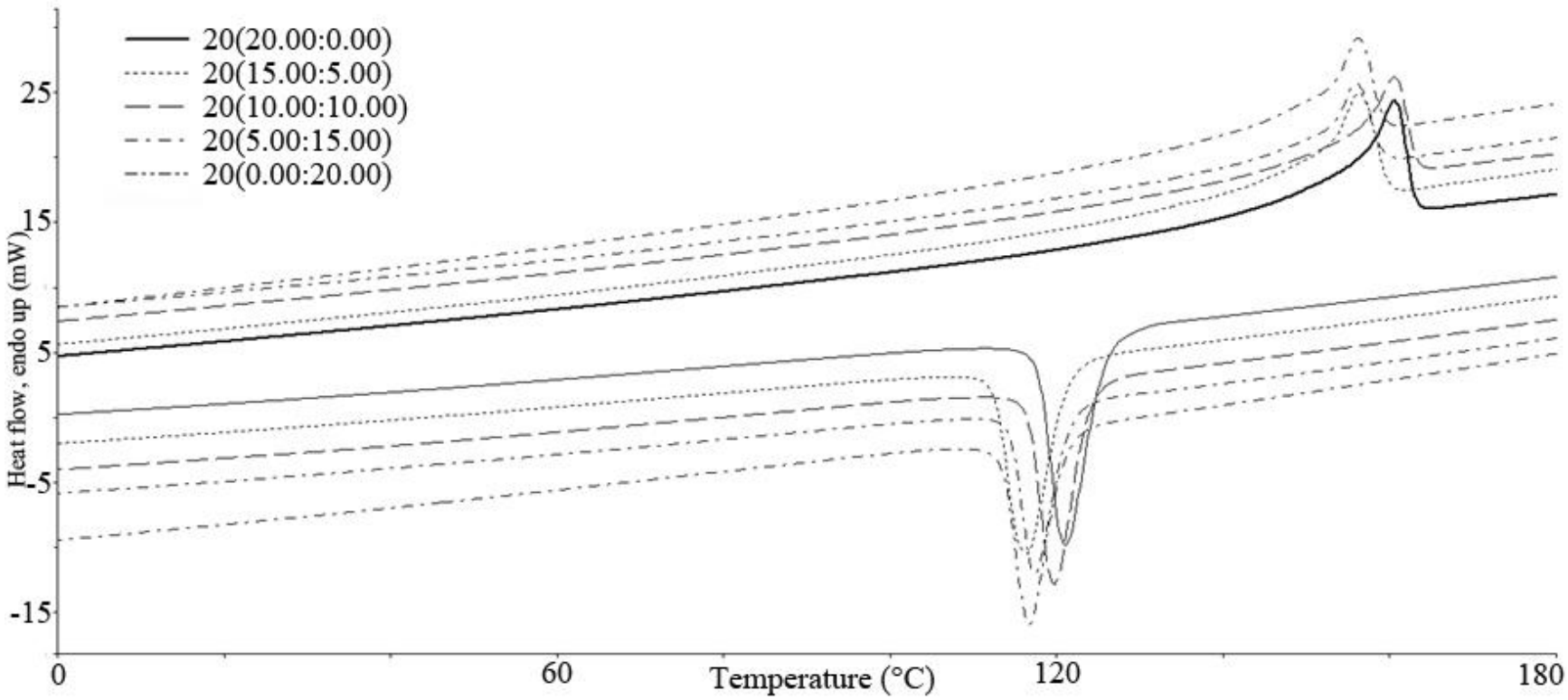

Figure 4.8: DSC curves of composites with 20% total V_f at different fibre proportion

For the hybrid composites, increasing the total V_f decreases the ΔH_m values (provided in Table 4.3). For hybrid composites with 75:25 V:V% fibre proportions, ΔH_m for the composites with total V_f 5, 10 and 20% are 103.6, 71.4 and 55.7 J/g, respectively. Similar trend was observed for hybrid composite with 50:50 V:V% and 25:75 V:V% fibre proportion. For hybrid composites with 50:50 V:V% fibre proportions, ΔH_m for the composites with total V_f 5, 10 and 20% are 90.0, 86.7 and 65.8 J/g, respectively. For hybrid composites with 25:75 V:V% fibre proportions, ΔH_m for the composites with total V_f 5, 10 and 20% are 82.9, 80.3 and 67.8 J/g, respectively.

Crystallisation behaviour

From Table 4.3, it was found that the degree of crystallinity (X_c) of AFRC would decrease with increasing fibre content. X_c for AFRC decreases from 44.5% to 41.8% as V_f increases from 5% to 10% and decreased further to 26.6% as V_f increased to 20%. Increasing the amount of aramid fibres in the composite system hinders the rearrangement of the polymers crystals, hence causing X_c to decrease. For CFRC, a mixed effect was observed. X_c increases from 38.4% to 47.2% when carbon fibre content was increased from 5% to 10%. When the fibre content was further increased to 20%, X_c reduced to 32.0%. Tan *et. al*. reported that increasing the amount of carbon fibre in the composite would increase the rate of crystallisation [76]. The researchers found that the nucleation of polypropylene started at the crossing point of two or more carbon fibres. However, at 20% fibre loading, the hindrance by the high amount of fibre could have caused crystallinity to be reduced.

For the hybrids, mixed effect was observed. For hybrid composites with 75:25 and 50:50 V:V% fibre proportions, X_c would decrease with increasing total V_f. X_c for hybrids

with 75:25 V:V% at 5, 10 and 20% total V_f are 49.6, 34.1 and 26.7%, respectively. For hybrids with 50:50 V:V% fibre composition, X_c for hybrids with total V_f 5, 10 and 20% are 43.1, 41.5 and 31.5%, respectively. However, hybrid composites with 25:75 V:V % fibre proportions exhibits a different trend. X_c would initially increase, from 31.7% to 38.4%, as total V_f increases from 5 to 10%. As the total V_f was increased to 20%, X_c decreased to 32.4%. The mixed effect could be due to the contrasting effect of aramid and carbon fibres on the crystalisation behaviour of the matrix. Nayak *et. al.* investigated the influence of bamboo/glass fibre on the thermal properties of polypropylene hybrid composites [69]. The researchers found that the addition of fibres increased X_c due to the formation of nucleation sites on the fibres.

4.2.2 The effect of fibre proportions

Varying the fibre proportions did not show any clear effect with respect to T_m, ΔH_m and X_c of the composites. T_m, ΔH_m and X_c values are provided in Table 4.3. No clear trend was observed. It can be inferred that the properties mentioned in the above statement are more sensitive towards the total V_f rather than the fibre proportions. However, improvement on the interfacial interaction between the fibre and the matrix could change this. It has been reported that improvement on the fibre-matrix interaction cause the fibres to have significant effect on the crystallisation behaviour of polypropylene [74].

In conclusion, the hybridisation of the fibres did not produce any significant effect on the melting temperature of the composite. This could be an advantage since that the hybrid can be processed using similar temperature as the single fibre composites.

4.3 Dynamic mechanical analysis (DMA)

Dynamic mechanical analysis is a technique used to study material viscoelastic properties. It is most useful for studying the viscoelastic properties of plastics and its composites. Researchers have harnessed the technique to evaluate material properties such the glass transition temperature (T_g), cross-linking effect, fatigue and other time-dependent properties [77-81]. The results presented here are the tan δ and storage modulus against temperature. The effect of fibre loading and hybridisation were investigated.

Figures 4.9 - 4.11 show the variation of tan δ of the composite as a function of temperature at different total fibre content. The curves were shifted vertically for clarity. Tan δ is expressed as the ratio of loss modulus to the storage modulus. Over the temperature range tested, only one clear transition region, indicated by a single damping maxima, was recorded. The temperature at which this peak is observed is generally known as the glass transition temperature (T_g). A material would behave glass-like (brittle) below T_g and rubber-like (ductile) above the threshold. As a simple guideline, materials with higher T_g will be more brittle at room temperature. The glass transition temperature data measured through dynamic mechanical analysis allows intelligent decisions to be made concerning the maximum use temperatures for composite [82]. Important information from the curves are recorded in Table 4.4.

McCrum *et al.* reported that the tan δ spectrum of pure PP shows three relaxation peaks at −80 °C (γ), 8 °C (β) and 100 °C (α) [83]. The γ peak is considered to be associated with the relaxation of small chain groups like methyl and methylene. The dominant β-relaxation is assigned to the T_g. The small α-relaxation peak can be attributed to lamellar slip.

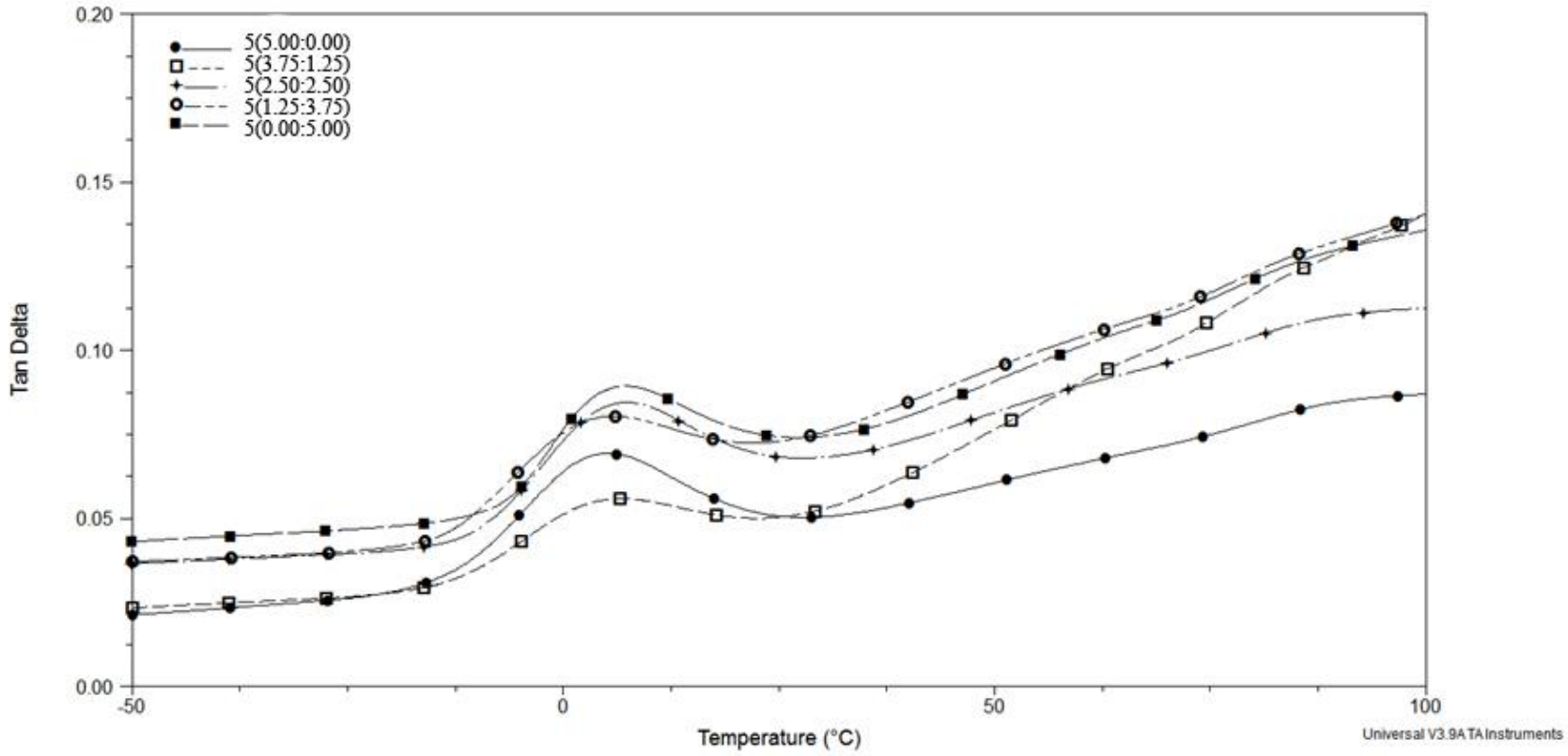

Figure 4.9: Tan delta-temperature behaviour for composites with 5% total V_f at different fibre proportions

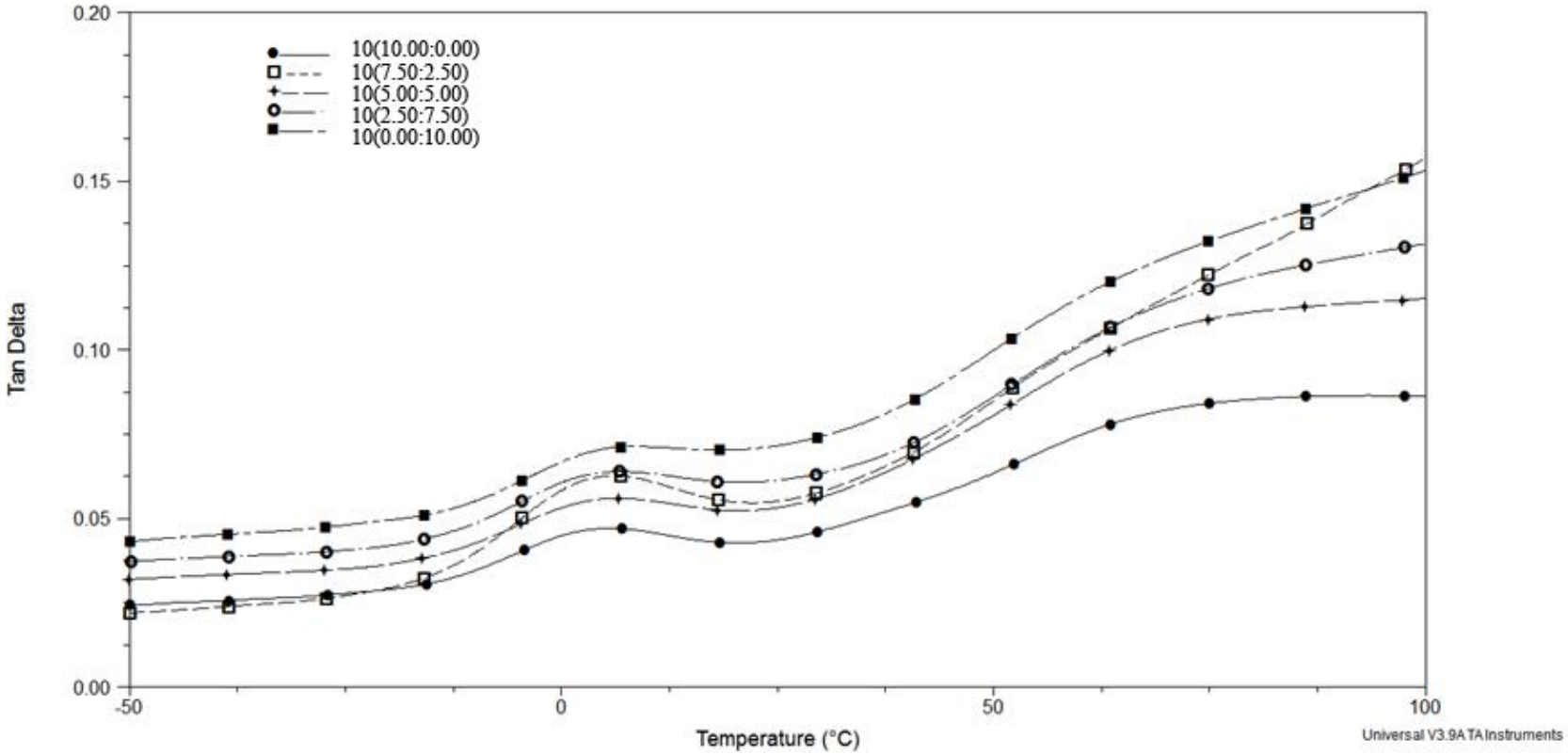

Figure 4.10: Tan delta-temperature behaviour for composites with 10% total V_f at different fibre proportions

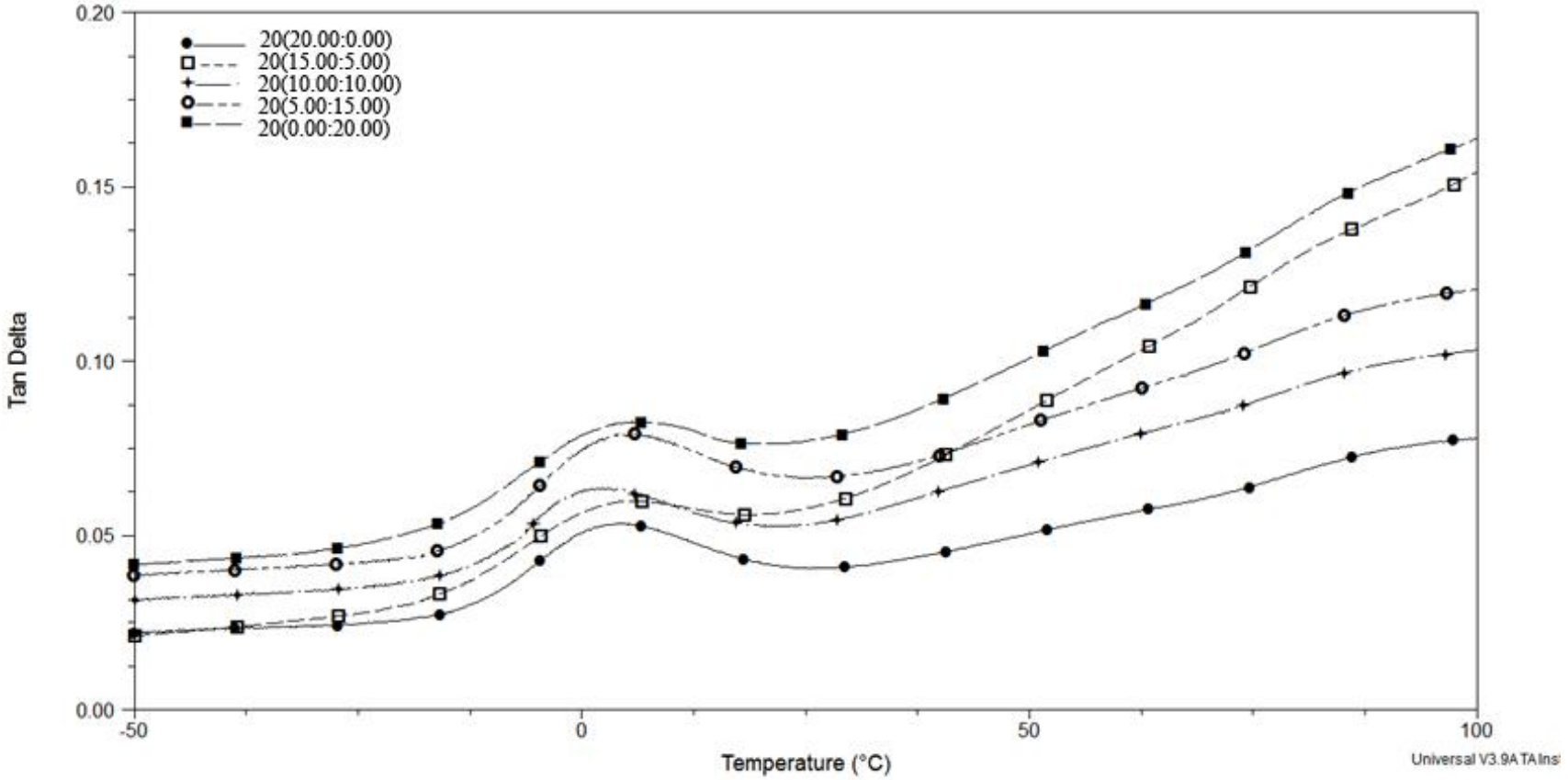

Figure 4.11: Tan delta-temperature behaviour for composites with 20% total V_f at different fibre proportions

Table 4.4: Thermomechanical data for all composites

Specimen	At 25°C			Tan δ_{max} ($x10^{-2}$)	T_g (°C)
	E' (GPa)	E" (MPa)	Tan δ ($x10^{-2}$)		
5(5.00:0.00)	2.3	108.2	4.8	5.2	6.1
5(3.75:1.25)	2.2	121.8	5.6	7.2	7.1
5(2.50:2.50)	2.5	135.3	5.4	6.2	5.2
5(1.25:3.75)	3.0	150.1	4.9	6.4	7.1
5(0.00:5.00)	4.0	176.8	4.4	5.0	6.6
10(10.00:0.00)	2.8	121.7	4.4	4.7	5.4
10(7.50:2.50)	3.4	139.7	4.1	4.4	6.2
10(5.00:5.00)	4.0	171.4	4.3	4.5	5.8
10(2.50:7.50)	4.6	214.4	4.7	4.6	7.3
10(0.00:10.00)	4.5	218.4	4.9	5.7	5.5
20(20.00:0.00)	4.2	169.9	4.1	5.3	4.7
20(15.00:5.00)	5.3	217.5	4.1	5.1	3.0
20(10.00:10.00)	5.5	264.5	4.8	6.0	4.3
20(5.00:15.00)	6.7	350.0	5.2	5.7	6.4
20(0.00:20.00)	8.9	456.9	5.2	5.3	5.8

4.3.1 The effect of total V_f

Glass transition temperature, T_g

For AFRC, T_g of the composites decreased with increasing aramid fibre content. T_g decreases from 6.1 °C to 5.4 °C and 4.7 °C as V_f was increased from 5% to 10% and 20%, respectively. Lower T_g may indicate that the amorphous region in the composite is more mobile. For CFRC, T_g decreases from 6.6 °C to 5.5 °C when the fibre content was increased from 5% to 10%. However, when the carbon content was further increased to 20%, the T_g rose slightly to 5.8 °C. For hybrid composites, the same trend was also observed. For example, T_g for hybrid with 75:25 V:V% at 5, 10 and 20% total V_f are 7.1 °C, 6.2 °C and 3.0 °C, respectively.

Storage modulus, E'

Storage modulus (E') values at 25 °C was also recorded. It is of interest due to the fact that most of the mechanical tests done to the specimens were done at room temperature. Figures 4.12 – 4.14 show the storage modulus curve of the composite as a function of temperature. The values at 25 °C are recorded in Table 4.4. Storage modulus is closely related to the load bearing capacity of a material and is linked to the flexural modulus. It is a measure of the energy stored in the material during a cycle and describes the elastic character or the solid-like nature of the material.

For AFRC, E'_{25} increases with increasing aramid content, from 2.3 GPa to 2.8 GPa and 4.2 GPa, when fibre loading was increased from 5% to 10% and 20%, respectively. This indicates that energy absorption increased with increasing fibre content. The storage

modulus always increase with addition of stiff fillers [84]. An even higher value can be obtained with aramid fibres which were surface treated.

For CFRC, similar trend was observed. E'_{25} increased from 4.0 GPa to 4.5 GPa and 8.9 GPa, as the carbon content increased from 5% to 10% and 20%, respectively. It can be seen that carbon fibre is stiffer than aramid fibre, hence the storage modulus for composites reinforced with carbon fibre is higher when compared to its counterpart.

For hybrid composite, increasing the total fibre content would result in the same trend as observed previously. For example, E' values for hybrid composite with fibre proportion 75:25 V:V% at 5, 10 and 20% V_f are 2.2 GPa, 3.4 GPa and 5.3 GPa, respectively.

Loss modulus, E"

Loss modulus is also referred as the imaginary (out-of-phase) modulus and is a measure of the viscous character or liquid-like nature of the material. It relates to the ability of the material to dissipate energy. Values for E''_{25} are provided in Table 4.4.

Increasing the fibre content in AFRC causes the $E"_{25}$ value to increase. $E"_{25}$ increases from 108.2 MPa to 121.7 MPa and 169.9 MPa as V_f was increased from 5% to 10% and 20%, respectively. For CFRC, similar trend was observed. $E"_{25}$ increases from 176.8 MPa to 218.4 MPa and 456.9 MPa as V_f was increased from 5% to 10% and 20%, respectively.

For the hybrid fibre composite, increasing V_f will increase the magnitude of $E"_{25}$. For example, $E"_{25}$ values for hybrid fibre composite with 50:50 V:V% fibre proportion at 5,

10 and 20% total V_f are 135.3 MPa, 171.4 MPa and 264.5 MPa. At a glance, it can be concluded that increasing the amount of fibre in the composite would improve the energy dissipation in the system.

Tan delta, tan δ

Tan δ, a mechanical loss factor, is the ratio of the loss modulus to the storage modulus. It represents the ratio of energy dissipated to energy stored per cycle of deformation and indicates the damping characteristics of the material.Values of tan δ at 25 °C were recorded in Table 4.4.

Increasing the fibre content in AFRC causes the tan δ_{25} value to decrease. Tan δ_{25} decreases from 4.8 to 4.4 and 4.1 as V_f was increased from 5% to 10% and 20%, respectively. For CFRC, the opposite was observed. Tan δ_{25} increases from 4.4 to 4.9 and 5.9 as V_f was increased from 5% to 10% and 20%, respectively.

For the hybrid fibre composite, mixed effect was observed. Hybrid fibre composite with 75:25 V:V% fibre proportions exhibit decreasing tan δ_{25} with increasing fibre content. Increasing the fibre content from 5% to 10% would cause the tan δ_{25} values to decrease from 5.6 to 4.1. However, increasing the V_f further to 20% did not change the tan δ_{25} values. Hybrid fibre composites with 50:50 and 25:75 V:V% showed similar trend. Increasing V_f from 5% to 10% would cause the tan δ_{25} to decrease. When V_f is further increased to 20%, tan δ_{25} value increased. For example, the tan δ_{25} values for hybrid composite with 25:75 V:V% at 5, 10 and 20% V_f are 4.9, 4.7 and 5.2, respectively.

4.3.2 The effect of fibre proportion

Storage modulus, E'

When materials with similar V_f were compared alongside, composites reinforced with carbon fibres tends to have higher T_g than composites reinforced with aramid fibres. For example, E' for CFRC at 10% V_f is 4.5 GPa while for AFRC the value is 2.8 GPa. This indicates that at room temperature, carbon reinforced composite is more brittle than aramid reinforced composites.

It was found that E'_{25} would increase with increasing amount of carbon fibre in the composite. From Table 4.4, it can be observed that the E'_{25} for 10(7.50:2.50), 10(5.00:5.00) and 10(2.50:7.50) (ascending carbon fibre content) are 3.4 GPa, 4.0 GPa and 4.6 GPa, respectively. Similar trend was observed in composites with 5% and 20% total V_f. It can be concluded that increasing the ratio of carbon fibre in the composite would increase the stiffness hence higher E'_{25}.

Loss modulus, E"

The effect of fibre proportions on the loss modulus of the composites are similar to the effect observed in storage modulus. Increasing the amount of carbon fibre in the composite would increase $E"_{25}$. For example, $E"_{25}$ values for composite with 20% total V_f are 169.9 MPa (20(20.00:0.00)), 217.5 MPa (20(15.00:5.00)), 264.5 MPa (20(10.00:10.00)), 350.5 MPa (20(5.00:15.00)) and 456.9 MPa (20(0.00:20.00)). Similar trend was observed for composites with total V_f 5% and 10%. From these observations, it could be deduced that increasing the amount of carbon fibre in the hybrid composite improves its energy dissipation, hence higher loss modulus values.

There were no discernable trends regarding the effect of fibre proportions in the hybrid composite towards T_g and tan δ.

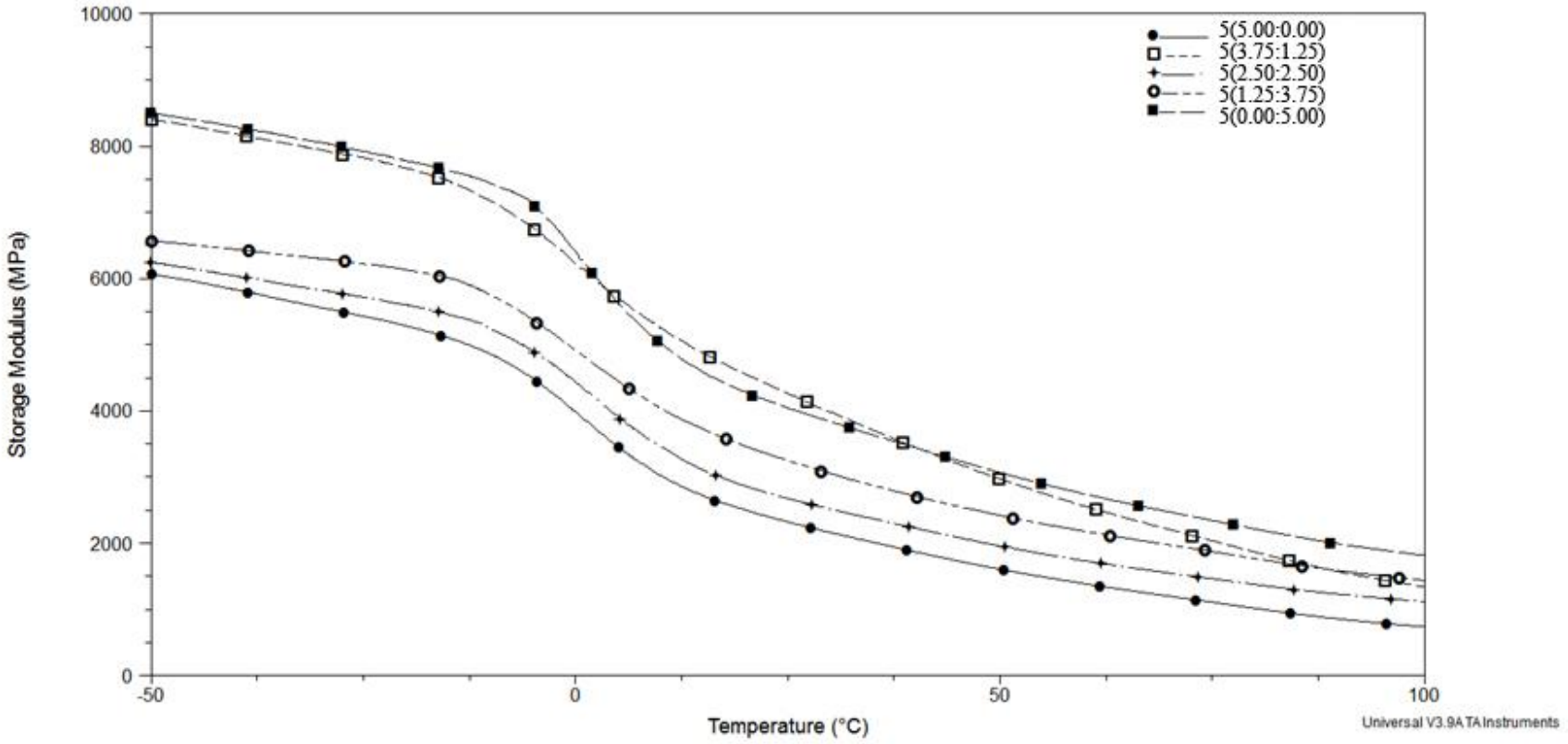

Figure 4.12: Storage modulus-temperature behaviour for composites with 5% total V_f at different fibre proportions

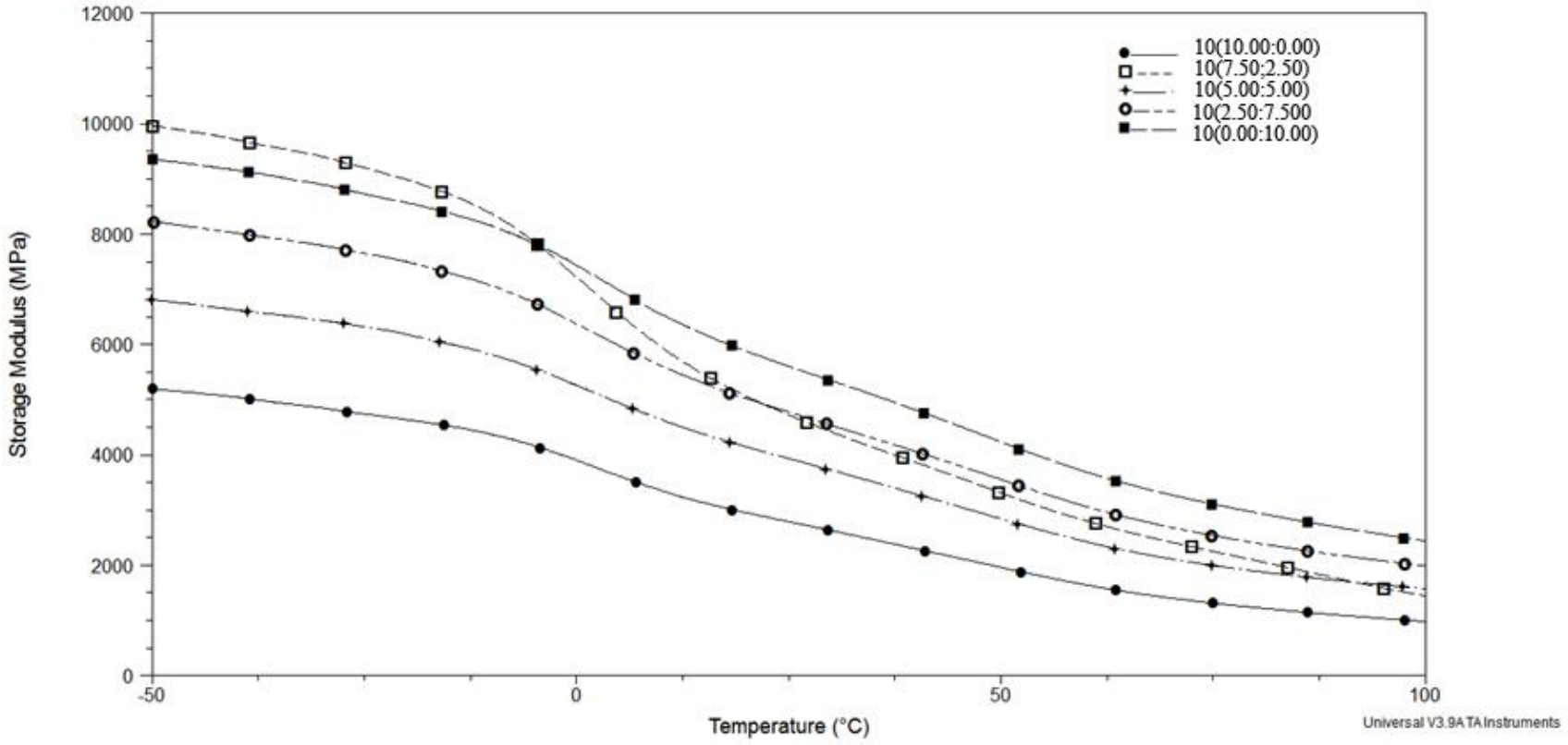

Figure 4.13: Storage modulus-temperature behaviour for composites with 10% total V_f at different fibre proportions

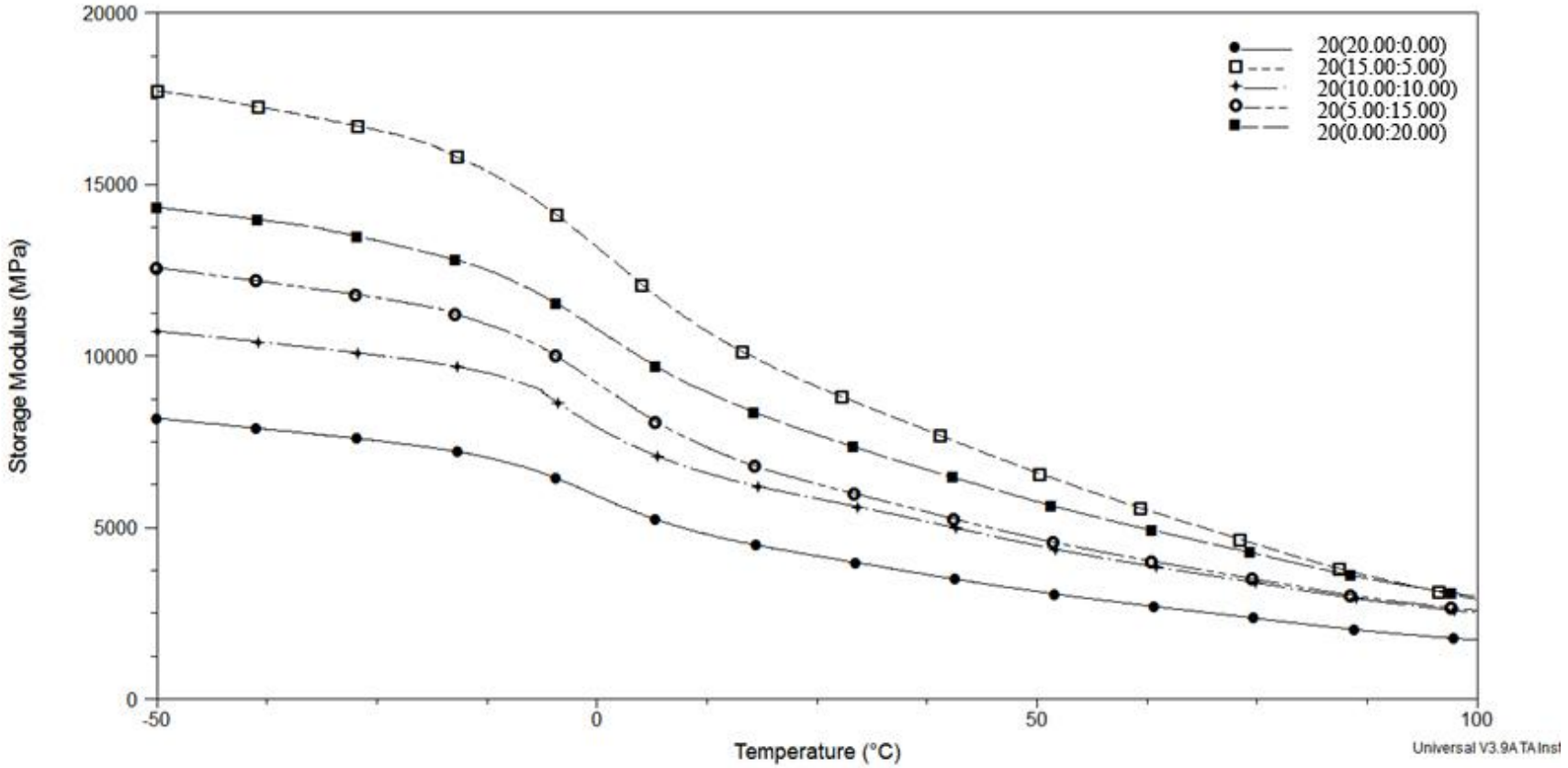

Figure 4.14: Storage modulus-temperature behaviour for composites with 20% total V_f at different fibre proportions

4.4 Tensile properties

Mechanical properties of a material are heavily influenced by both the tensile properties of the reinforcement fibres and the properties of the matrix. Depending on the intended application, reinforcing fibres are added to plastics to improve their mechanical properties. Plastic composite has the advantage of lower weight and production cost when compared to traditional materials such as steel. In this study, the effect of fibre volume fraction (V_f) and hybridisation on the tensile properties was studied. The Young's modulus, tensile strength and tensile strain of the composites are provided in Table 4.5.

4.4.1 The effect of total V_f

Young's Modulus, E

To better illustrate the effect of V_f on the tensile properties of the composite, histogram of Young's modulus, tensile strength and tensile strain against the V_f of the composites are provided in Figure 4.15 - 4.17. From the figures, it can be derived that for all the composites, increasing the total V_f would increase the modulus. Young's modulus for the AFRC increased from 3.26 GPa to 3.48 GPa as the fibre loading was increased from 5% to 10%. The modulus further increased to 3.93 GPa as the fibre loading was further increased to 20%. For CFRC, the modulus increased from 3.03 GPa to 3.63 GPa as the fibre loading was increased from 5% to 10%. The modulus further increased to 4.65 GPa as the fibre loading was further increased to 20%. For hybrid fibre composite with 50:50 V:V% fibre proportion, modulus increased from 2.98 GPa to 3.67 GPa as the total volume fraction was increased from 5% to 10%. When the total V_f was increased further to 20%, the modulus

increased to 4.38 GPa. CFRC with 20% V_f exhibit the highest modulus (4.65 GPa). Tensile properties of the composites are provided in Table 4.5.

Table 4.5: Tensile properties for all composites

Specimen	Young's modulus (GPa)	Tensile strength (MPa)	Tensile strain (%)
5(5.00:0.00)	3.26	38.51	7.71
5(3.75:1.25)	3.11	35.47	8.69
5(2.50/2.50)	2.98	32.19	8.96
5(1.25/3.75)	3.08	34.09	8.42
5(0.00/5.00)	3.03	34.43	7.71
10(10.00:0.00)	3.48	43.33	6.71
10(7.50:2.50)	3.63	37.82	6.67
10(5.00:5.00)	3.67	35.00	6.49
10(2.50:7.50)	3.44	33.06	6.20
10(0.00:10.00)	3.63	30.84	7.00
20(20.00:0.00)	4.65	30.56	5.42
20(15.00:5.00)	4.82	48.04	4.55
20(10.00:10.00)	4.38	40.38	5.75
20(5.00:15.00)	4.53	32.87	5.46
20(0.00:20.00)	3.93	50.53	5.17

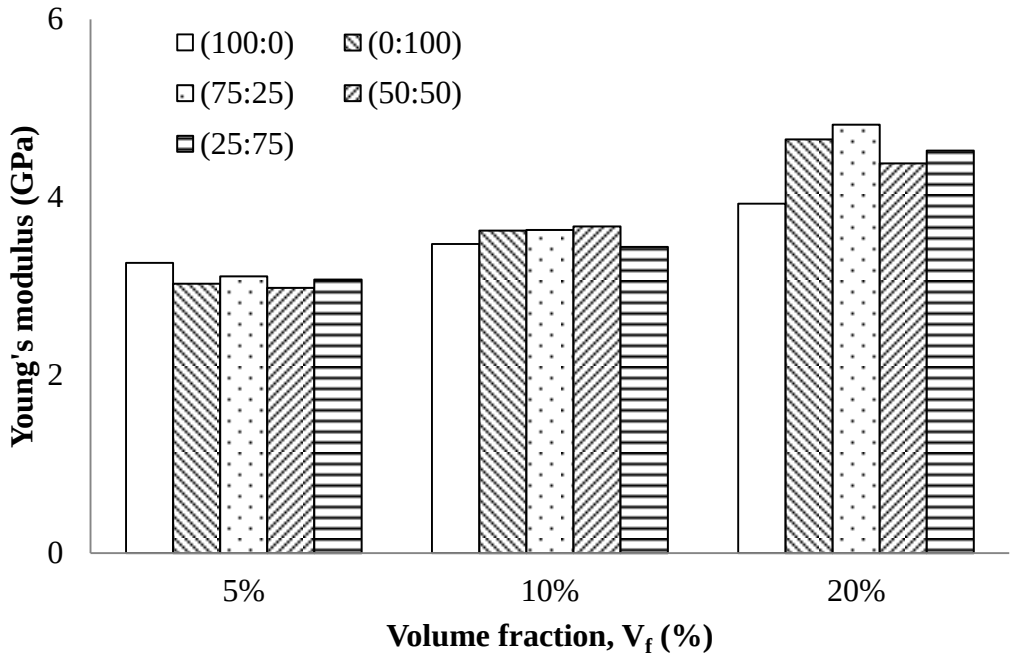

Figure 4.15: Young's modulus of all composite at different total V_f

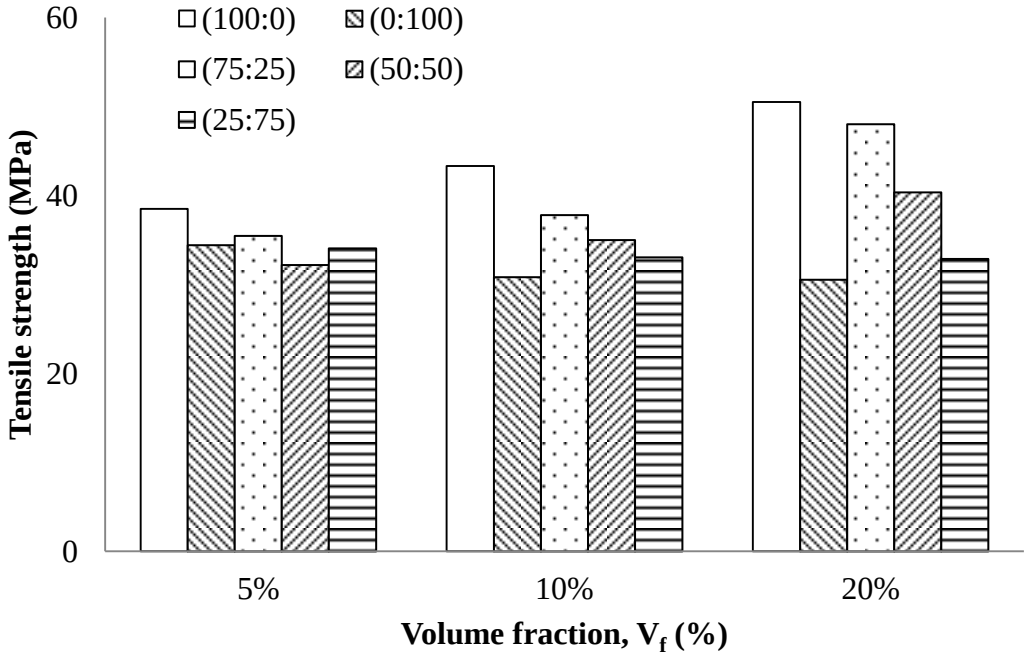

Figure 4.16: Tensile strength of all composites at different total V_f

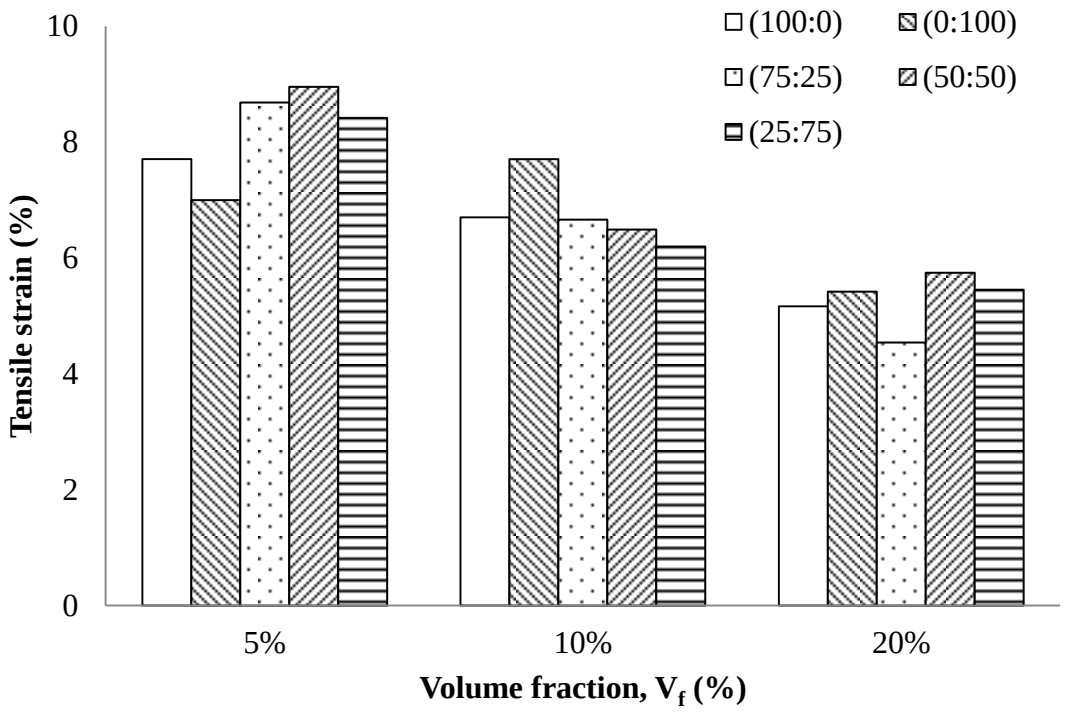

Figure 4.17: Tensile strain of all composites at different total V_f

The main factors affecting the Young's modulus are the fibre content, stiffness and orientation, and matrix stiffness [85]. Thomason and Vlug have reported similar trends in glass reinforced polypropylene [86]. The researchers found that the modulus of the composite would increase when the fibre concentration was increased. Further increasing the fibre concentration beyond the optimal level (40% w/w) would negatively impact the modulus of the material by introducing voids and undispersed fibre bundles which could act as stress concentrators.

Tensile strength

The tensile strength for AFRC decreases with increasing fibre content. The tensile strength for aramid reinforced composite with 5%, 10% and 20% V_f are 38.51, 43.33 MPa and 30.56 MPa, respectively. Arroyo *et. al.* reported that addition of aramid fibres increases the modulus but decreases the tensile strength of the composite [87]. The researchers suggested that a good contact between the fibres and the matrix exists due to a strong mechanical adhesion created by the different expansion coefficients of both materials. However, once the material starts to flow in a tensile test, the fibres begin to slide smoothly at the interface due to an increment of the temperature caused by the interfacial shear. So, a great effort is needed to unstick the fibres from the matrix, but once the fibres are debonded, they slide very smooth at the interface giving rise to voids in the polymer matrix which in turn decreases the tensile strength and elongation at break in the presence of aramid fibres.

For CFRC, the tensile strength increases with increasing fibre content. The tensile strength for CFRC at 5%, 10% and 20% V_f are 34.43, 30.84 and 50.53 MPa, respectively. The increase in tensile strength is due to the reinforcement effect by the fibres. Similar observation was reported by Fu *et. al*. [43]. For hybrid composite, two different trends were observed. For hybrid with fibre proportion of 75:25 and 50:50 V:V%, the tensile strength increases with increasing total fibre volume fraction. For example, the tensile strength for hybrid fibre composite with 75:25 V:V% fibre proportion at 5%, 10% and 20% V_f are 35.5, 37.8 and 48.0 MPa, respectively. However, for hybrid with 25:75 V:V% fibre proportion, the tensile strength was not significantly affected by V_f. The tensile strength for hybrid fibre composite with 25:75 V:V% fibre proportion at 5%, 10% and 20% V_f are 34.1, 33.1 and 32.9 MPa, respectively. AFRC with 20% V_f exhibit the highest strength (50.53 MPa).

The modulus of carbon fibre is comparatively higher than that of the aramid fibre, whereas the extensibility of carbon is low compared to the aramid fibre. This results in an early carbon fibre failure which transfers a high stress to the aramid fibres. A sufficient amount of aramid fibre needs to be present in the composite for it to successfully withstand the sudden stress transfer. Without sufficient fibres, the aramid fibres will fail almost at the same time of the carbon fibre, hence no improvement to the tensile strength of the composite. This is the reason why the hybrid composite with 75:25 and 50:50 V:V% fibre proportion showed improvement in tensile strength while hybrid with 25:75 V:V% fibre proportion did not.

In another study by Thomason *et al.*, they found that the tensile strength of polypropylene laminates increases with increase in fibre content up to 60% w/w [88]. Another important factor which affects the tensile strength of a composite is the compatibility between the fibre sizing and the matrix. Excellent compatibility between these two components would produce strong interfacial adhesion. The interfacial interaction is very important because it determines the efficiency of load transfer from the matrix to the fibres [88].

Tensile strain

Generally, tensile fracture strain would decrease with increasing fibre content. The fracture strain of AFRC decreases from 7.71% to 6.71% and 5.17% as the fibre content increased from 5% to 10% and 20%, respectively. Similar trend was observed for CFRC and the hybrids. Similar trend was observed in CFRC and the hybrid fibre composites. The fracture strain of CFRC decreases from 7.71% to 7.00% and 5.42% as the fibre content increased from 5% to 10% and 20%, respectively. For hybrid with 25:75 V:V%, the tensile strain

decreases from 8.42% to 6.20% and 5.46% as the fibre content increased from 5% to 10% and 20%, respectively.

The reduction in the fracture strain value is expected. As the modulus of the material increases, it becomes stiffer and less ductile. Stiffer material would resist any changes to its shape, in this case, elongation. The molecular structure needs to be able to rearrange effectively in order to have high fracture strain value. In fibre reinforced composites, the matrix is constrained by the fibres and thus matrix flow is minimal, especially with high fibre content. Increasing the fibre content would increase the constraint on the matrix thus limiting chain mobility [68]. Thomason has reported similar observation in his study of glass fibre reinforced polyamide 6,6. He stated that the fracture strain value of the composite is significantly dependent on the residual fibre length, fibre diameter and fibre concentration [89].

4.4.2 The effect of fibre proportion

Through SEM, the effect of the fibre proportion on the failure mechanism was observed. SEM micrograph of the tensile fracture surface for CFRC is provided in Figure 4.18. It can be seen in the image shows flat fracture surface which indicates that the composite failed in a brittle manner. Materials that fails in brittle mode is very rigid, which explains its high tensile modulus values. However, the crack propagation occurs almost instantly, evident by the lack of plastic deformation observed on the fracture surface. This corresponds to the sudden drop in its stress against strain curve provided by the instrument.

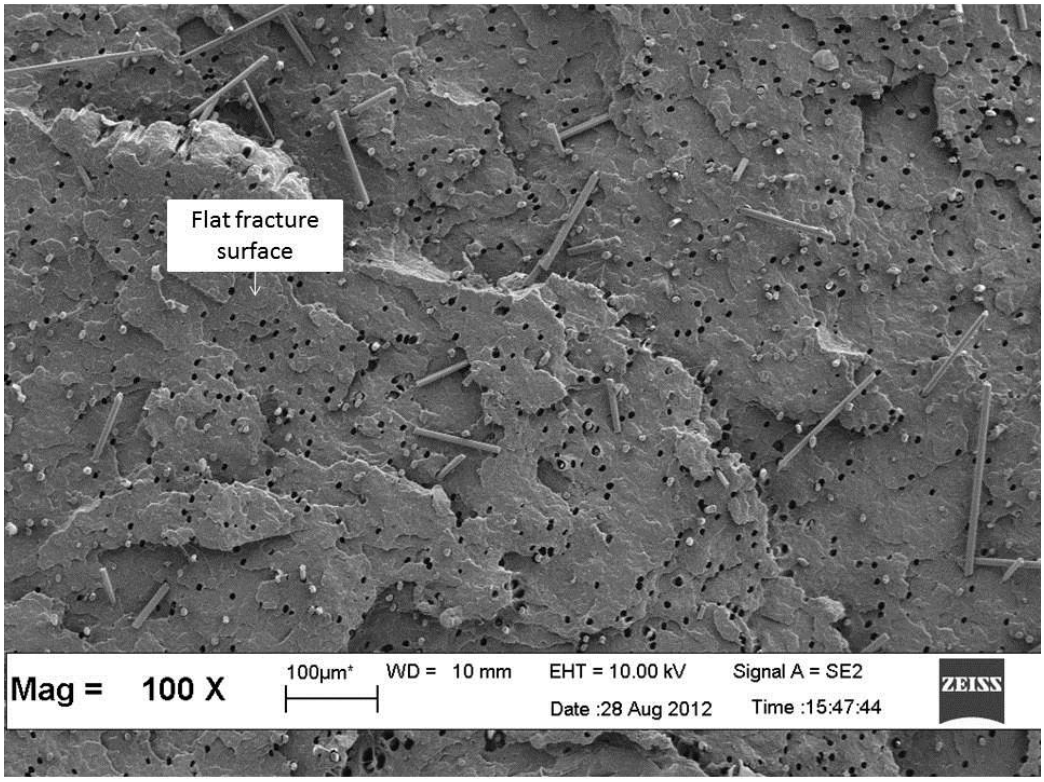

Figure 4.18: Tensile fracture surface for 5(0.00:5.00)

The fracture surface of AFRC and hybrid fibre reinforced composites on the other hand showed a mix of ductile and brittle failure. SEM images of the tensile fracture surface for AFRC and hybrid composite are provided in Figures 4.19 and 4.20. As carbon fibres are replaced by aramid fibres in the composite, the failure mode of the composite was also affected from fully brittle (Figure 4.18) to a mix of brittle and ductile failures (Figures 4.19-4.20). In addition, the differences between the failure mechanisms of the fibres themselves are apparent in the micrograph. Figure 4.21 reveals that both these fibres behave differently during failure. The fracture surface on the ends of the carbon fibre is clean and flat, displaying the classical Griffiths brittle fracture [90]. This type of failure usually occurs in three-dimensionally bonded materials with no yield mechanism. The fibrillar nature of the aramid fibre failure is also clearly observed in this image.

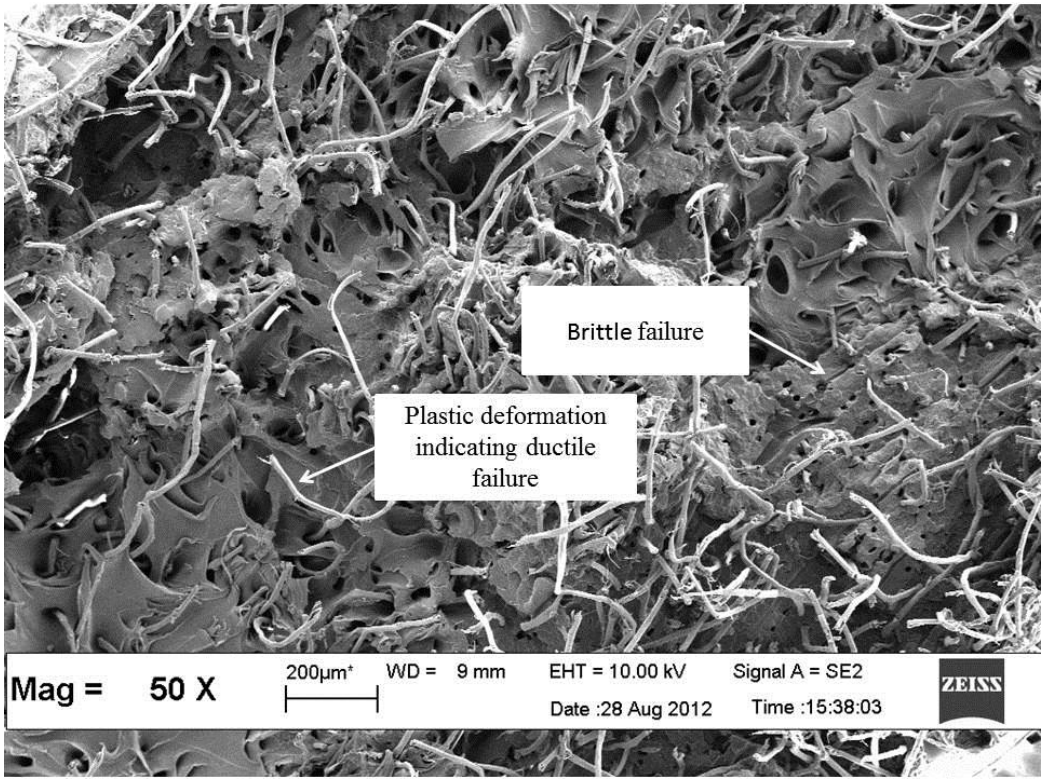

Figure 4.19: Tensile fracture surface for 5(5.00:0.00**)**

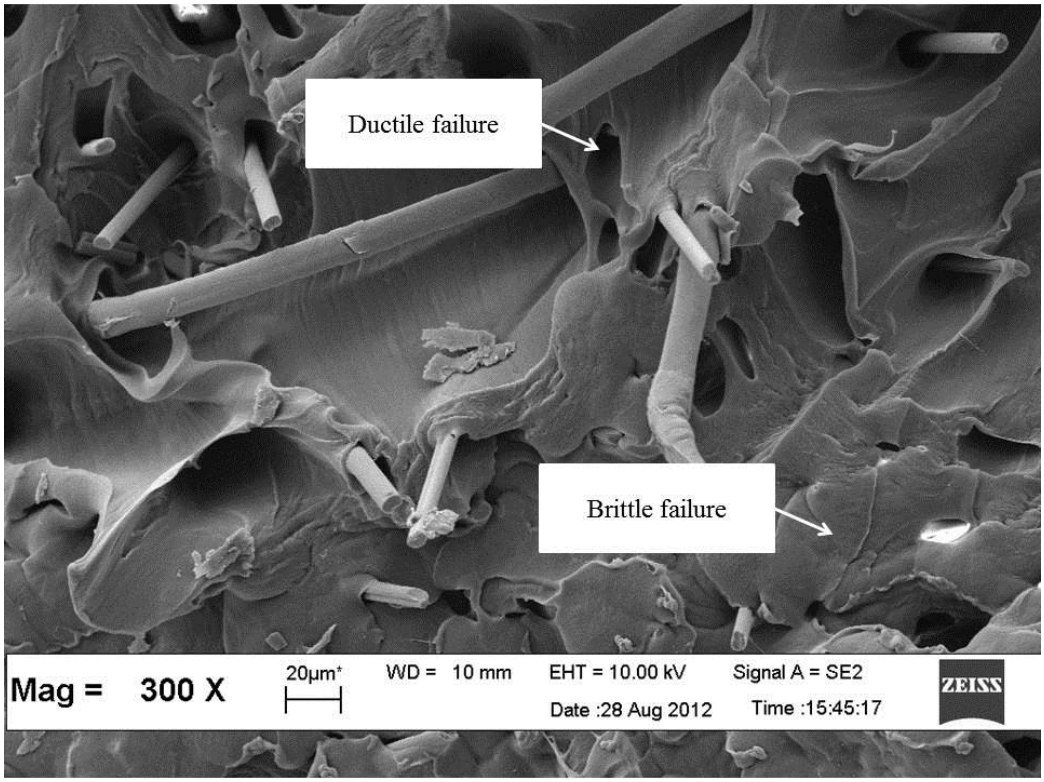

Figure 4.20: Tensile fracture surface for 5(2.50:2.50)

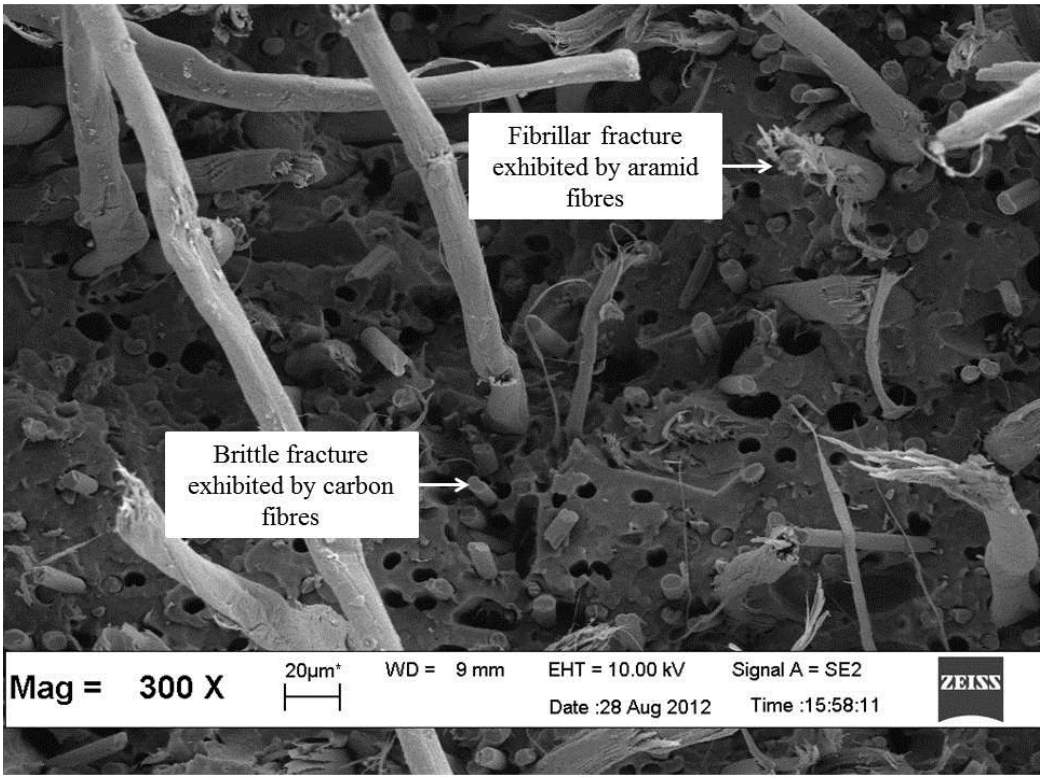

Figure 4.21: Tensile fracture surface of 20(10.00:10.00)

Simple rule of mixture

In order to study the effect of hybridisation, the rule of mixture was employed. The rule of mixture would provide a baseline from which comparisons can be made so that any synergy can be observed. The equation used is as follows:

$$P = P_A V_A + P_B V_B \tag{4.1}$$

where P_A and P_B are the material property of composites reinforced with only A or B fibres while V_A and V_B are the volume fraction of the respective fibres.

There are several assumptions made when employing the simple rule of mixture. The assumptions are:

1. Fibres are uniformly distributed throughout the matrix.
2. Perfect bonding between fibres and matrix.
3. Matrix is free of voids.
4. Applied loads are either parallel or normal to the fibre direction.
5. Lamina is initially in a stress-free state (no residual stresses).
6. Fibre and matrix behave as linearly elastic materials.

The experimental and theoretical values for tensile modulus and tensile strength were plotted in Figures 4.22– 4.24.

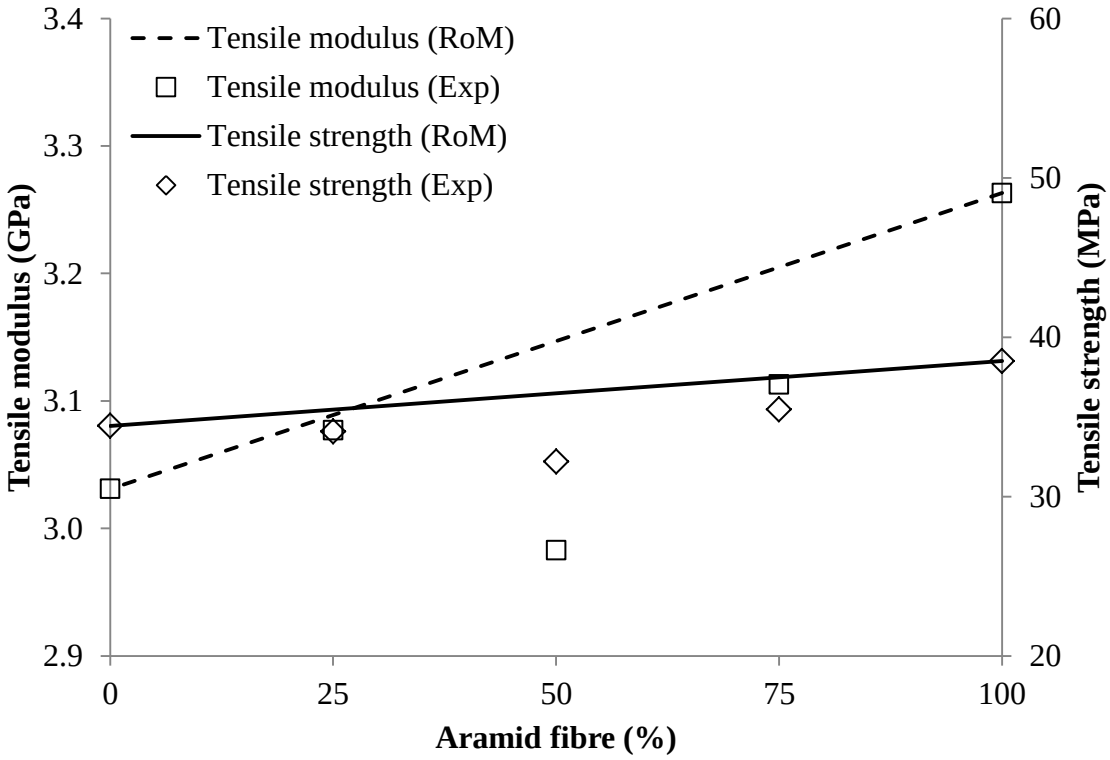

Figure 4.22: Experimental and calculated Young's modulus and tensile strength for composite with 5% total V_f

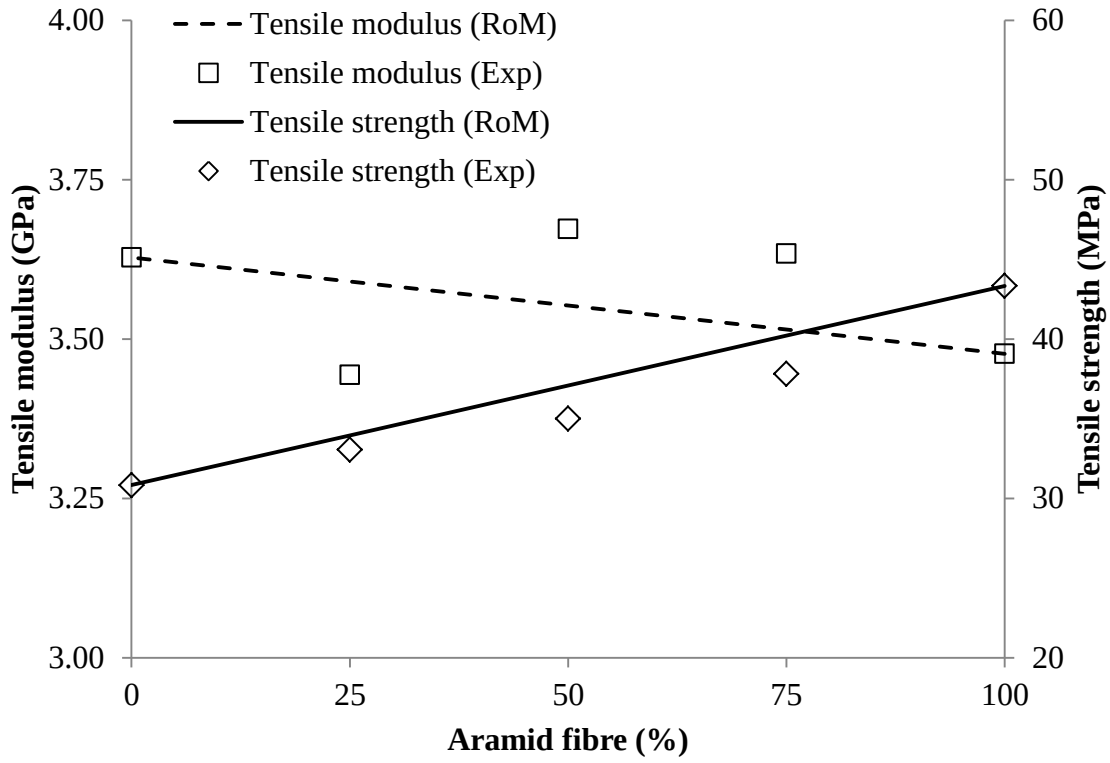

Figure 4.23: Experimental and calculated Young's modulus and tensile strength for composite with 10% total V_f

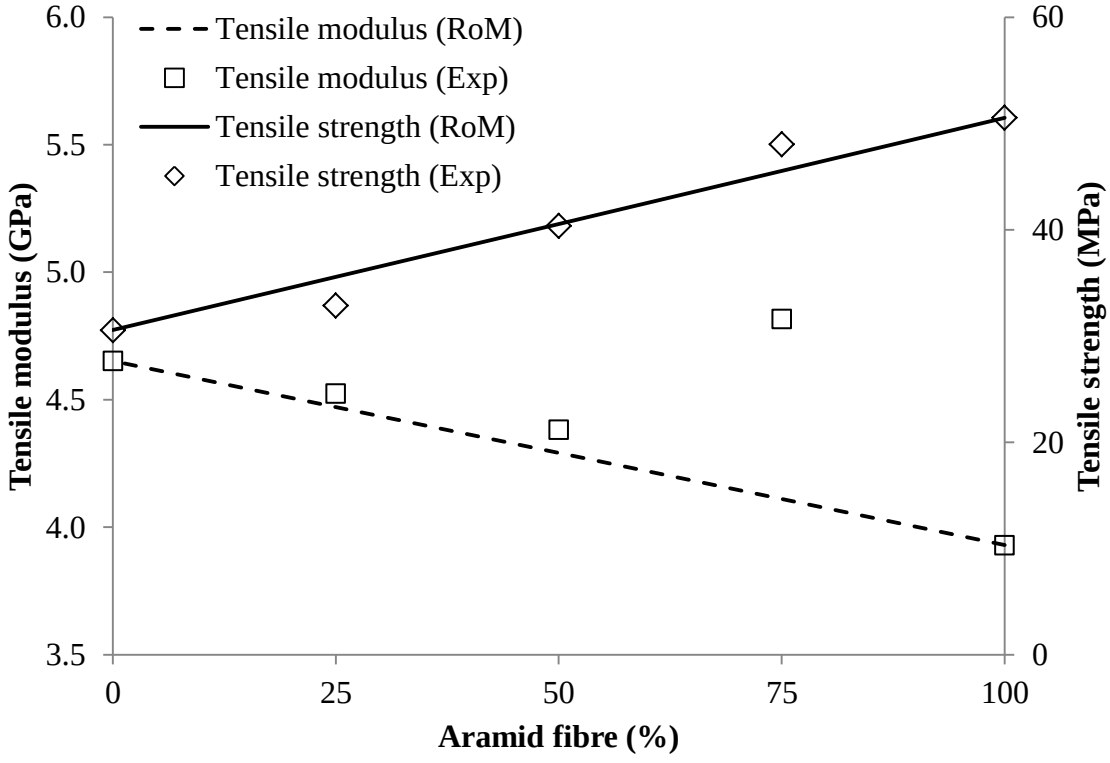

Figure 4.24: Experimental and calculated Young's modulus and tensile strength for composite with 20% total V_f

A positive or negative synergy effect in hybrid composite is defined as a positive or negative deviation of a certain mechanical properties from the rule-of-mixtures behaviour [30]. Positive synergy is highly preferable since it produces a composite with better properties than the sum of its components.

Young's modulus, E

At 5% total V_f, all the hybrids showed negative synergy effect for both the Young's modulus. At 10% total V_f, hybrids with 75:25 and 50:50 V:V% showed positive synergy for Young's modulus. However, hybrid with 25:75 V:V% shows lower negative synergy effect. At 20% V_f, all the hybrids showed positive synergy for their Young's modulus, especially hybrid with 75:25 V:V% which exhibited the highest Young's modulus value (4.82 GPa) among all the composites tested.

Young's modulus defines the linear part of the stress-strain curve where no deformation or crack propagation has yet to occur. It is less sensitive to flaws in the composite than the tensile strength. However, improvement in interfacial bonding [91] and intermingling of fibres would definitely improve the tensile properties of a hybrid composite. Sreekala *et al.* have reported that for their phenol-formaldehyde-glass fibre-OPEFB fibre hybrid composite, the high tensile modulus observed in their hybrid reinforced with 0.96 OPEFB V_f was due to excellent fibres intermingling [92]. You *et al.* have also reported similar results [93]. One of their hybrid, designated E-VE, which consists of randomly dispersed carbon and glass fibres, showed the highest hybrid effect when compared to their skin-core hybrids. These studies further emphasize the importance of fibre dispersion and mixing in the composite.

Tensile strength

At 5% and 10% total V_f, all the hybrids showed negative synergy effect for tensile strength. At 20% V_f, hybrid with 75:25 V:V% showed positive synergy effect while hybrid 50:50 V:V% showed value (40.38 MPa) on par with the value predicted by rule-of-mixtures. Hybrid with 25:75 V:V% showed negative synergy.

In a hybrid composite, the properties of the composite are mainly dependent on the modulus and elongation at break, of the individual reinforcing fibres. It was expected for the experimental values to deviate from the calculated values because by applying the simple rule of mixture, the fibre-fibre interaction was not accounted for. The fibre-fibre interaction plays a major role in determining fibre orientation and the average fibre length in the composite which significantly affects the strength of the composite [30, 88, 94].

4.5 Flexural properties

Flexural testing studies the bending behaviour of a material. In flexural tests, most of the specimens fail in ductile mode. Flexure testing is often done on relatively flexible materials such as polymers, wood and composites. Specimens under flexural test underwent a range of stresses across its depth. At the edge of the object on the inside of the bend (concave face) the stress will be at its maximum compressive value. At the convex face, the stress will be at its maximum tensile values. Flexural strength is defined as the maximum stress in the outermost fibre. This is calculated at the surface of the specimen on the convex or tension side. Flexural modulus is calculated from the slope of the stress vs. deflection curve. Specimen deflection is usually measured by the cross-head position. The value for flexural modulus, flexural strength and flexural displacement are illustrated in Figure 4.25 - 4.27.

4.5.1 The effect of total V_f

Flexural modulus

For single fibre reinforced composites, increasing the total V_f will increase the flexural modulus value. For AFRC, the flexural modulus initially did not change when V_f was increased from 5 to 10%. However, as V_f was further increased to 20%, the modulus increased from 1.89 GPa to 2.93 GPa. For CFRC, flexural modulus increases from 2.09 GPa (5% V_f) to 2.30 GPa (10% V_f) and 3.61 GPa (20% V_f). Carbon fibre reinforced composites are shown to have higher flexural modulus compared to its aramid fibre reinforced counterparts. This is due to the higher modulus and also rigidity of the carbon fibre itself whereas aramid fibre is easily bendable.

For all hybrid composites, increasing the total V_f also produces similar trend. For example, for hybrid composite with 50:50 V:V% fibre composition, flexural modulus increases from 1.70 GPa (5% V_f) to 2.00 GPa (10% V_f) and 3.10 GPa (20% V_f).

Flexural strength

The flexural strength for aramid fibre reinforced composite increases with increasing V_f. The flexural strength for composites reinforced with 5%, 10% and 20% aramid fibre are 56.94 MPa, 55.68 MPa and 72.66 MPa, respectively. For carbon fibre reinforced composites, it showed that the flexural strength decreases with increasing V_f. The flexural strength for composites reinforced with 5%, 10% and 20% carbon fibre are 53.78 MPa, 49.12 MPa and 49.15 MPa, respectively. Hybrid composites showed similar trend to aramid reinforced composites where the increase of total V_f increases the flexural strength of the composite. For example, the flexural strength for hybrid composites with 50:50 V:V% at 5, 10 and 20% V_f are 43.85 MPa, 50.87 MPa and 64.77 MPa, respectively.

Flexural displacement

The flexural displacement for all composites was independent of total V_f. The value did not change significantly with increasing V_f.

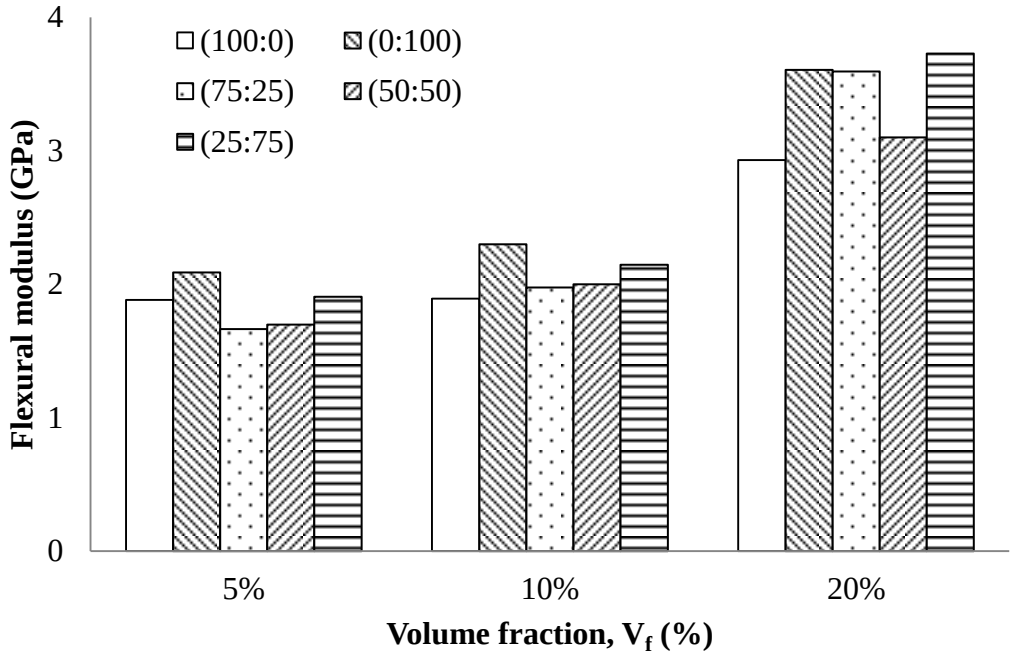

Figure 4.25: Flexural modulus of all composites at different total V_f

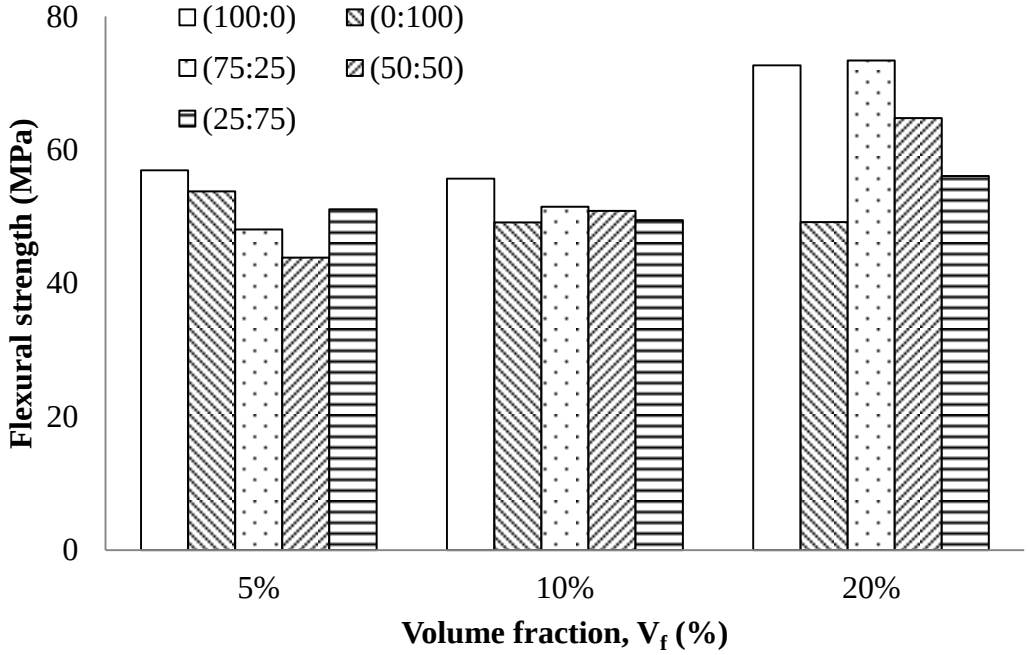

Figure 4.26: Flexural strength of all composites at different total V_f

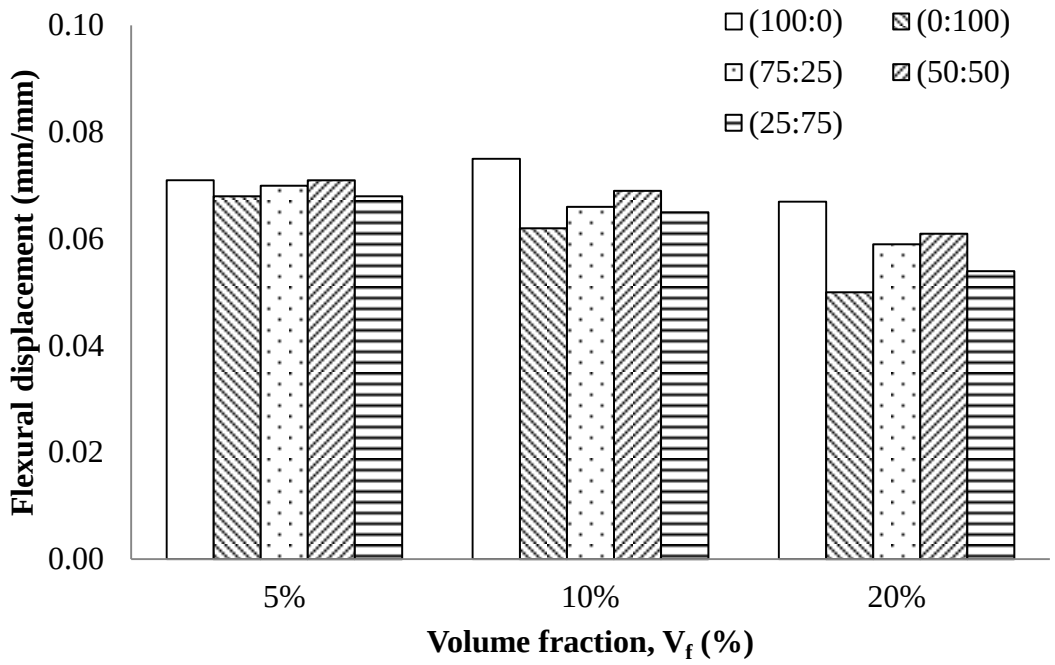

Figure 4.27: Flexural displacement of all composites at different total V_f

4.5.2 The effect of fibre proportion

Flexural modulus

There were no significant trends observed with regard to the effect of fibre proportion on the flexural modulus of the composites.

Flexural strength

There were no significant trends observed with regard to the effect of fibre proportion on the flexural modulus of the composites at 5% and 10% V_f. However, at 20% V_f, increasing the carbon fibre proportion causes the flexural strength to decrease. The flexural strength

for hybrid fibre composites at 20% V_f are 73.40 MPa (75:25 V:V%), 64.77 MPa (50:50 V:V%) and 56.08 MPa (25:75 V:V%).

Carbon fibre is very brittle and will easily break when bent. Its ability to strongly resist bending contributes to the excellent flexural modulus values exhibited by carbon fibre reinforced composites unlike aramid fibres which are rope-like in nature. However, once the bending threshold for the fibre is exceeded, the carbon would fail in a brittle manner. Carbon fibre is anisotropic, where it is very strong when the tensile stress applied is along its fibre length. In flexural tests, both compression and tensile forces acts upon the specimen. Aramid fibre on the other is not as stiff as carbon fibre but is more difficult to break. The aramid fibres were held into place by the matrix and the stresses acting upon the matrix were transferred to the fibres. More energy is needed to break aramid fibres due to its molecular arrangement and its failure mechanism.

Simple rule of mixture

Simple rule of mixture equation was also applied to study the synergistic effect of hybridization on the flexural properties of the composite. The calculated and experimental values for the composites are illustrated in Figures 4.28 – 4.30.

Flexural modulus

For hybrid fibre composites with 5% and 10% total V_f, flexural modulus showed negative synergy. For example, the flexural modulus for 5(2.50:2.50) is 1.70 GPa much lower than the calculated values, 2.00 GPa. However, for hybrid composites with 20% total V_f, positive synergy was observed. For example, the flexural modulus for 20(15.00:5.00) is 3.60 GPa, higher than the calculated value, 3.10 GPa.

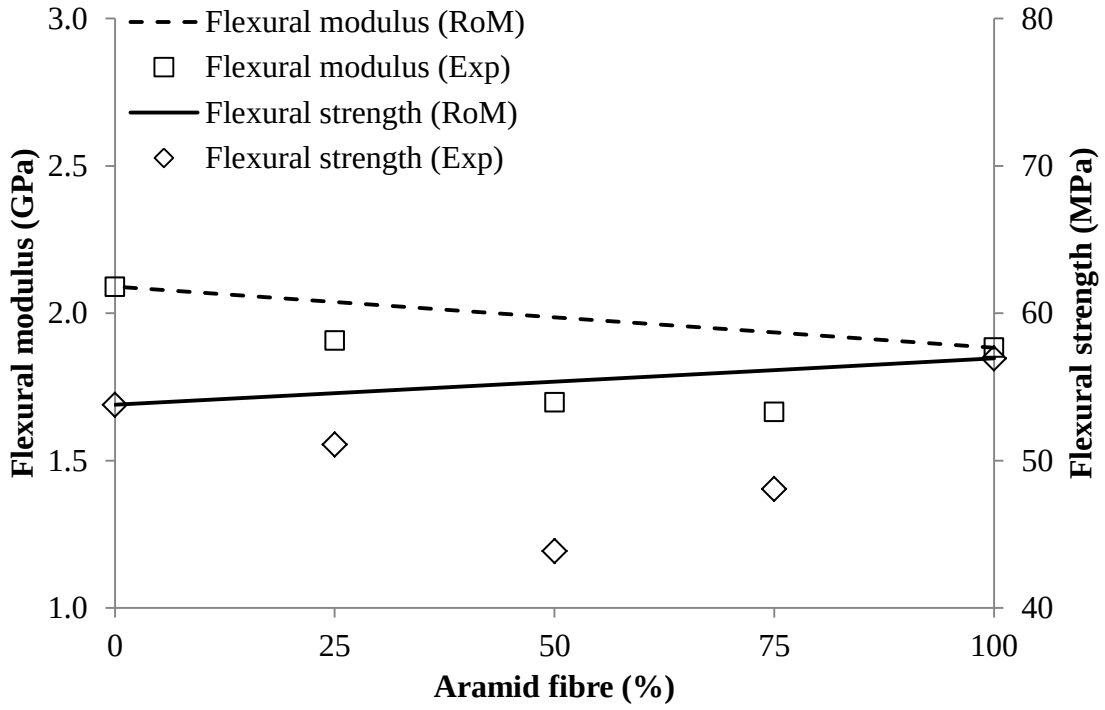

Figure 4.28: Experimental and calculated flexural modulus and flexural strength for composite with 5% total V_f

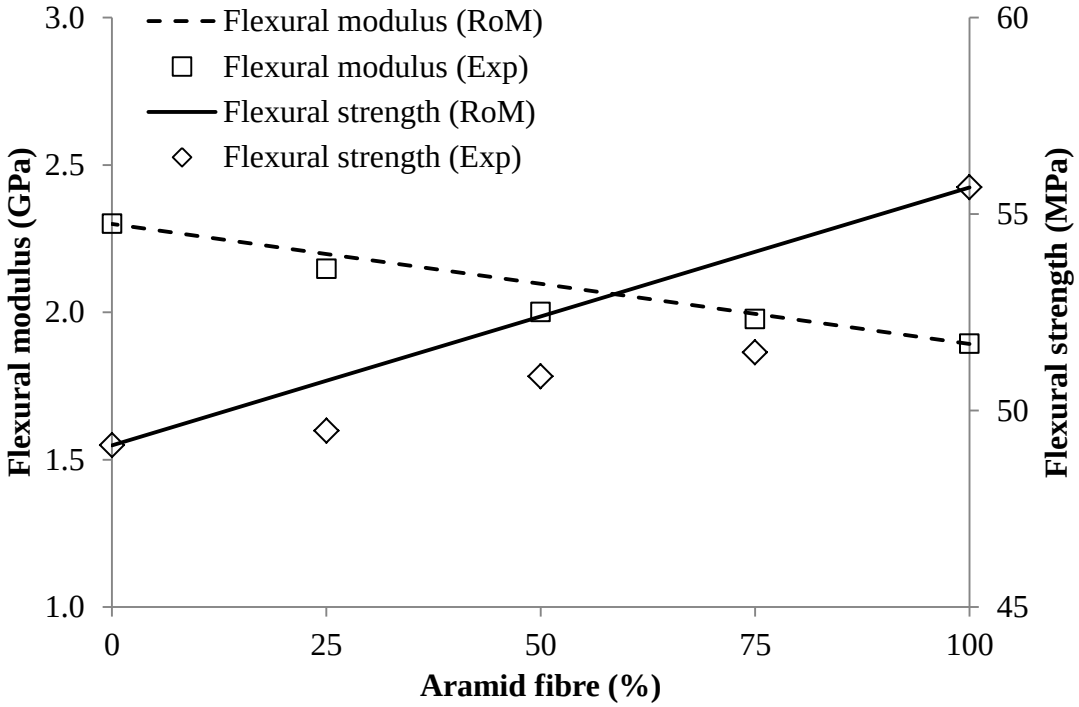

Figure 4.29: Experimental and calculated flexural modulus and flexural strength for composite with 10% total V_f

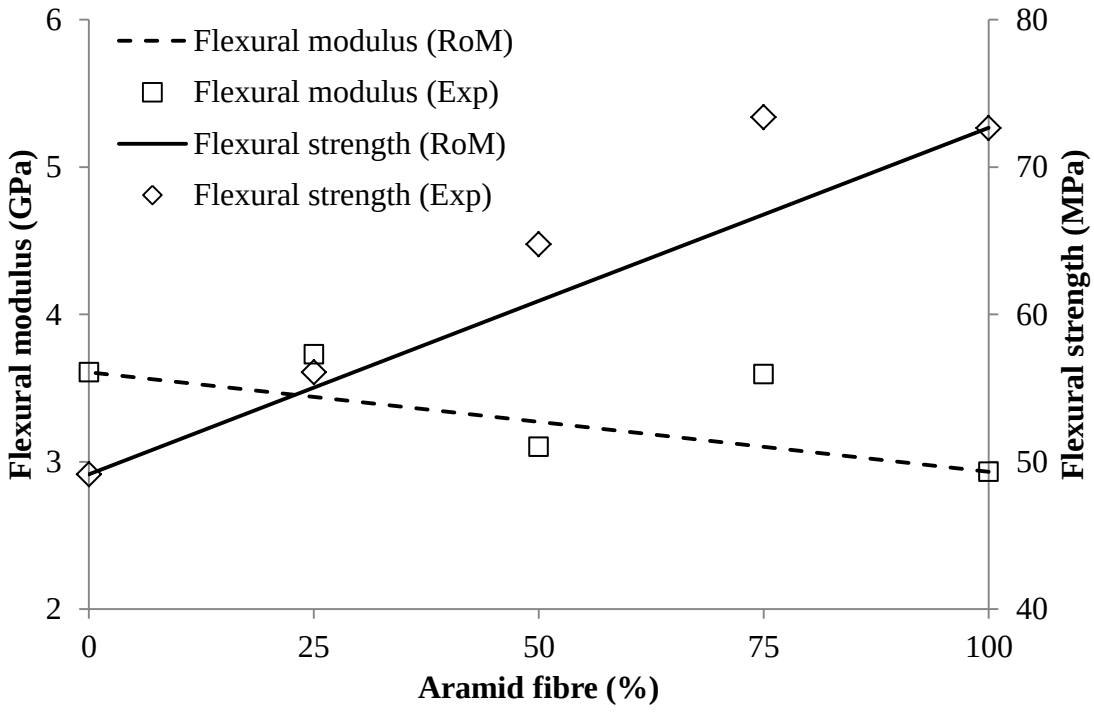

Figure 4.30: Experimental and calculated flexural modulus and flexural strength for composite with 20% total V_f

Flexural strength

Hybrid fibre composites with 5% and 10% total V_f showed negative synergy effect. The flexural strength for 10(5.00:5.00) is 50.87 MPa, lower than the calculated value (52.40 MPa). Hybrid composites with 20% V_f showed positive synergy effect. For example, the flexural strength for 20(15.00:5.00) is 73.40 MPa, which is higher than the calculated value (66.79 MPa).

4.6 Impact properties

Information on the impact behaviour of material is very important. Scientists have sought to improve the impact resistance of polymeric materials. Impact resistance or toughness is defined as the ability of a material to withstand sudden impact without fracturing [95]. A material with high impact resistance is able to absorb more energy and disperse the energy efficiently. In order to produce material with outstanding impact toughness, balance between strength and ductility is required.

Impact energy of a material is the amount of energy required to fracture in a given volume of the material. Impact strength is the energy needed to propagate the crack through the material. The crack propagation energy is related to the toughness of the material and the distance travelled by the crack tip during failure. Brittle material typically have low impact energy due to the lower amount of energy needed for the crack to propagate during fracture [96].

Impact tests produced energy vs. time graphs for each tested specimens. There are two important parameters that were extracted from these graphs, fracture energy (W) and peak load (P). Fracture energy or work of fracture can be defined as total work required to fracture the sample, per unit area of new surface produced or the total amount of energy dissipated during crack growth [97]. Fracture energy is obtained by calculating the area under the graph prior to sample fracture. Peak load was obtained from the highest point in the graph prior to fracture.

Various energy dissipating mechanism operate when a discontinuous fibre-reinforced composite fractures from an existing notch. Deformation and fracture of the matrix takes place in an area in front of the crack tip. At the same time the applied load,

transferred by shear to the fibres, may exceed the strength of the fibre-matrix interface and fibre debonding may occur. Transfer of stress may still be possible to a debonded fibre via frictional forces along the interface. Fibres may fracture if the fibre stress level exceeds the local fibre strength. Fibres which have fractured away from the crack interface will be pulled-out of the matrix which may also involve energy dissipation [98].

The relationship between W and the critical strain energy release rate (G_c) and specimen geometry function (BDΦ) is given by,

$$W = G_C BD\Phi \tag{4.2}$$

where B and D are the width and depth of the specimen, respectively. A correction factor, Φ is given by,

$$\phi = \frac{1}{2}\left(\frac{a}{D}\right) + \frac{1}{18\pi}\left(\frac{S}{D}\right)\frac{1}{\left(\frac{a}{D}\right)} \tag{4.3}$$

where a and S are notch depth (crack length) and the specimens support span respectively.

A plot of W against BDΦ produced a straight line, where its slope is equal to the G_c of the materials. G_c is the total energy absorbed by test specimen divided by its net cross section area and is used to measure the energy necessary for crack initiation.

The resistance to crack propagation or fracture toughness of the aramid, carbon and hybrid composites is characterized by measuring the critical strain energy release rate (G_c) and the critical stress intensity factor (K_c) of single edge notched (SEN) specimens in three point bending mode according to ASTM E23 [60].

Critical stress intensity factor (K_c) is a function of loading, crack size, and structural geometry. K_c indicates the resistance of the material to unstable crack growth [99]. The

relationship between the critical stress intensity factor (K_c) with nominal fracture stress (σ), geometry correction factor (Y) and notch or crack length (a) is given by,

$$\sigma Y = \frac{K_c}{\sqrt{a}} \tag{4.4}$$

In three-point bend test, σ is given by simple bending theory as,

$$\sigma = \frac{6PS}{4BD^2} \tag{4.5}$$

For the three-point bend test specimen, where S/D is equal to 4, Y is given by,

$$Y = 1.93 - 3.07\left(\frac{a}{D}\right) + 14.53\left(\frac{a}{D}\right)^2 - 25.11\left(\frac{a}{D}\right)^3 + 25.80\left(\frac{a}{D}\right)^4 \tag{4.6}$$

A plot of σY against $a^{-0.5}$ produced a straight line, where its slope is equal to the K_c of the materials. There are three types of K depending on their mode of fracture. Refer to Figure 4.31. In this work, mode I (crack opening) is of interest.

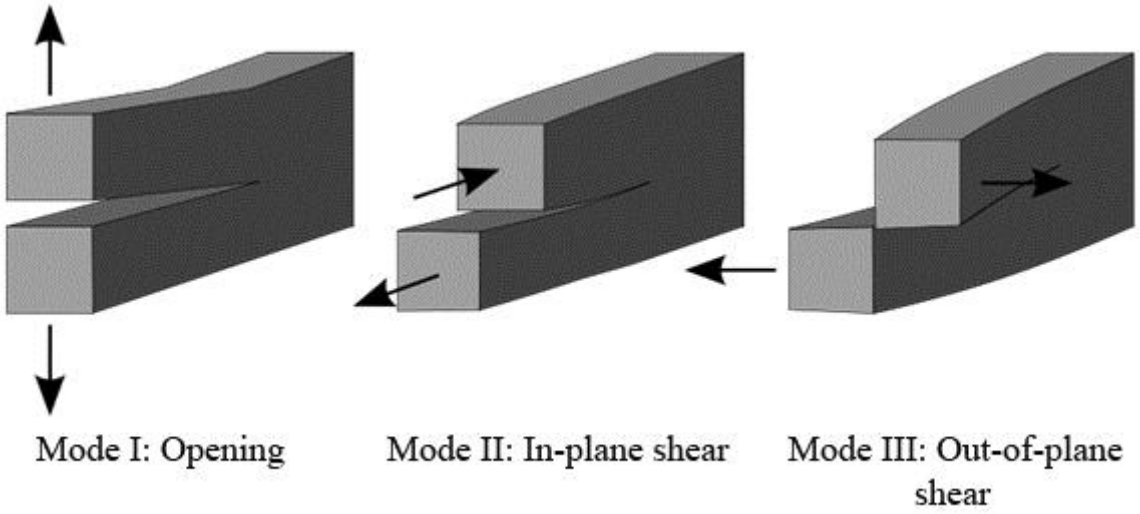

Figure 4.31: Different crack loading modes.

4.6.1 The effect of total V_f

Fracture energy, W

It was observed that increasing the notch to depth ratio (a/D) would cause the fracture energy to lower. The fracture energy for composite 5% (100/0) at 0.1 a/D is 332.8 mJ. W lowers to 127.5 mJ, 75.1 mJ and 59.9 mJ as the a/D increases to 0.2, 0.3 and 0.4, respectively. Refer to Figure 4.32. Similar observation was made for carbon fibre reinforced composites and the hybrid composite (Figure 4.33 and Figure 4.34). As stated before, fracture energy is related to the distance where the crack needs to travel during failure. Higher a/D ratio means that the crack is longer, hence shorter distance for the crack to propagate (smaller fracture area) resulting in lower fracture energy value [100].

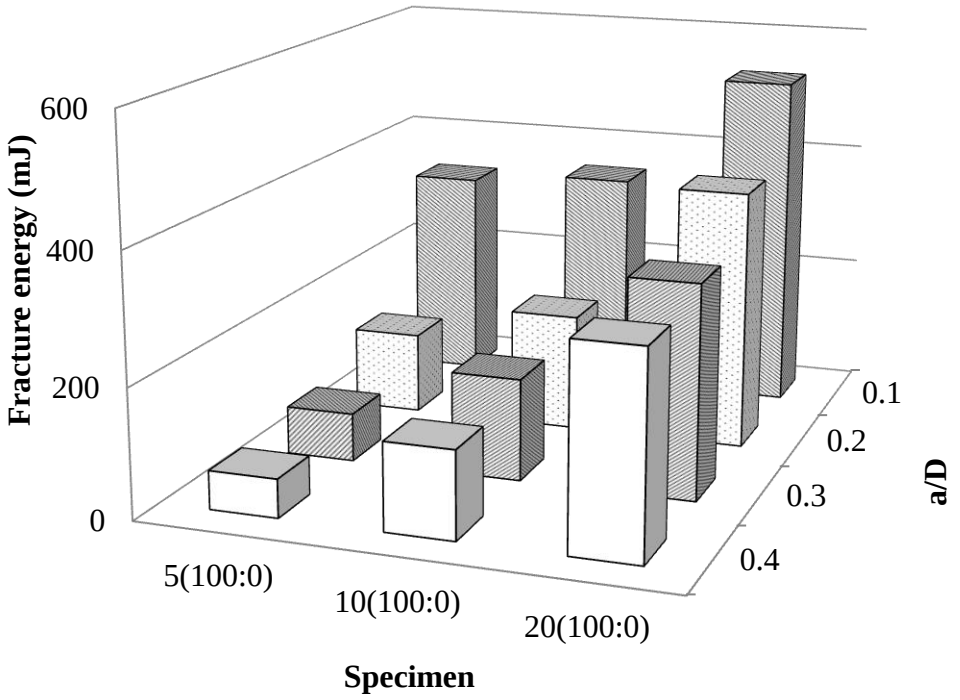

Figure 4.32: Fracture energy for aramid fibre reinforced composite at different V_f

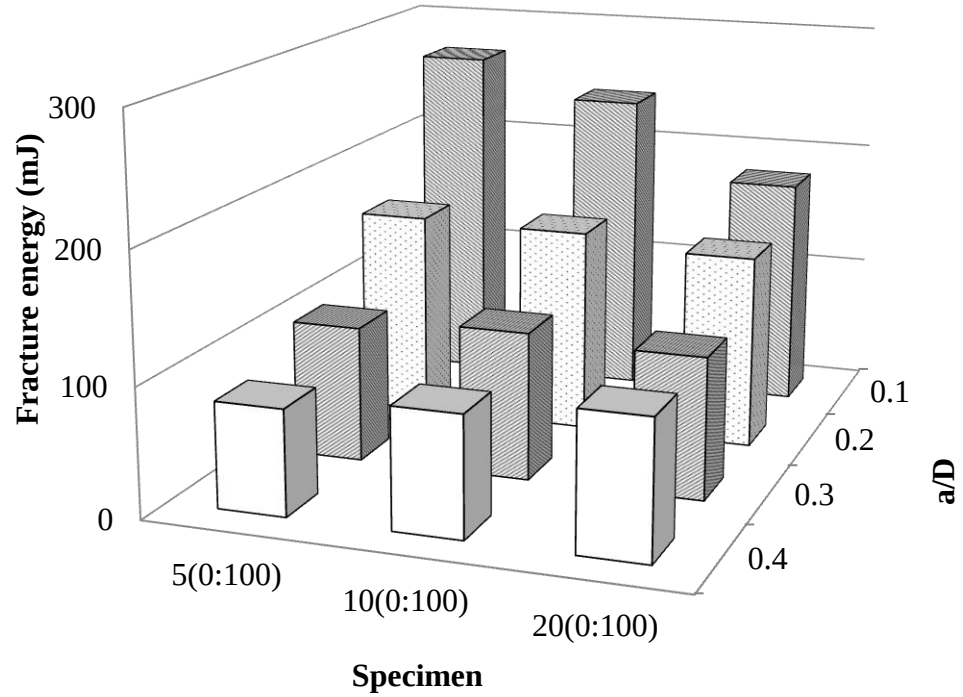

Figure 4.33: Fracture energy for carbon fibre reinforced composite at different V_f

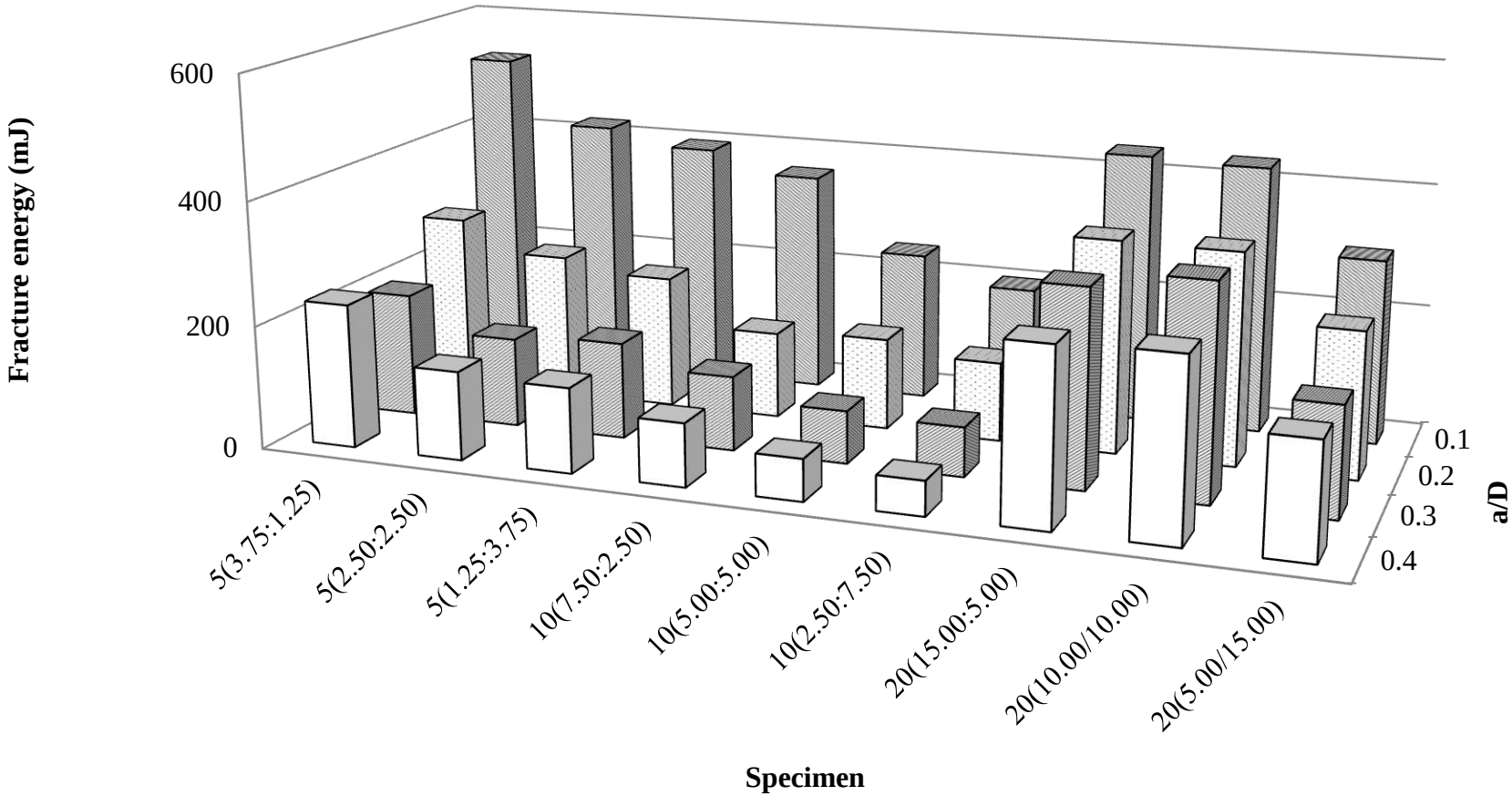

Figure 4.34: Fracture energy for hybrid fibre reinforced composite at different V_f and different fibre proportions.

The effect of fibre loading on the fracture energy of the composite depends on the type of fibre employed. Fracture energy for AFRC at 0.2 a/D increases from 127.5 mJ to 183.8 mJ and 405.4 mJ as the V_f was increased from 5% to 10% and 20%, respectively. As we all know, aramid fibre has excellent impact properties and has been utilised as bulletproof vests. Their high degree of toughness, associated with the failure mechanism of aramids, and damage tolerance promotes good impact performance. When aramid fibres break, they do not fail by brittle cracking, as do glass or carbon fibres. Instead, the aramid fibres fail by a series of small fibril failures, where the fibrils are molecular strands that make up each aramid fibre and are oriented in the same direction as the fibre itself. These many small failures absorb much energy and result in very high toughness [101]. The presence of aramid fibres in the composite would hamper the crack propagation process by forcing the crack lines to travel around the fibre ends, resulting in higher fracture energy. These fibrillar fractures can be observed in Figure 4.35.

The fracture energy for CFRC decreases as the amount of carbon fibre was increased. Fracture energy for carbon reinforced composite at 0.1 a/D decreases from 270.3 mJ to 241.0 mJ and 180 mJ as the fibre content increases from 5% to 10% and 20%, respectively. Carbon fibre reinforced composite is stiff but brittle. Brittle materials tend to have poor impact properties. Increasing the amount of carbon fibre of the composite will further reduce the impact resistance of the material. The fracture surface can be observed in Figure 4.36. It can be clearly seen that the fracture is a brittle fracture. An interesting observation is that the fibres at the core of the composite tend to be aligned perpendicularly to the melt flow while fibres near the surface of the composite tend to be aligned parallel to the melt flow.

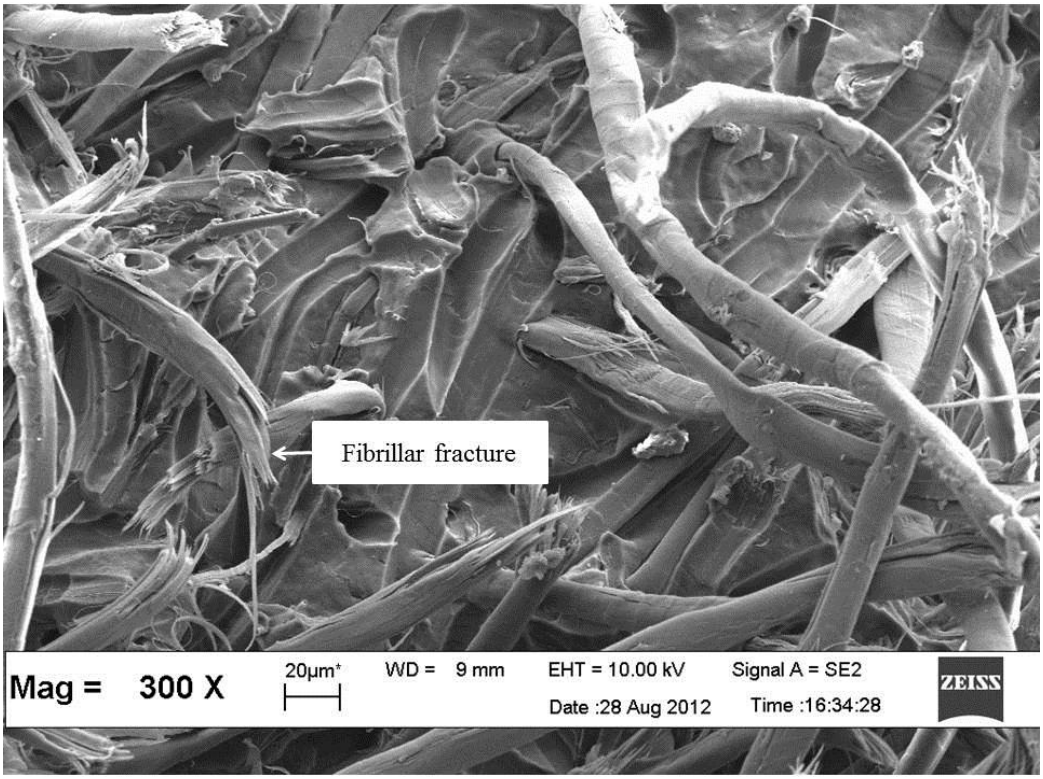

Figure 4.35: Impact fracture surface of 20(20.00:0.00)

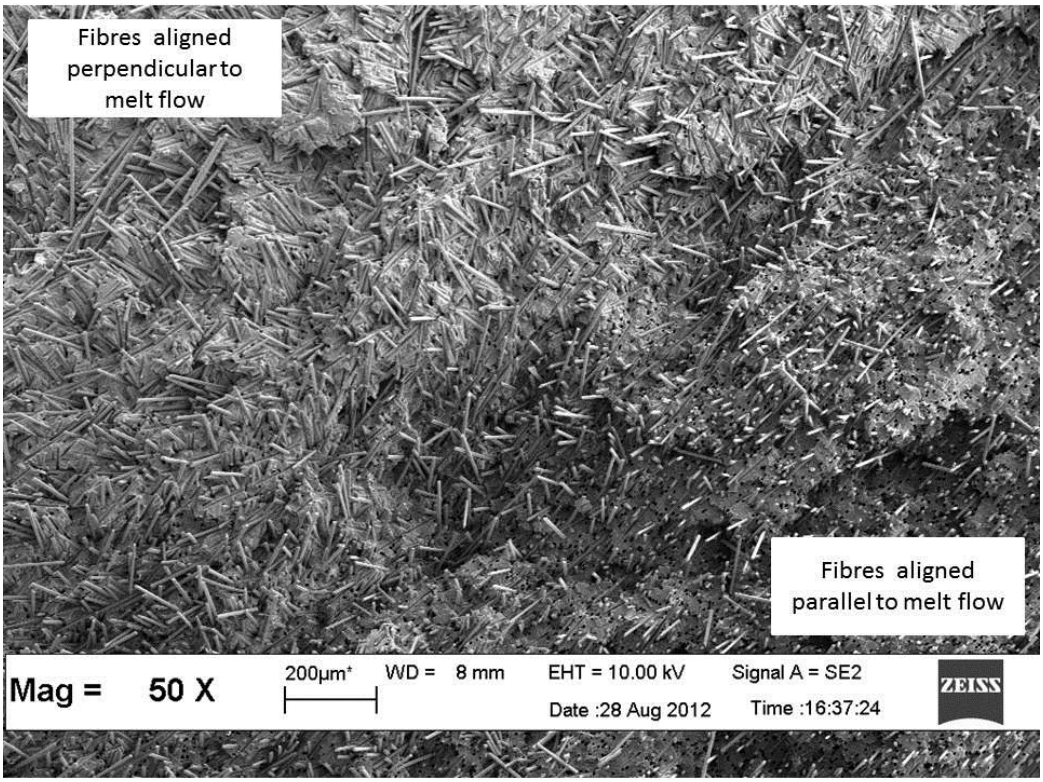

Figure 4.36: Impact fracture surface of 20(0.00:20.00)

For hybrid fibre composites, increasing the total V_f results in mixed effect. Refer to Figure 4.34. For example, the fracture energy for hybrid composite with 50:50 V:V% fibre proportion for a/D 0.2 at V_f 5, 10 and 20% are 235.7 mJ, 148.6 mJ and 342.7 mJ, respectively. The fracture surface for the hybrid fibre composite can be observed in Figure 4.37. Important information can be extracted from the image. Firstly, the surface of the fibres in the hybrid fibre composite, as well as AFRC and CFRC previously, are clean. This indicates that the interfacial interaction between the matrix and the fibres in use are poor. Secondly, the carbon fibres in the hybrid fibre composites tend to break near the surface of the matrix, which indicates that during failure, the crack propagates through most of the carbon fibres, resulting in brittle fracture.

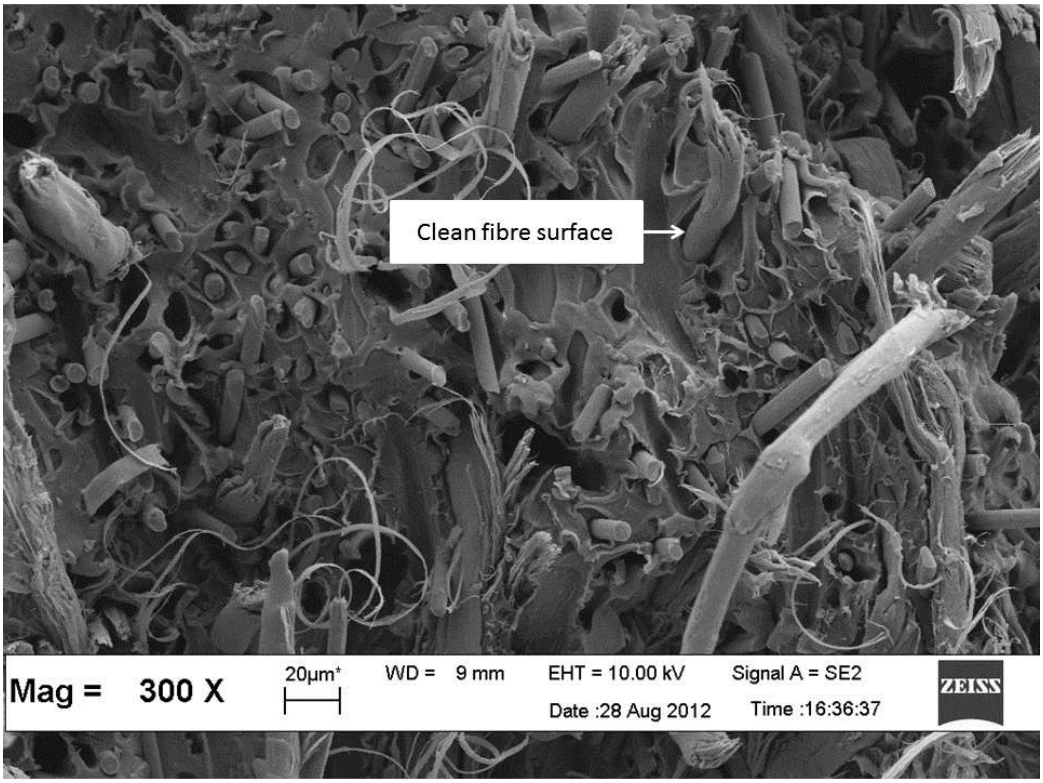

Figure 4.37: Impact fracture surface of 20(10.00:10.00)

Critical energy release rate, G_c

An example of the W against BDΦ plot is given in Figure 4.38. Similar graphs were plotted for all the composites and their G_c values were tabulated in Table 4.6.

Strain energy release rate (G) defines the energy dissipated during fracture per unit of newly formed surface and only when G exceed the critical value, G_c, would the crack grow and failure occurs. Generally, the trend observed with regard to G_c is in agreement with the trends earlier observed in W.

The trend observed for G_c of the AFRC is the same as observed for W. G_c values for AFRC at 5, 10 and 20% V_f are 4.76, 6.41 and 10.51 $kJ.m^{-2}$, respectively. G_c increases with increasing V_f due to more energy needed to form new surface. The fibres would hinder crack propagation by forcing it around the fibre ends. Aramid fibre is very strong and the fibre itself doesn't fail in a brittle manner.

G_c value for CFRC decreases with increase in carbon fibre content. G_c values for CFRC at 5, 10 and 20% V_f are 5.46, 4.51 and 3.96 $kJ.m^{-2}$, respectively. This is due to increase in brittleness of the composite caused by increased presence of carbon fibres. Brittle materials generally have low G_c. Various researchers have reported similar observation [102].

For hybrid fibre composites, mixed effect was observed. For example, for hybrid fibre composites with 50:50 V:V% fibre proportion, G_c values at 5, 10 and 20% V_f are 6.82, 4.17 and 10.26 $kJ.m^{-2}$, respectively. Similar trend was observed for hybrid fibre composites with fibre proportion of 75:25 and 25:75 V:V%. Hybrid fibre composites with 75:25 V:V% fibre proportion, G_c values at 5, 10 and 20% V_f are 8.77, 5.84 and 10.01 $kJ.m^{-2}$, respectively. AFRC with 20% V_f exhibited the highest G_c value at 10.51 $kJ.m^{-2}$

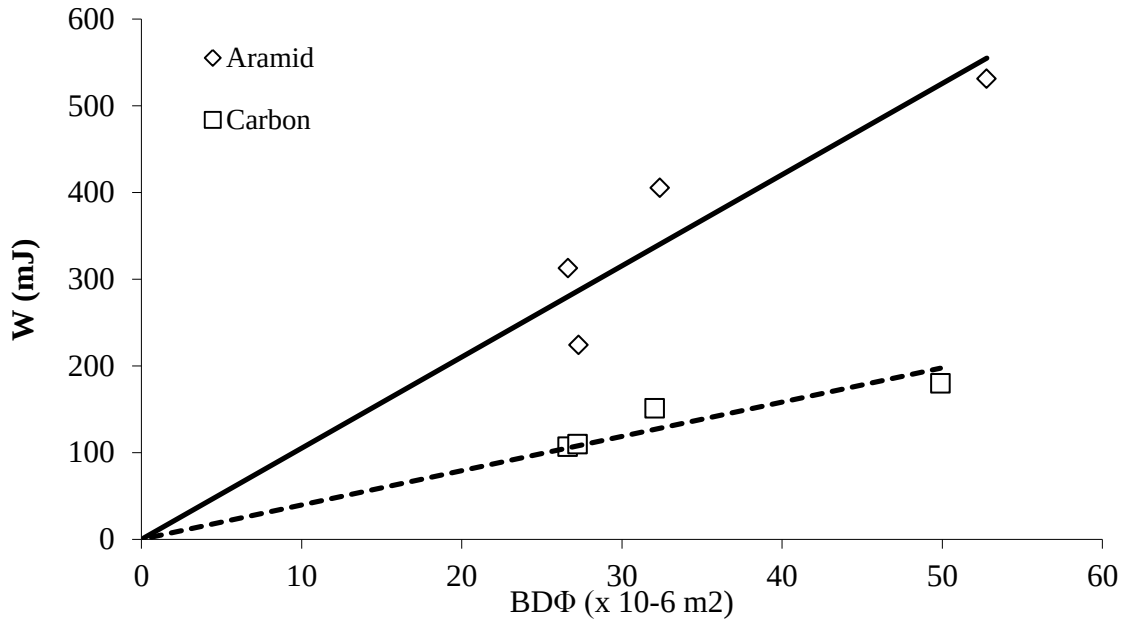

Figure 4.38: W against BDΦ plot for ARFC and CFRC at 5% V_f

G_c of the composite can be further enhanced by improving the interfacial interaction of the fibres and the matrix especially for composites reinforced with aramid fibres. Polypropylene is non-polar while aramid fibre is polar. Therefore, it is highly unlikely that there is any significantly strong interaction between these two components. Enhancement can be made via surface treatment of the aramid fibres or introducing compatibiliser into the system.

Table 4.6: G_c and K_c for all composites

Specimen	G_c (kJ.m^{-2})	K_c (MPa.m$^{1/2}$)
5(5.00:0.00)	4.76	2.87
5(3.75:1.25)	8.77	3.10
5(2.50:2.50)	6.82	3.12
5(1.25:3.75)	6.42	3.00
5(0.00:5.00)	5.46	2.75
10(10.00:0.00)	6.41	3.04
10(7.50:2.50)	5.84	3.47
10(5.00:5.00)	4.17	3.17
10(2.50:7.50)	3.17	3.17
10(0.00:10.00)	4.51	3.25
20(20.00:0.00)	10.51	3.38
20(15.00:5.00)	10.01	3.30
20(10.00:10.00)	10.26	3.30
20(5.00:15.00)	7.36	3.72
20(0.00:20.00)	3.96	3.39

Peak load, P

Peak load is the maximum force needed to cause the fracture of the sample. It depicts the highest point on the load-deflection curve and is a function of the damage resistance of a material. The peak load values for all the composites are illustrated in Figure 4.39 – 4.41.

For AFRC, peak load increases when V_f is increased from 5% to 10% and then decreased when the V_f is further increased to 20%. P values for AFRC with 0.2 a/D at 5, 10 and 20% V_f are 381.5, 432.0 and 479.5 N, respectively. For carbon fibre reinforced composites, the peak load of the composite improves with increase in carbon fibre content. P values for CFRC with 0.2 a/D at 5, 10 and 20% V_f are 421.4, 465.1 and 496.8 N, respectively. The increase is due to an increase in the stiffness of the material. The presence of fibres restricts the movement of the polymer chains resulting in increased stiffness, improving its resistance to deformation. When a notched specimen is subjected to impact loading in 3 point bending mode, there are several steps involved prior to crack propagation. One of the steps involves deformation of the matrix at the crack tip, resulting in crack opening (mode I). For stiffer materials, more energy is needed to initiate deformation, hence higher P. With regard to the hybrid fibre composite, varying the total V_f did not affect the P of the composite significantly.

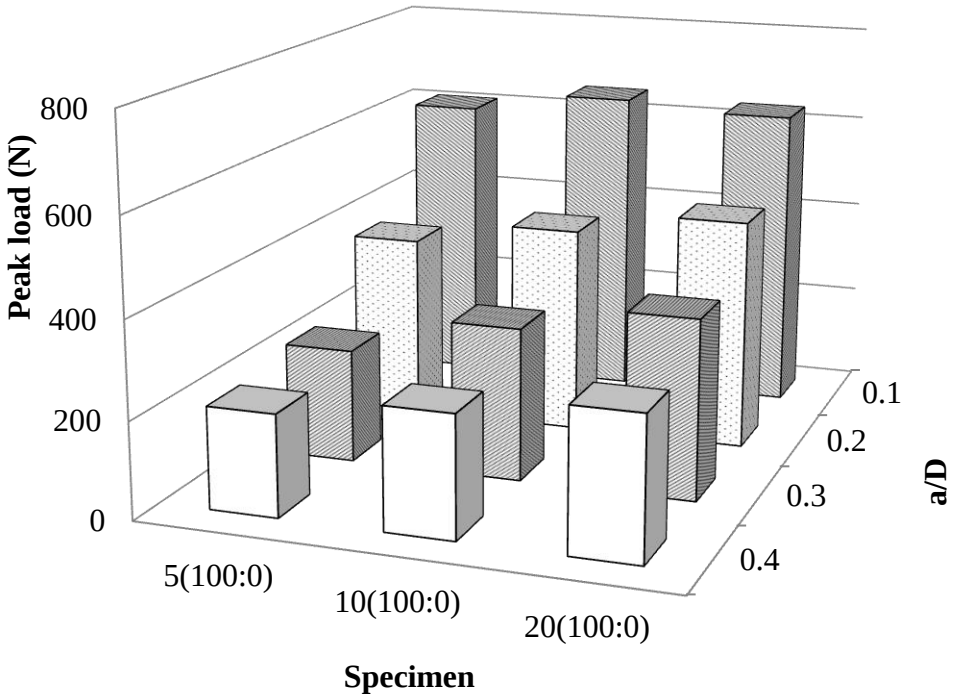

Figure 4.39: Peak load for aramid fibre reinforced composite at different V_f

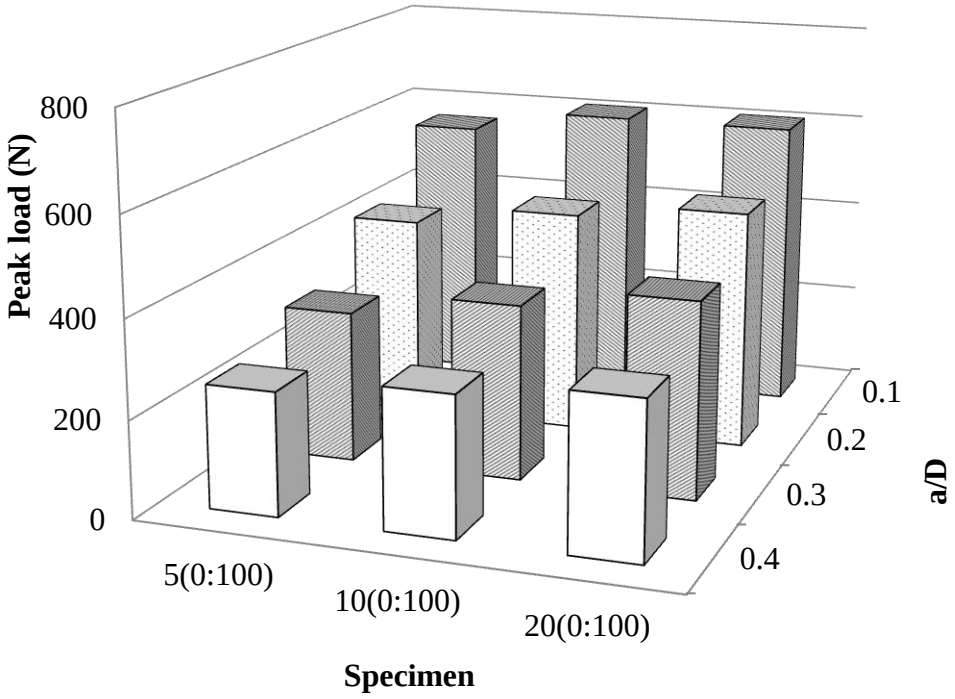

Figure 4.40: Peak load for carbon fibre reinforced composite at different V_f

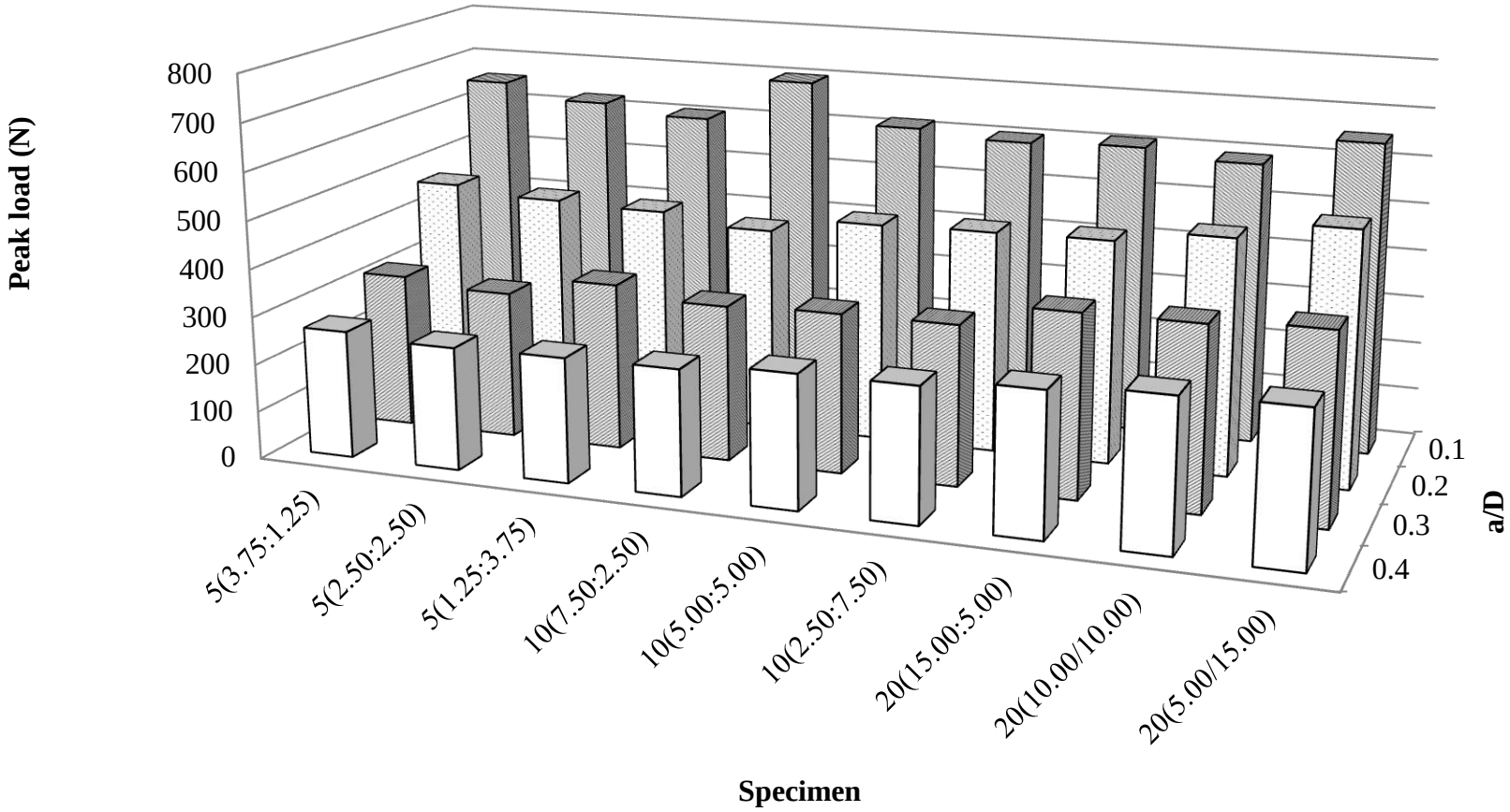

Figure 4.41: Peak load for hybrid fibre reinforced composite at different V_f

Critical stress intensity factor, K_c

An example of σY against $a^{-0.5}$ plot is illustrated in Figure 4.42. K_c values for all the composites are extracted from their respective figures of σY against $a^{-0.5}$ and tabulated in Table 4.6.

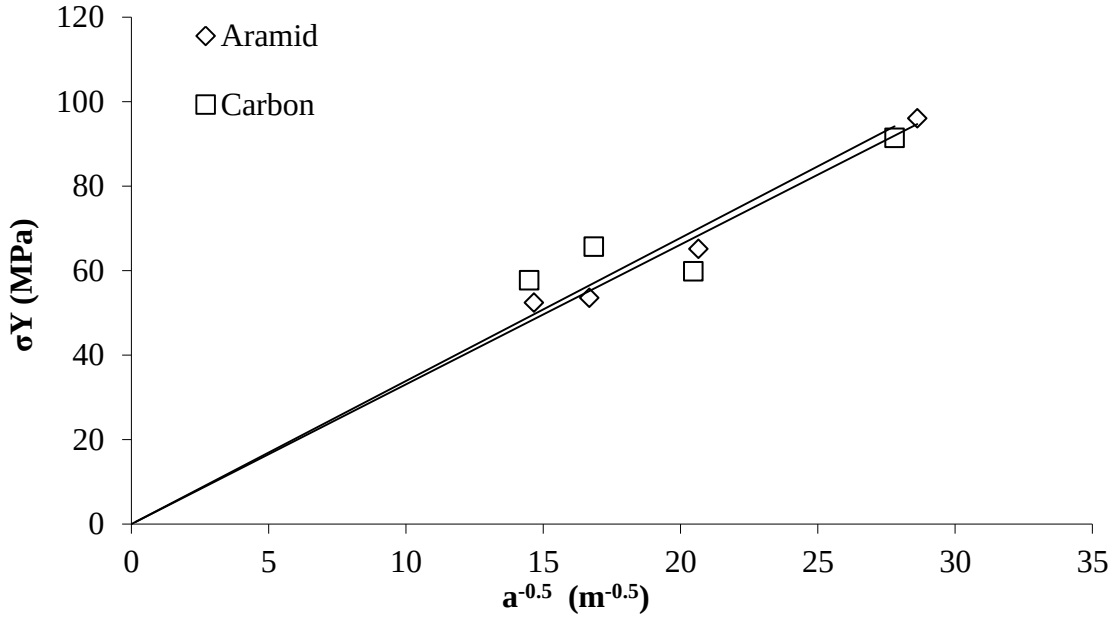

Figure 4.42: σY against $a^{-0.5}$ plot for ARFC and CFRC at 5% V_f

The trend observed for K_c are in agreement with the trend observed in P. K_c for AFRC and CFRC increases with increase in fibre loading. K_c for AFRC at 5, 10 and 20% V_f are 2.87, 3.04 and 3.38 MPa.$m^{1/2}$. K_c for CFRC at 5, 10 and 20% V_f are 2.75, 3.25 and 3.39 MPa.$m^{1/2}$. K_c is more sensitive towards the rigidity of the material and describes the initial process of failure (crack initiation at the notch tip). Hassan *et al.* has reported that the

increment in G_c and K_c values with increase in V_f is an expected observation [103]. Fibres will control the fracture behaviour of the composite with increasing fibre loading.

At a glance, it would seem that increasing the V_f would improve the impact resistance for both composites. However, this conclusion is incorrect. It is important that we study the impact behaviour of a material through more than one parameter or there will be a risk of misunderstanding the actual impact behaviour of the composite. Although K_c for both aramid and carbon fibre reinforced composites both increased with increasing V_f, one must note that the G_c for aramid reinforced composites increased while G_c for carbon reinforced composites decreased.

Taking into account both values, it is understood that for CFRC, increasing V_f would improve the ability of the composite to resist crack initiation. However, due to the brittle nature of the composite, there is little resistance towards crack propagation, which is reflected by G_c. CFRC, especially at high V_f, will fail catastrophically once crack is initiated. The composite would fail in a brittle manner, almost instantaneously due to the unimpeded crack growth. On the other hand, for AFRC, increasing the amount of aramid fibres improves the ability of the composite to resist crack initiation and also requires more energy to propagate the fracture. The increase in energy would mean that total failure of the composite would require more time, which could be the difference in a life or death situation.

For hybrid composites, varying the total V_f did not affect K_c significantly. For example, K_c for hybrid fibre composite with 50:50 V:V% fibre proportion at 5, 10 and 20% V_f are 3.12, 3.17 and 3.30 $MPa.m^{1/2}$, respectively. However, it is worth noting that all

hybrid composites tested have higher K_c value than its non-hybrid counterpart. Refer to Table 4.6. Hybrid 20(5.00:15.00) exhibited the highest K_c (3.76 MPa.$m_{1/2}$).

4.6.2 The effect of fibre proportion

Fracture energy, W

For hybrid fibre composites with the same total V_f, increasing the proportion of carbon fibre in the mixture resulted in decreasing fracture energy. Refer to Figure 4.34. For example, the fracture energy for hybrid composite 10(7.50:2.50), 10(5.00:5.00) and 10(2.50:7.50) at a/D 0.1 are 361.4, 242.8 and 200.1 mJ, respectively. Similar trend is observed for hybrid with total V_f 5% and 20%. For example, the fracture energy for hybrid fibre composites at 5% V_f with 0.1 a/D are 656.8, 625.4 and 606.1 mJ, respectively. The reduction in fracture energy is due to the increasing amount of brittle carbon fibre into the system.

Critical strain energy release rate, G_c

Rule of mixture (RoM) was employed to study the synergistic effect of hybridization on G_c for the hybrid composites. The calculated and experimental G_c values for the composites are illustrated in Figure 4.43 – 4.45. It can be seen that there is positive synergy effect on G_c for for hybrid fibre composites with 5 and 20% total V_f. For example, G_c for 5(2.50:2.50) is 6.82 kJ.m^{-2}, higher than the calculated value via RoM (5.11 kJ.m^{-2}). However, negative synergy was observed for hybrid fibre composites with 10% V_f. G_c for 10(5.00:5.00) is 4.17 kJ.m^{-2}, lower than the calculated value via RoM (5.46 kJ.m^{-2})

There are several factors that can contribute to the deviation between the experimental and calculated values. Negative synergy can be due to the presence of flaws in the system, such as voids, undispersed fibre bundles and poor interfacial interaction. These flaws act as a stress concentrator and weaken the composite causing it to fail prematurely. On the other hand, theoretical predictions through RoM would assume that the composite system is without flaws.

It is well documented that the reinforcing effect of fibres in a composite will increase with increase in fibre loading up to an optimum level. When the fibre content exceeds the optimum level, the improvement in the mechanical properties would start to level off and even decrease as the content is further increased. This observation is caused by the wetting problem faced by the composite. Interfacial interaction between fibre and matrix is one of the most important components in a composite. Good interfacial interaction would allow stress to be transferred from the matrix to the fibre in an efficient manner, producing superior composite. However, when fibre content is too high, the fibres and matrix do not mix well. As a result, various defects such as voids and undispersed fibre bundles are present in the mix. These flaws act as a stress concentrator and weaken the composite causing it to fail prematurely.

Critical stress intensity factor, K_c

No direct relationship between K_c and the fibre proportions was observed. The rule of mixture was applied to study the effect of hybridization on K_c. Rule of mixture would provide a baseline in which the effect of hybridization can be referred to. The expected values calculated via rule of mixture ignore any fibre-fibre interaction or any flaws (voids

or fibre breakage) that would be present in the hybrid composite. The experimental and calculated values for all the composites are illustrated in Figure 4.43– 4.45.

Hybrid composites with 5% total V_f showed positive synergy regardless of fibre proportions. For example, the experimental K_c for hybrid 5(2.50:2.50) is 3.12 MPa.m$^{1/2}$, which is higher than the calculated value of 2.81 MPa.m$^{1/2}$.

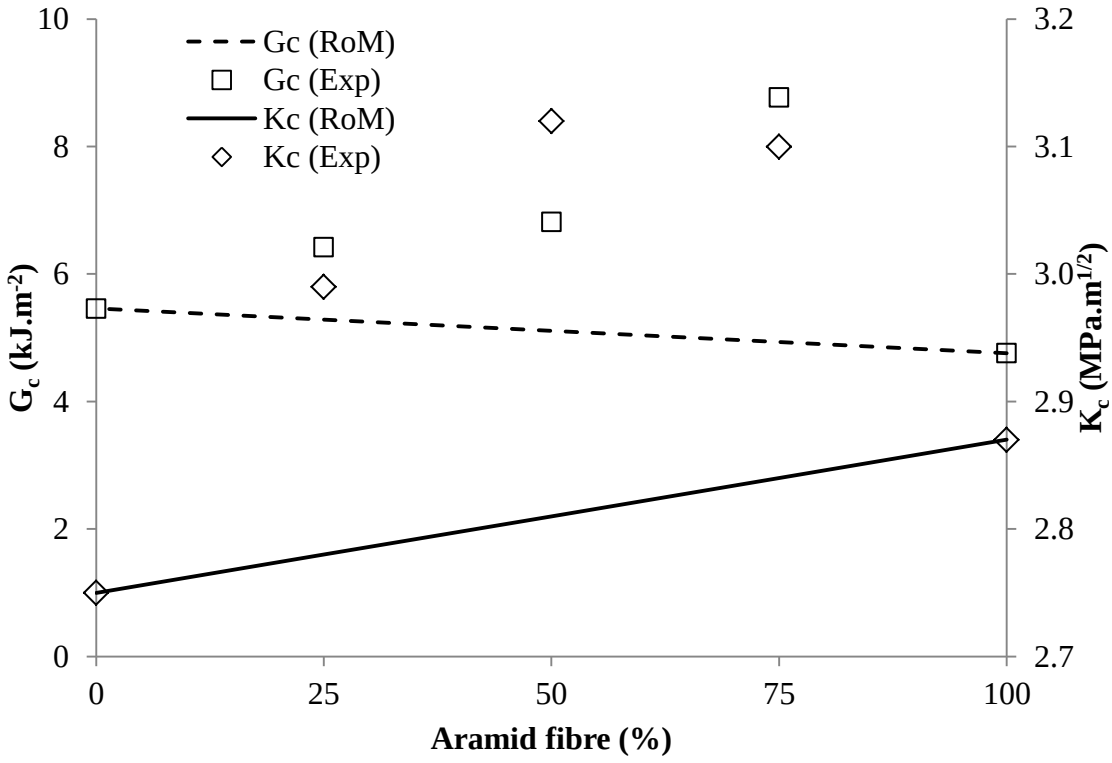

Figure 4.43: Experimental and calculated G_c and K_c for composite with 5% total V_f

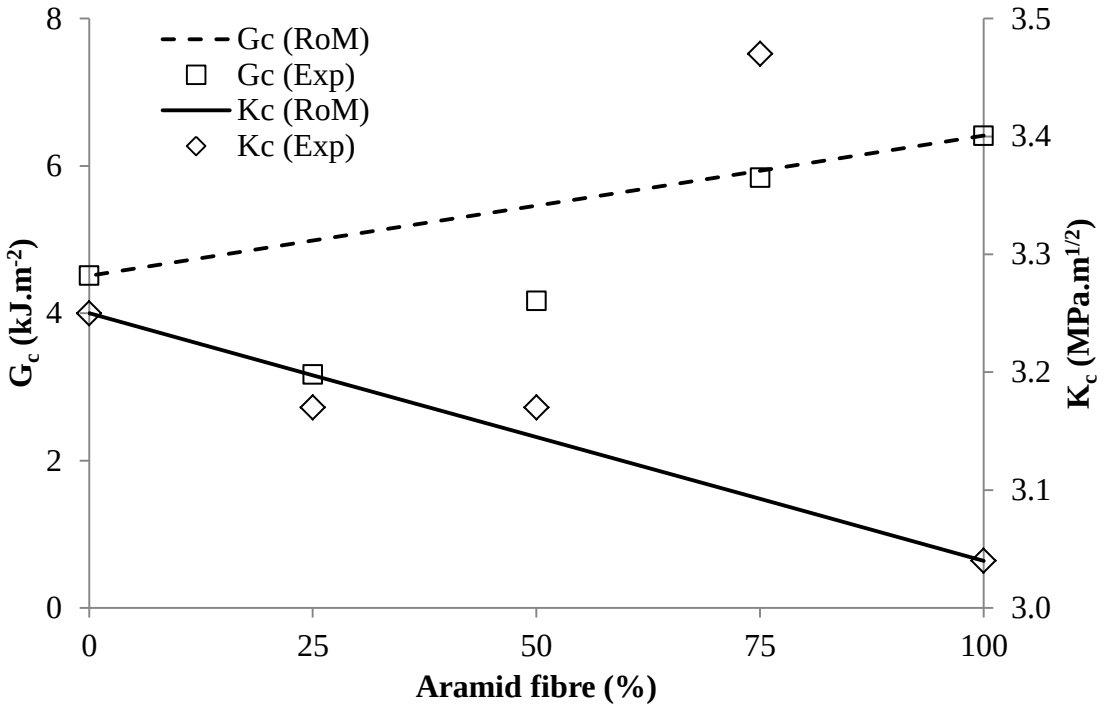

Figure 4.44: Experimental and calculated G_c and K_c for composite with 10% total V_f

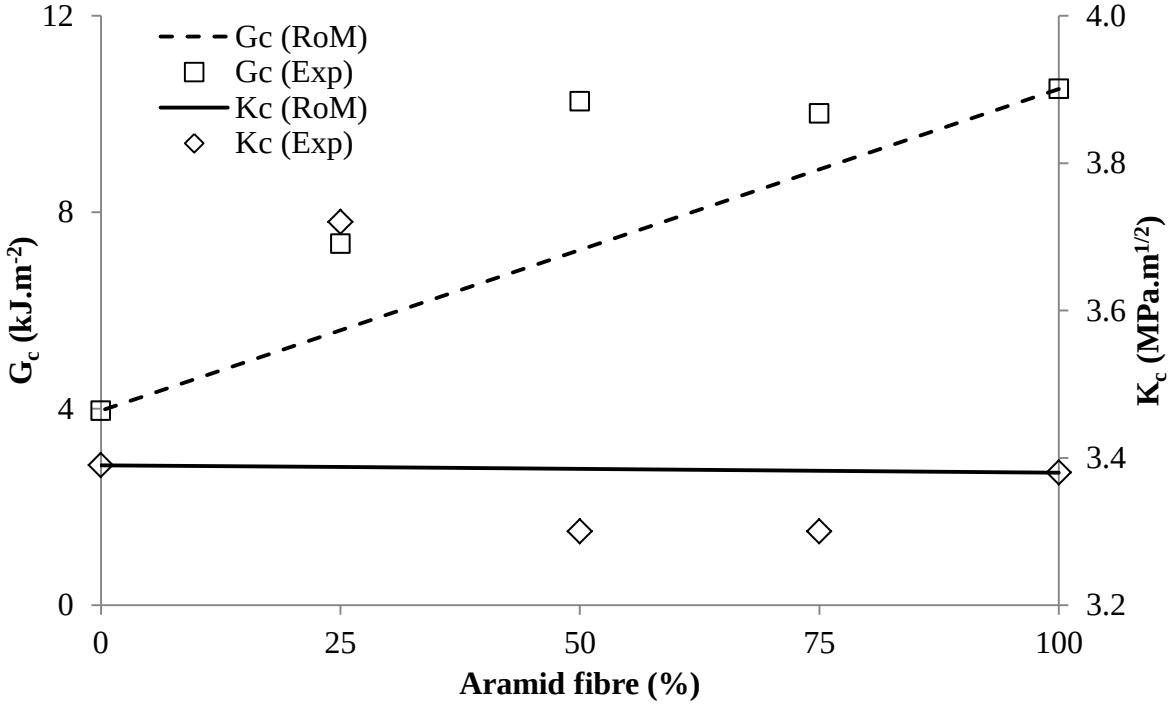

Figure 4.45: Experimental and calculated G_c and K_c for composite with 20% total V_f

For hybrid with 10% total V_f, mixed effect was observed. Both composite, 10(7.50:2.50) and 10(5.00:5.00), showed positive synergy while hybrid 10(2.50:7.50) showed negative synergy. The experimental K_c for hybrid 10(7.50:2.50) is 3.47 MPa.m$^{1/2}$, which is higher than the calculated value of 3.09 MPa.m$^{1/2}$. On the other hand, experimental K_c for hybrid 10(2.50:7.50) is 3.17 MPa.m$^{1/2}$, which is slightly lower than the calculated value of 3.20 MPa.m$^{1/2}$.

For hybrid composites with 20% total V_f, only 20(5.00:15.00) showed positive synergy. The experimental K_c for hybrid 20(5.00:15.00) is 3.72 MPa.m$^{1/2}$, which is higher than the calculated value of 3.39 MPa.m$^{1/2}$.

Figure 4.46 plots G_c and K_c for all the composite tested for comparison. From the plot, composite 20(20.00:0.00) is determined to have the highest G_c value. For K_c, hybrid composite 20(5.00:15.00) has the highest value. Among the hybrid composite, 20(15.00:5.00) and 20(10.00:10.00) showed the most promise since its G_c value is almost as high as 20(20.00:0.00) and its K_c is comparatively higher than the others. In general, the objective of improving the impact properties of the composite through hybridization was achieved.

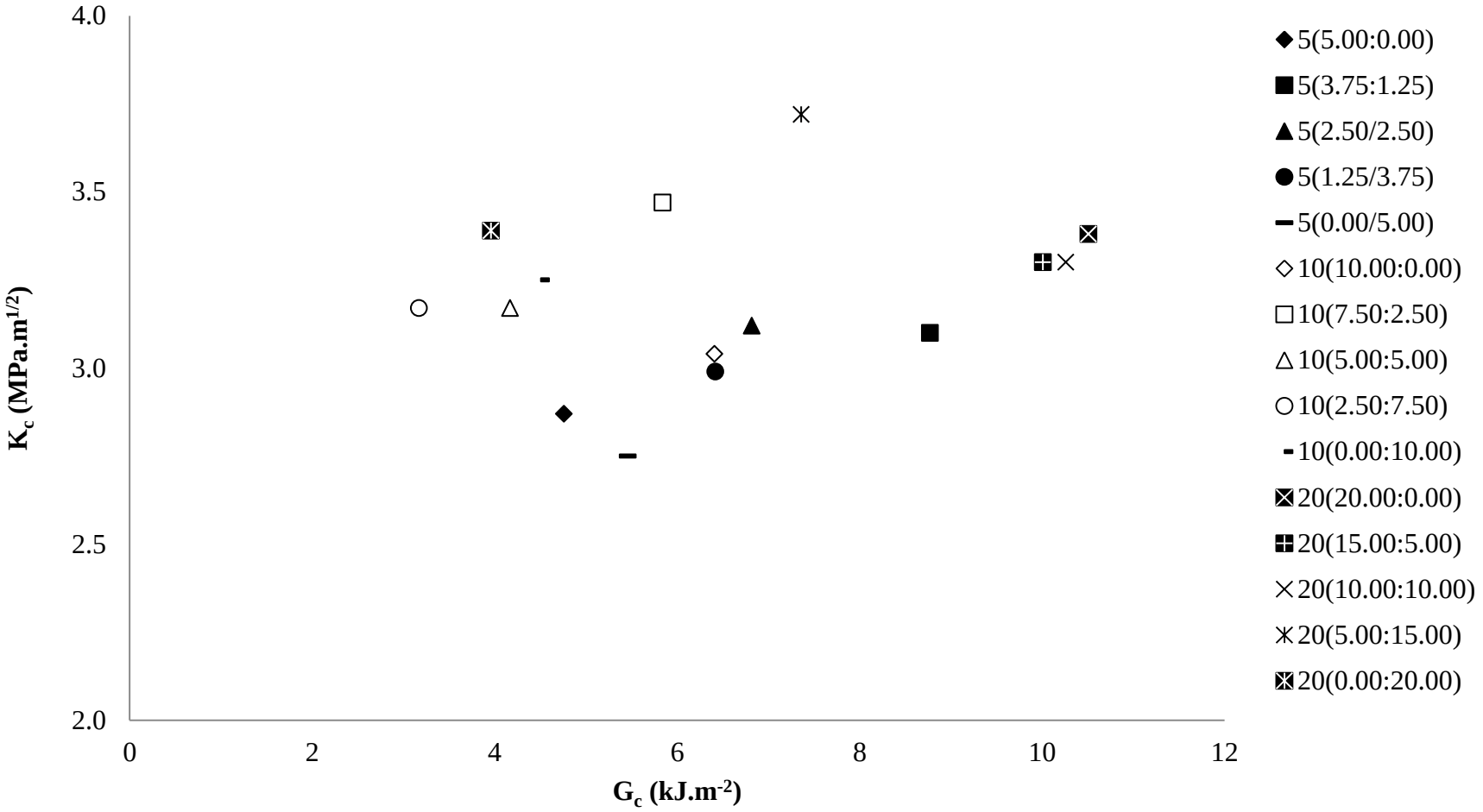

Figure 4.46: K_c and G_c values for all composites

CHAPTER 5

CONCLUSION AND SUGGESTION FOR FUTURE WORKS

5.1 Conclusion

From the determination of thermal and mechanical properties of the composites and the effect of hybridisation, the following conclusions have been made:

i. Intimately mixed hybrid aramid/carbon fibre reinforced polypropylene composites were successfully prepared and moulded via extrusion and injection moulding.

ii. From TGA, it was found that hybridisation improved the thermal stability of the composites. The hybrid composites possess better thermal stability than its single fibre reinforced counterparts. From DSC, it was found that the melting temperature and the degree of crystallinity of the composites were not significantly affected by hybridisation. This means that the hybrid can be processed using the same temperature as the single fibre composites.

iii. Hybridisation improves the tensile modulus and strength of the composites. Fracture strain on the other hand is more sensitive towards the total V_f regardless of the fibre proportions. Flexural modulus increases with increasing total V_f, regardless of fibre proportions. Flexural strength was negatively affected by hybridisation. Flexural displacement on the other hand did not show any significant trend. The impact properties of the composite were significantly improved with hybridisation. Hybridisation produced composites with relatively high G_c and K_c values

iv. From the SEM micrographs, it was found that the interfacial bonding between the fibres and the matrix was weak, based on the clean fibre surface during fracture. It

was an expected observation since no surface treatment or compatibilisers were used in the preparation of the composites.

5.2 Suggestions for Future Works

i. The interfacial interaction between the fibre and the matrix can be improved by introducing coupling agents such maleic anhydride or through fibre surface treatment.

ii. The effect of temperature on the mechanical properties of the composites can be tested.

iii. The composites could also be subjected to weathering studies. This is especially important since aramid fibres are hygroscopic and sensitive to UV.

iv. The fibre length distribution in the hybrid composite could be studied to further understand the fibre-fibre interaction that occurs during processing.

REFERENCES

1. Zangenberg, J., P. Brøndsted, and M. Koefoed, *Design of a fibrous composite preform for wind turbine rotor blades.* Materials & Design, 2014. **56**(0): p. 635-641.

2. Carley, J.F., *Whittington's dictionary of plastics: edited by James F. Carley*. 1993: CRC PressINC.

3. Mallick, P.K., *Fibre Reinforced Composites: Materials, Manufacturing and Design*. 2008, Boca Raton, Florida: CRC Press.

4. De, S.K. and J.R. White, *Short Fibre: Polymer Composites*. 1996: Woodhead Pub.
5. Ahmad, J., *Machining of Polymer Composites*. 2008: Springer.

6. Mazumdar, S.K., *Composite Manufacturing: Materials, Product and Process Engineering*. 2002, Boca Raton, Florida: CRC Press.

7. de Freitas, M. and L. Reis, *Failure mechanisms on composite specimens subjected to compression after impact.* Composite Structures, 1998. **42**(4): p. 365-373.

8. Peijs, A.A.J.M., R.W. Venderbosch, and P.J. Lemstra, *Hybrid composites based on polyethylene and carbon fibres Part 3: Impact resistant structural composites through damage management.* Composites, 1990. **21**(6): p. 522-530.

9. Cao, Y., J. Feng, and P. Wu, *Simultaneously improving the toughness, flexural modulus and thermal performance of isotactic polypropylene by α-β crystalline transition and inorganic whisker reinforcement.* Polymer Engineering & Science, 2010. **50**(2): p. 222-231.

10. Karger-Kocsis, J., *Polypropylene Structure, Blends and Composites V.1: Structure and Morphology*. 1995: Chapman & Hall.

11. Natta, G. and P. Corradini, *Structure and properties of isotactic polypropylene.* Il Nuovo Cimento Series 10, 1960. **15**(1): p. 40-51.

12. Maier, C. and T. Calafut, *Polypropylene: The Definitive Users Guide*. 1998: Plastics Design Library.

13. *Ullmann's Encyclopedia of Industrial Chemistry*. 2003: John Wiley & Sons.

14. Andrews, M.C. and R.J. Young, *Analysis of the deformation of aramid fibres and composites using Raman spectroscopy.* Journal of Raman Spectroscopy, 1993. **24**(8): p. 539-544.

15. S van der Zwaag, et al., *Chain stretching in aramid fibres.* Polymer Communications, 1987. **28**: p. 276-277.

16. Zhang, H., et al., *Effects of solar UV irradiation on the tensile properties and structure of PPTA fiber.* Polymer Degradation and Stability, 2006. **91**(11): p. 2761-2767.

17. Dobb, M.G., R.M. Robson, and A.H. Roberts, *The ultraviolet sensitivity of Kevlar 149 and Technora fibres.* Journal of Materials Science, 1993. **28**(3): p. 785-788.

18. Brown, J.R., et al., *Photochemical Ageing of Kevlar® 49.* Textile Research Journal, 1983. **53**(4): p. 214-219.

19. Tanaka, K., et al., *Characterization of the aramid/epoxy interfacial properties by means of pull-out test and influence of water absorption.* Composites Science and Technology, 2002. **62**(16): p. 2169-2177.

20. Komai, K., S. Shiroshita, and K. Okamoto, *Effects of Water Absorption and Cryogenic Temperature on Strength of ArFRP*. Journal of the Society of Materials Science, Japan, 1997. **46**(2): p. 157-162.

21. Cervenka, A.J., D.J. Bannister, and R.J. Young, *Moisture absorption and interfacial failure in aramid/epoxy composites.* Composites Part A: Applied Science and Manufacturing, 1998. **29**(9–10): p. 1137-1144.

22. Komai, K., K. Minoshima, and K. Tanaka, *Delamination induced by low-velocity impact and influence of water absorption on delamination and CAI of FRPs.* Nippon Kikai Gakkai Ronbunshu, A Hen/Transactions of the Japan Society of Mechanical Engineers, Part A, 1997. **63**(610): p. 1198-1204.

23. Komai, K., et al., *Effects of stress waveform and water absorption on the fatigue strength of angle-ply aramid fiber/epoxy composites.* International Journal of Fatigue, 2002. **24**(2–4): p. 339-348.

24. Fitzer, E., *Carbon fibres and their composites*. 1985: Springer-Verlag.

25. Chand, S., *Review Carbon fibers for composites.* journal of materials science, 2000. **35**(6): p. 1303-1313.

26. Minus, M. and S. Kumar, *The processing, properties, and structure of carbon fibers.* JOM, 2005. **57**(2): p. 52-58.

27. White, J.R., *Fibre reinforcements for composite materials (Composite materials series, volume 2) Edited by A. R. Bunsell (Series Editor: R. B. Pipes), Elsevier Science Publishers, Amsterdam, 1988, pp. ix + 537, price US£171.00, Dfl 325.00. ISBN 0–444–42801-1 (Series: ISBN 0–444–42525-X).* Journal of Chemical Technology & Biotechnology, 1990. **48**(3): p. 388-388.

28. Thomas, S. and L.A. Pothan, *Natural Fibre Reinforced Polymer Composites: From Macro to Nanoscale*. 2009: Éd. des Archives contemporaines.

29. Hancox, N.L., *Fibre composite hybrid materials*. 1981: Applied Science.

30. Marom, G., et al., *Hybrid effects in composites: conditions for positive or negative effects versus rule-of-mixtures behaviour.* journal of materials science, 1978. **13**(7): p. 1419-1426.

31. Pan, N. and R. Postle, *The Tensile Strength of Hybrid Fibre Composites: A Probabilistic Analysis of the Hybrid Effects.* Philosophical Transactions of the Royal Society of London. Series A: Mathematical, Physical and Engineering Sciences, 1996. **354**(1714): p. 1875-1897.

32. Tadmor, Z. and C.G. Gogos, *Principles of Polymer Processing*. 2006: Wiley.

33. Manas-Zloczower, I., *Mixing and Compounding of Polymers: Theory and Practice*. 2009: Hanser.

34. Chung, C.I., *Extrusion of Polymers: Theory and Practice*. 2000: Hanser Gardner Publications.

35. Rauwendaal, C., *Polymer Extrusion*. 2001: Hanser Gardner Publications.

36. Osswald, T.A., *Polymer processing fundamentals*. 2006: Hanser.

37. *Handbook of Polypropylene and Polypropylene Composites*. 2003: Marcel Dekker Incorporated.

38. Lobo, H. and J.V. Bonilla, *Handbook of Plastics Analysis*. 2003: Marcel Dekker.

39. Hartikainen, J., et al., *Polypropylene hybrid composites reinforced with long glass fibres and particulate filler.* Composites Science and Technology, 2005. **65**(2): p. 257-267.

40. Lin, L.-Y., et al., *Preparation and characterization of layered silicate/glass fiber/epoxy hybrid nanocomposites via vacuum-assisted resin transfer molding (VARTM).* Composites Science and Technology, 2006. **66**(13): p. 2116-2125.

41. Mingzhu Pan, S.Y. Zhang, and Dingguo Zhou, *Preparation and Properties of Wheat Straw Fiber-polypropylene Composites. Part II. Investigation of Surface Treatments on the Thermo-mechanical and Rheological Properties of the Composites.* Journal of Composite Materials, 2010. **44**(9): p. 1061-1073.

42. Idicula, M., et al., *Dynamic mechanical analysis of randomly oriented intimately mixed short banana/sisal hybrid fibre reinforced polyester composites.* Composites Science and Technology, 2005. **65**(7-8): p. 1077-1087.

43. Fu, S.Y., et al., *Tensile properties of short-glass-fiber- and short-carbon-fiber-reinforced polypropylene composites.* Composites Part A: Applied Science and Manufacturing, 2000. **31**(10): p. 1117-1125.

44. Jacob, M., S. Thomas, and K.T. Varughese, *Mechanical properties of sisal/oil palm hybrid fiber reinforced natural rubber composites.* Composites Science and Technology, 2004. **64**(7-8): p. 955-965.

45. Velmurugan, R. and V. Manikandan, *Mechanical properties of palmyra/glass fiber hybrid composites.* Composites Part A: Applied Science and Manufacturing, 2007. **38**(10): p. 2216-2226.

46. Deng, S., et al., *Evaluation of fibre tensile strength and fibre/matrix adhesion using single fibre fragmentation tests.* Composites Part A: Applied Science and Manufacturing, 1998. **29**(4): p. 423-434.

47. Tjong, S.C., et al., *Short glass fiber-reinforced polyamide 6,6 composites toughened with maleated SEBS.* Composites Science and Technology, 2002. **62**(15): p. 2017-2027.

48. Rijsdijk, H.A., M. Contant, and A.A.J.M. Peijs, *Continuous-glass-fibre-reinforced polypropylene composites: I. Influence of maleic-anhydride-modified polypropylene on mechanical properties.* Composites Science and Technology, 1993. **48**(1–4): p. 161-172.

49. Chow, C.P.L., X.S. Xing, and R.K.Y. Li, *Moisture absorption studies of sisal fibre reinforced polypropylene composites.* Composites Science and Technology, 2007. **67**(2): p. 306-313.

50. Dhakal, H.N., Z.Y. Zhang, and M.O.W. Richardson, *Effect of water absorption on the mechanical properties of hemp fibre reinforced unsaturated polyester composites.* Composites Science and Technology, 2007. **67**(7–8): p. 1674-1683.

51. Chen, H., M. Miao, and X. Ding, *Influence of moisture absorption on the interfacial strength of bamboo/vinyl ester composites.* Composites Part A: Applied Science and Manufacturing, 2009. **40**(12): p. 2013-2019.

52. Almgren, K.M., et al., *Effects of Moisture on Dynamic Mechanical Properties of Wood Fiber Composites Studied by Dynamic FT-IR Spectroscopy.* Journal of Reinforced Plastics and Composites, 2008. **27**(16-17): p. 1709-1721.

53. Bradley, W.L. and T.S. Grant, *The effect of the moisture absorption on the interfacial strength of polymeric matrix composites.* journal of materials science, 1995. **30**(21): p. 5537-5542.

54. Rozman, H.D., et al., *Polypropylene–oil palm empty fruit bunch–glass fibre hybrid composites: a preliminary study on the flexural and tensile properties.* European Polymer Journal, 2001. **37**(6): p. 1283-1291.

55. Mishra, S., et al., *Studies on mechanical performance of biofibre/glass reinforced polyester hybrid composites.* Composites Science and Technology, 2003. **63**(10): p. 1377-1385.

56. Rezaei, F., et al., *Development of Short-Carbon-Fiber-Reinforced Polypropylene Composite for Car Bonnet.* Polymer-Plastics Technology and Engineering, 2008. **47**(4): p. 351-357.

57. Hassan, A., et al., *Interfacial shear strength and tensile properties of injection-molded, short- and long-glass fiber-reinforced polyamide 6,6 composites.* Journal of Reinforced Plastics and Composites, 2011. **30**(14): p. 1233-1242.

58. ASTM, *ASTM Standard D638 Standard test method for tensile properties of plastics*, 2010, ASTM International.

59. ASTM, *ASTM Standard D760 Standard test methods for flexural properties of unreinforced and reinforced plastics and electrical insulating materials*, 2010, ASTM International.

60. ASTM, *ASTM Standard E23 Standard test methods for notched bar impact testing of metallic materials*, 2012, ASTM International.

61. Hassan, A., et al., *Tensile, Impact and Fiber Length Properties of Injection-Molded Short and Long Glass Fiber-Reinforced Polyamide 6,6 Composites.* Journal of Reinforced Plastics and Composites, 2004. **23**(9): p. 969-986.

62. Rezaei, F., R. Yunus, and N.A. Ibrahim, *Effect of fiber length on thermomechanical properties of short carbon fiber reinforced polypropylene composites.* Materials & Design, 2009. **30**(2): p. 260-263.

63. Rezaei, F., et al., *Effect of fiber loading and fiber length on mechanical and thermal properties of short carbon fiber reinforced polypropylene composite.* The Malaysian Journal of Analytical Sciences, 2007. **11**(1): p. 181-188.

64. Bourbigot, S., X. Flambard, and F. Poutch, *Study of the thermal degradation of high performance fibres—application to polybenzazole and p-aramid fibres.* Polymer Degradation and Stability, 2001. **74**(2): p. 283-290.

65. Maity, J., et al., *Direct fluorination of Twaron fiber and the mechanical, thermal and crystallization behaviour of short Twaron fiber reinforced polypropylene composites.* Composites Part A: Applied Science and Manufacturing, 2008. **39**(5): p. 825-833.

66. Golebiewski, J. and A. Galeski, *Thermal stability of nanoclay polypropylene composites by simultaneous DSC and TGA.* Composites Science and Technology, 2007. **67**(15–16): p. 3442-3447.

67. Abu-Sharkh, B.F. and H. Hamid, *Degradation study of date palm fibre/polypropylene composites in natural and artificial weathering: mechanical and thermal analysis.* Polymer Degradation and Stability, 2004. **85**(3): p. 967-973.

68. Karsli, N.G. and A. Aytac, *Effects of maleated polypropylene on the morphology, thermal and mechanical properties of short carbon fiber reinforced polypropylene composites.* Materials & Design, 2011. **32**(7): p. 4069-4073.

69. Nayak, S.K., S. Mohanty, and S.K. Samal, *Influence of short bamboo/glass fiber on the thermal, dynamic mechanical and rheological properties of polypropylene hybrid composites.* Materials Science and Engineering: A, 2009. **523**(1–2): p. 32-38.

70. Cui, Y.-H., et al., *Fabrication and properties of nano-ZnO/glass-fiber-reinforced polypropylene composites.* Journal of Vinyl and Additive Technology, 2010. **16**(3): p. 189-194.

71. Abdelmouleh, M., et al., *Short natural-fibre reinforced polyethylene and natural rubber composites: Effect of silane coupling agents and fibres loading.* Composites Science and Technology, 2007. **67**(7–8): p. 1627-1639.

72. Bhattacharyya, A.R., et al., *Crystallization and orientation studies in polypropylene/single wall carbon nanotube composite.* Polymer, 2003. **44**(8): p. 2373-2377.

73. Yamada, K., et al., *Molecular Weight Dependence of Equilibrium Melting Temperature and Lamellar Thickening of Isotactic Polypropylene with High Tacticity.* Journal of Macromolecular Science, Part B, 2003. **42**(3-4): p. 733-752.

74. Cao, Y., J. Feng, and P. Wu, *DSC and morphological studies on the crystallization behavior of β-nucleated isotactic polypropylene composites filled with Kevlar fibers.* Journal of Thermal Analysis and Calorimetry, 2010. **103**(1): p. 339-345.

75. Tan, J.K., T. Kitano, and T. Hatakeyama, *Crystallization of carbon fibre reinforced polypropylene.* Journal of Materials Science, 1990. **25**(7): p. 3380-3384.

76. Tan, J., T. Kitano, and T. Hatakeyama, *Crystallization of carbon fibre reinforced polypropylene.* journal of materials science, 1990. **25**(7): p. 3380-3384.

77. Afaghi-Khatibi, A. and Y.-W. Mai, *Characterisation of fibre/matrix interfacial degradation under cyclic fatigue loading using dynamic mechanical analysis.* Composites Part A: Applied Science and Manufacturing, 2002. **33**(11): p. 1585-1592.

78. Kanny, K., et al., *Dynamic mechanical analyses and flexural fatigue of PVC foams.* Composite Structures, 2002. **58**(2): p. 175-183.

79. Rooj, S., et al., *Influence of "expanded clay" on the microstructure and fatigue crack growth behavior of carbon black filled NR composites.* Composites Science and Technology, 2013. **76**(0): p. 61-68.

80. Papadimitriou, K.D., et al., *Covalent cross-linking in phosphoric acid of pyridine based aromatic polyethers bearing side double bonds for use in high temperature polymer electrolyte membrane fuelcells.* Journal of Membrane Science, 2013. **433**(0): p. 1-9.

81. Sakurai, K., T. Maegawa, and T. Takahashi, *Glass transition temperature of chitosan and miscibility of chitosan/poly(N-vinyl pyrrolidone) blends.* Polymer, 2000. **41**(19): p. 7051-7056.

82. Goertzen, W.K. and M.R. Kessler, *Dynamic mechanical analysis of carbon/epoxy composites for structural pipeline repair.* Composites Part B: Engineering, 2007. **38**(1): p. 1-9.

83. MacCrum, N.G., B.E. Read, and G. Williams, *Anelastic and dielectric effects in polymeric solids*. 1967: Dover Publications, Incorporated.

84. Díez-Gutiérrez, S., et al., *Dynamic mechanical analysis of injection-moulded discs of polypropylene and untreated and silane-treated talc-filled polypropylene composites.* Polymer, 1999. **40**(19): p. 5345-5353.

85. Thomason, J.L., *The influence of fibre length, diameter and concentration on the modulus of glass fibre reinforced polyamide 6,6.* Composites Part A: Applied Science and Manufacturing, 2008. **39**(11): p. 1732-1738.

86. Thomason, J.L. and M.A. Vlug, *Influence of fibre length and concentration on the properties of glass fibre-reinforced polypropylene: 1. Tensile and flexural modulus.* Composites Part A: Applied Science and Manufacturing, 1996. **27**(6): p. 477-484.

87. Arroyo, M., R. Zitzumbo, and F. Avalos, *Composites based on PP/EPDM blends and aramid short fibres. Morphology/behaviour relationship.* Polymer, 2000. **41**(16): p. 6351-6359.

88. Thomason, J.L., et al., *Influence of fibre length and concentration on the properties of glass fibre-reinforced polypropylene: Part 3. Strength and strain at failure.* Composites Part A: Applied Science and Manufacturing, 1996. **27**(11): p. 1075-1084.

89. Thomason, J.L., *The influence of fibre length, diameter and concentration on the strength and strain to failure of glass fibre-reinforced polyamide 6,6.* Composites Part A: Applied Science and Manufacturing, 2008. **39**(10): p. 1618-1624.

90. Llorca, J., *Fiber fracture* 2002: Elsevier Science & Technology Books.

91. Mittal, R.K. and V.B. Gupta, *The strength of the fibre-polymer interface in short glass fibre-reinforced polypropylene.* journal of materials science, 1982. **17**(11): p. 3179-3188.

92. Sreekala, M.S., et al., *The mechanical performance of hybrid phenol-formaldehyde-based composites reinforced with glass and oil palm fibres.* Composites Science and Technology, 2002. **62**(3): p. 339-353.

93. You, Y.-J., et al., *Hybrid effect on tensile properties of FRP rods with various material compositions.* Composite Structures, 2007. **80**(1): p. 117-122.

94. Thomason, J.L., *Micromechanical parameters from macromechanical measurements on glass reinforced polypropylene.* Composites Science and Technology, 2002. **62**(10–11): p. 1455-1468.

95. Nicholson, *The Chemistry of Polymers*. 2011: Royal Society of Chemistry.

96. Ku, H., et al., *Drop Weight Impact Test Fracture of Vinyl Ester Composites: Micrographs of Pilot Study.* Journal of Composite Materials, 2005. **39**(18): p. 1607-1620.

97. Richardson, O.W., *Polymer engineering composites*. 1977: Applied Science Publishers.

98. Thomason, J.L. and M.A. Vlug, *Influence of fibre length and concentration on the properties of glass fibre-reinforced polypropylene: 4. Impact properties.* Composites Part A: Applied Science and Manufacturing, 1997. **28**(3): p. 277-288.

99. Masud, A., A.K.B. Zaman, and A. Al-Khaled, *Effects of environment on fracture toughness of glass fiber/polyester composite.* Journal of Mechanical Engineering, 2007. **38**: p. 38-44.

100. Hassan, A., A.A. Hassan, and M.I. Mohd Rafiq, *Impact properties of injection molded glass fiber/polyamide-6 composites: effect of testing parameters.* Journal of Reinforced Plastics and Composites, 2011. **30**(10): p. 889-898.

101. Reis, P.N.B., et al., *Impact response of Kevlar composites with filled epoxy matrix.* Composite Structures, 2012. **94**(12): p. 3520-3528.

102. Iqbal, K., et al., *Impact damage resistance of CFRP with nanoclay-filled epoxy matrix.* Composites Science and Technology, 2009. **69**(11–12): p. 1949-1957.

103. Hassan, A., et al., *Extrusion and pultrusion compounded carbon fibre reinforced PA 6,6 composites: impact properties of injection moulded specimens.* Malaysian Journal of Science, 2003. **22**: p. 105-110.